RESEARCH

2007-36

Cone Penetration Testing in Pavement Design

LRRB
LOCAL ROAD RESEARCH BOARD

Take the steps... Research...Knowledge...Innovative Solutions!

Transportation Research

Technical Report Documentation Page

1. Report No.	2.	3. Recipients Accession No.
MN/RC 2007-36		

4. Title and Subtitle	5. Report Date
Cone Penetration Testing In Pavement Design	September 2007
	6.

7. Author(s)	8. Performing Organization Report No.
William Dehler and Joseph Labuz	

9. Performing Organization Name and Address	10. Project/Task/Work Unit No.
Department of Civil Engineering University of Minnesota 500 Pillsbury Drive SE Minneapolis, MN 55455	11. Contract (C) or Grant (G) No. (c) 81655 (wo) 163

12. Sponsoring Organization Name and Address	13. Type of Report and Period Covered
Minnesota Department of Transportation 395 John Ireland Boulevard, Mail Stop 330 St. Paul, Minnesota 55155	Final Report 14. Sponsoring Agency Code

15. Supplementary Notes
http://www.lrrb.org/PDF/200736.pdf

16. Abstract (Limit: 200 words)

The objective of this work was to show that cone penetration testing (CPT) can be used for pavement applications, specifically estimating resilient modulus and organic content. A series of undisturbed samples were obtained from borings directly adjacent to CPT soundings. These samples underwent both laboratory resilient modulus and bender element testing. A statistical analysis was then performed on these results in conjunction with the data obtained from the CPT soundings to determine the feasibility of developing correlations between field and laboratory measurements of moduli. A relationship was developed between Young's modulus determined by bender element testing and that determined by resilient modulus testing. However, the correlation did not apply to the field-based seismic measurements of stiffness from the CPT soundings.

The analysis presented with respect to the identification of highly organic soils via CPT testing shows that at this point the model identified using the discriminate analysis method is not currently sufficient to use in practice. The 10% increase in correctly classified soils, however, holds promise for the future, and the introduction of additional independent parameters within a significantly larger data set can be easily analyzed using the methods and tools presented here.

17. Document Analysis/Descriptors	18. Availability Statement
resilient modulus, bender element, CPT piezocone, organic content	No restrictions. Document available from: National Technical Information Services, Springfield, Virginia 22161

19. Security Class (this report)	20. Security Class (this page)	21. No. of Pages	22. Price
Unclassified	Unclassified	116	

Cone Penetration Testing In Pavement Design

Final Report

Prepared by:

William Dehler
Joseph Labuz

Department of Civil Engineering
University of Minnesota

September 2007

Published by:

Minnesota Department of Transportation
Research Services Section
MS 330
395 John Ireland Boulevard.
St. Paul, Minnesota 55155

Acknowledgements

The authors would like to thank the Local Road Research Board and the Minnesota Department of Transportation for their assistance with funding and providing data for analysis.

Table of Contents

List of Tables

List of Figures

Executive Summary

The cone penetration test (CPT) is popular in geotechnical site investigations, replacing the standard penetration test in many instances. The focus of this research surrounds furthering the uses of the CPT for pavement applications with emphasis on estimating resilient modulus and organic content.

In analyzing the feasibility of using the CPT to estimate the resilient modulus of soil, a series of undisturbed samples were obtained from borings directly adjacent to CPT soundings. These samples underwent both laboratory resilient modulus and bender element testing. A statistical analysis was then performed on these results in conjunction with the data obtained from the CPT soundings to determine the feasibility of developing correlations between field and laboratory measurements of moduli.

An attempt was made to develop a model to assist in predicting soils with problematic organic content. The analysis was performed on existing CPT soundings and their accompanying SPT borings, provided by Mn/DOT, using MatLAB statistical software. The analysis presented with respect to the identification of highly organic soils via CPT testing shows that the model identified using the discriminate analysis method is not currently sufficient to use in practice. The 10% increase in correctly classified soils, however, holds promise for the future, and the introduction of additional independent parameters within a significantly larger data set can be easily analyzed using the methods and tools presented.

This research showed that it is reasonable to use small strain seismic measurements of material stiffness to estimate stiffness values represented by resilient modulus. A relationship was developed between Young's modulus determined by bender element testing and that determined by resilient modulus testing. However, the correlation did not apply to the field-based seismic measurements of stiffness from the CPT soundings.

Chapter 1
Introduction

The Cone Penetration Test (CPT) has been gaining in popularity in the field of geotechnical engineering. Many consultants use it as their primary exploration tool, replacing the Standard Penetration Test (SPT). The focus of this research surrounds furthering the uses of the CPT for pavement applications.

1.1 Overview & Purpose

This research focuses on two aspects of the CPT. It looks into the feasibility of using the data obtained from the CPT to estimate the resilient modulus (M_R) of soil for use in pavement design, and it addresses the problem of identifying highly organic soils using the CPT.

In analyzing the feasibility of using the CPT to predict the resilient modulus of soil, a series of undisturbed samples were obtained from borings directly adjacent to CPT soundings. These samples underwent both laboratory resilient modulus and bender element testing. A statistical analysis was then performed on these results in conjunction with the data obtained from the CPT soundings to determine the feasibility of developing correlations between field and laboratory measurements of moduli.

In addition, the Minnesota Department of Transportation (Mn/DOT) would like to use the CPT as its primary exploration tool. However, it is often difficult to discern between soft clays, sensitive soils, and organic rich soils. An attempt was made to develop a model to assist in predicting whether or not a particular soil has a problematic organic content. The analysis was performed on existing CPT soundings and their accompanying SPT borings, provided by Mn/DOT, using MatLAB statistical analysis software.

Together, the results of this research will serve to make better use of the Cone Penetration Test in the fields of geotechnical and pavement engineering, and pave the way for future research into the prediction of design parameters from CPT results.

1.2 Organization

The remainder of this report is broken up into four chapters. The next chapter provides the necessary background information on each of the key elements of the analyses. Chapters 3 and 4 address the measurement of moduli and the modelling of organic content. Finally, the report concludes with a summary and recommendations for future work.

Chapter 2
Background and Literature Review

2.1 Cone Penetration and Resilient Modulus Testing

Use of the Cone Penetration Test (CPT) has been increasing in popularity among geotechnical engineering studies due primarily to its increased test speed and accuracy as compared to the traditional Standard Penetration Test (SPT) borings (Olsen 1994). In practice, the CPT has become known for delineation of soil stratigraphy and estimation of soil parameters such as friction angle and undrained shear strength (Robertson and Campanella 1983). One additional advantage to CPT exploration is the ability to perform analysis in real time due to the continuous digital data record (Olsen 1994).

As described further in Section 3.2.1, the CPT involves advancement of an instrumented cone into the ground at approximately 2 cm/s (0.79 in./s). Standard CPT cones are equipped to measure tip resistance and skin friction during penetration, via internal load cells, to obtain a nearly continuous record that is related to the soil profile. Most cones currently in operation are also equipped to measure pore water pressure via appropriate transducers and detect seismic wave arrivals through the use of geophones. The data obtained from the CPT have been correlated to multiple soil properties such as friction angle, shear strength, and soil type by Robertson and Campanella (1983) and Olsen (1994), among others. One correlation where little research has been done is the prediction of resilient modulus.

Through the development of the new AASHTO design guides for both flexible and rigid pavements, the industry has been trending toward increased use of resilient modulus values in design. A material's resilient modulus, originally defined by Seed et al. (1962), is the ratio of applied dynamic deviator stress to the resilient or recovered strain under a transient dynamic load pulse (Gudishala 2004). The resilient modulus concept was further developed by the Strategic Highway Research Program in 1987, and additional refinements were made through 1996 when the Long Term Pavement Performance Protocol P46 was proposed by the Federal Highway Administration (FHWA), as reviewed by Davich et al. (2004). The current protocol, used in this research, was established by National Cooperative Highway Research Program (NCHRP) Project No. 1-28A.

The resilient modulus (M_R) is determined by repeated cyclic loading of a standard soil specimen (either re-compacted or undisturbed) under various combinations of confining and deviator stress designed to mimic loading due to traffic. The resilient modulus is calculated from the final five load cycles as the ratio of the applied deviator stress to the recoverable strain and is generally considered a measure of a secant Young's modulus.

Though widely accepted as the best available predictor of pavement performance, the resilient modulus test is considered too time consuming and costly to run for every roadway design. As a result, other correlations have been developed to predict the resilient modulus using laboratory and in situ testing devices (Gudishala 2004). Correlations between M_R and California Bearing Ratio (CBR), undrained shear strength, and unconfined compressive strength have been suggested by Heukelom and Klomp (1962), Duncan and Buchignani (1976), and Thompson and

Robnett (1979), among others. In addition, correlations between M_R and in situ testing apparatus, such as the falling weight deflectometer, Humboldt soil stiffness gauge, and dynamic cone penetrometer, have also been developed (Siekmeier et al. 1999; Webster et al. 1994; Powell et al. 1984; Harr 1966; Egorov 1965).

At this time, the majority of resilient modulus values used in design are based upon constitutive models, such as the universal model (George 2004). These models, however, still require sampling of soils and laboratory testing to determine the parameters. One purpose of this research is to perform a preliminary analysis regarding the feasibility of using in situ testing, CPT in particular, to predict M_R for roadway design without the need for sampling and laboratory testing.

Mohammad et al. (2000) performed a similar investigation to that discussed here. The research focused upon the feasibility of using a combination of CPT data and laboratory index property test results to predict M_R. Three correlations were developed for common fine-grained and coarse-grained Louisiana soils using cone tip resistance (q_c), sleeve friction (f_s), unit weight (γ), moisture content (w), applied stresses (σ), and soil properties:

$$\frac{M_R}{\sigma_c^{0.55}} = \frac{1}{\sigma_v}\left(31.79q_c + 74.81\frac{f_s}{w}\right) + 4.08\frac{\gamma_d}{\gamma_w} \tag{2.1}$$

$$\frac{M_R}{\sigma_3^{0.55}} = \frac{1}{\sigma_1}\left(47.03q_c + 170.40\frac{f_s}{w}\right) + 1.67\frac{\gamma_d}{\gamma_w} \tag{2.2}$$

$$\frac{M_R}{\sigma_c^{0.55}} = 6.66\frac{q_c\sigma_b}{\sigma_v^2} - 32.09\frac{f_s}{q_c} + 0.52\frac{\gamma_d}{w\gamma_w} \tag{2.3}$$

Equation 2.1 is for in-situ, fine-grained soils; equation 2.2 is for fine-grained soils under in-situ stresses and traffic loading, and equation 2.3 is for coarse-grained soils under in-situ conditions. The subscripts c, v, d, w, and b stand for confining, vertical, dry, water, and bulk, respectively. Mohammed et al. (2000) concluded that even though the correlations developed using end bearing, friction, and moisture content as parameters were successful, additional testing on other soil types is needed before any conclusions can be drawn. Because M_R is a measure of soil stiffness, which is not necessarily related to strength, this work addressed the feasibility of using seismic measurements performed by CPT testing for prediction of resilient modulus without the use of supplementary laboratory data.

2.2 Bender Element and Resilient Modulus Testing

Studies involving wave propagation in soil gained popularity in the 1930's (Hardin and Richart 1963). Since then, the use of wave propagation in geophysical exploration has become common place and technologies are being rapidly developed and applied to new fields. One of the technologies to have come into place more recently is the use of wave propagation in both field and laboratory testing of soil for geotechnical engineering and design. The methods to be analyzed for possible use in predicting resilient modulus from seismic measurements are based upon existing research showing the relationship between moduli determined by laboratory

seismic testing to the resilient modulus by Baig and Nazarian [16] and Davich et al. (2004), among others.

First introduced to soil testing by Shirley and Hampton (1978), bender element testing has often been used to measure small strain soil stiffness (Lings and Greening 2001). Bender elements (Figure 2.1) consist of thin-pieces of piezo-ceramic material sandwiched together such that when energized by a voltage pulse (such as a sine wave), vibration results. Depending upon their orientation, bender elements can be made to vibrate horizontally (bend) or vertically (extend), creating both shear and compression waves, respectively. When used in pairs, bender/extender elements can be made to react to the seismic wave generated by the other, thereby allowing for the measurement of seismic wave arrival times and the subsequent determination of a soil's seismic wave speed, Poission's ratio, and shear and Young's moduli (Davich et al. 2004; Swenson et al. 2006).

Figure 2.1. Bender elements housed in resilient modulus platens.

Chapter 3
Prediction of Resilient Modulus

3.1 Specimen Index Properties

Resilient modulus testing was carried out on eight (8) undisturbed cohesive soil specimens from various depths at three project sites across Minnesota: TH 14 in Owatonna, TH 61 in Forest Lake, and TH 14 in Florence. Each specimen was taken from the bottom 25 - 178 mm (1 - 7 in.) of its respective Shelby tube. Of the eight (8) Shelby tubes, seven (7) contained enough additional soil to perform index property testing, including:

- Grain Size Distribution (with hydrometer)
- In Situ Density and Moisture Content
- Organic Content
- Atterberg Limits

Based upon the results of the index testing, it appears the majority of the soils used in this research consist of Loam (as classified using the Mn/DOT textural triangle) with Silty Loam and Clay Loam present as well. Results of the index property testing are summarized in Table 3.1 and the data sheets are included in Appendix H.

Table 3.1. Summary of soil index properties.

Source	Depth (ft)	Mn/DOT Class	Mn/DOT Class (-10)	Clay (%)	Silt (%)	Sand (%)	Organic (%)	In Situ Moisture Content (%)	In Situ Density (kg/m^3)	In Situ Density (pcf)
Florence	8.5-10.5	Loam	Loam	15.8	46.6	37.6	2.4	19.6	2056	128.4
Florence	13.5-15.5	Clay Loam	Silty Clay Loam	26.3	47.8	25.9	4.8	18.5	2192	136.8
Forest Lake	13.5-15.5	Loam	Loam	14.4	36.6	49.0	2.6	12.6	2143	133.8
Forest Lake	18.5-20.5	Silty Loam	Loam	12.5	36.5	51.0	2.3	14.7	2140	133.6
Owatonna	3.5-5.5	Loam	Loam	11.5	41.2	47.3	2.9	15.4	2093	130.7
Owatonna	8.5-10.5	Loam	Loam	13.8	36.3	49.9	2.8	16.6	2046	127.7
Owatonna	13.5-15.5	Loam	Loam	14.3	39.9	45.8	2.3	15.4	2111	131.8
Min				11.5	36.3	25.9	2.3	12.6	2046	127.7
Max				26.3	47.8	51.0	4.8	19.6	2192	136.8
Mean				15.5	40.7	43.8	2.9	16.1	2112	131.8
St. Dev.				5.0	4.8	9.0	0.9	2.4	52	3.2

3.2 Equipment and Procedures

3.2.1 Cone Penetration Test

Cone penetrometer testing was performed in accordance with American Society for Testing and Materials (ASTM) standard D 3441. The primary pieces are the following:

- truck mounted CPT rig
- standard seismic piezocone
- data acquisition system

The CPT rig (Figure 3.1) consists of a hydraulically leveled truck within which is housed a hydraulic clamp and pushing system (Figure 3.2) that clamps to each section of the push rods and advances the cone at a rate of approximately 20 mm/s (0.79 in./s).

Figure 3.1. Cone penetration test (CPT) truck.

Figure 3.2. CPT hydraulic cone advancement system.

The seismic piezocone is equipped to record tip resistance, sleeve friction, pore water pressure, and seismic wave arrivals (Figure 3.3).

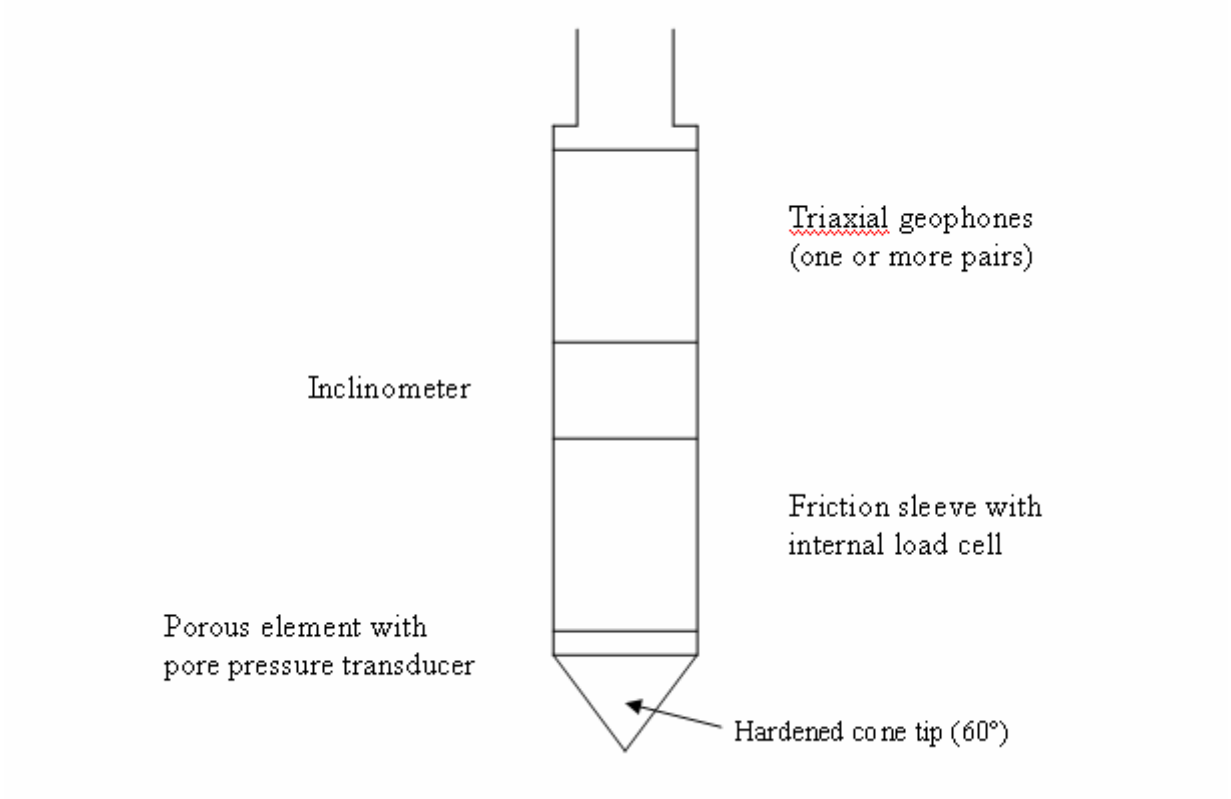

Figure 3.3. Basic seismic CPT piezocone arrangement.

Tip resistance and sleeve friction are measured by internal load cells. Pore water pressure is generally measured using porous stones that have been saturated by glycerin (or other viscous fluid). Note that the pore water pressure is that resulting from the advancement of the cone, and is not considered the in situ pore water pressure. Each of the above data types are recorded at 20 mm increments during advancement. Seismic events are triggered at the surface by hitting the leveling pad of the truck with a sledge hammer (some CPT rigs are equipped with an internal hydraulic hammer). The arrival waves are recorded by one or more pairs of triaxial geophones (accelerometers) mounted behind the tip of the cone. The number of pore pressure transducers and geophones often varies with cone manufacturer.

The data acquisition system (Figure 3.4) consists of a personal computer program that records data in real time in 1 s increments. Advancement is monitored in real time to help avoid damaging the cone during advancement in hard layers.

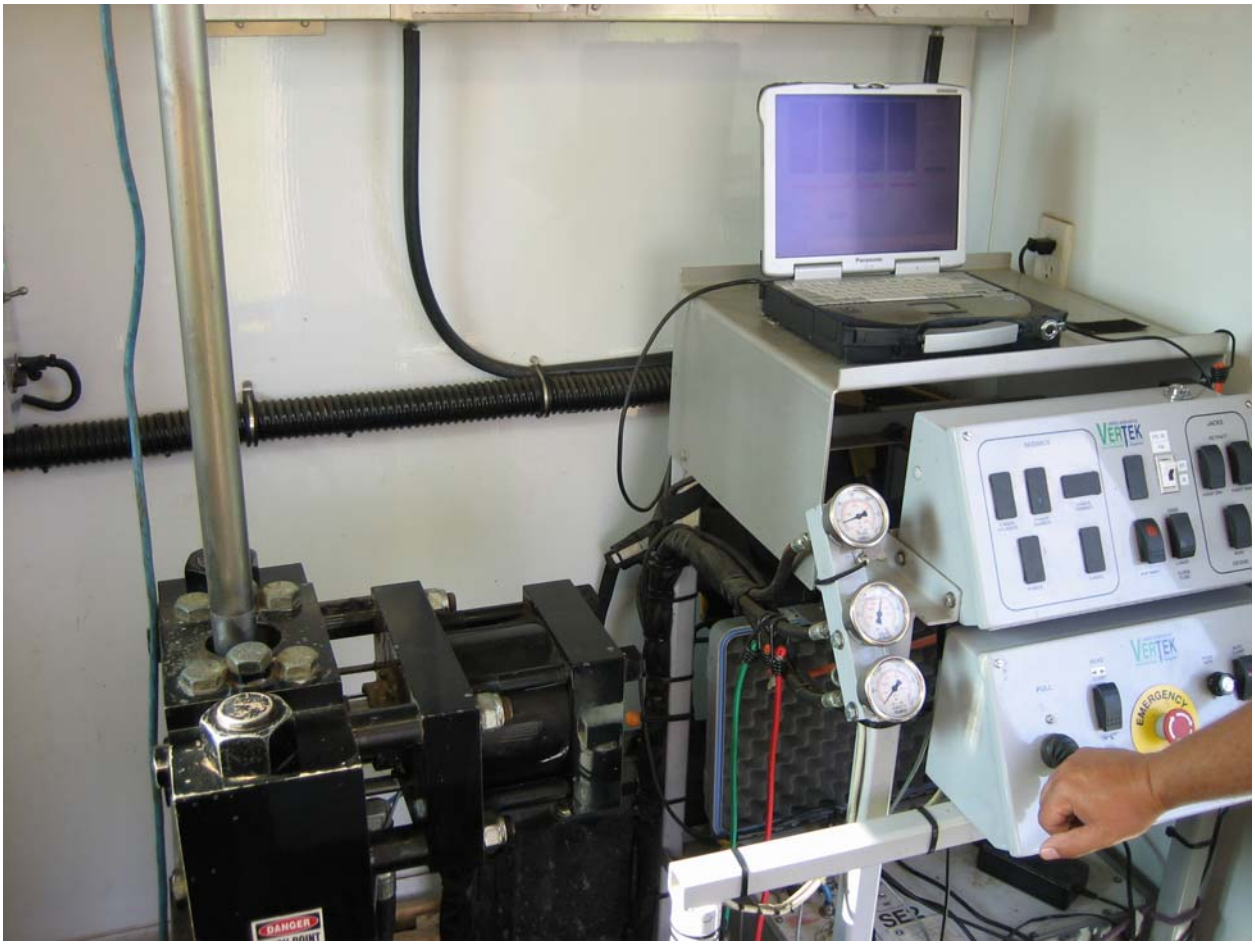

Figure 3.4. CPT data acquisition system.

3.2.2 Resilient Modulus Test

As stated in Section 2.1, resilient modulus testing consists of the measurement of recoverable deformation during cyclic loading of a specimen under a series of deviator and confining stress variations. The procedure followed was from the NCHRP 1-28A protocol for undisturbed samples of fine grained/cohesive (type 4) materials, where the specimen was subjected to a series of 16 different stress states under cyclic loading (Table 3.2).

Table 3.2. NCHRP 1-28A procedure – resilient modulus of fine grained/cohesive materials (Witczak 2004).

Sequence #	No. Repetitions	Confining Pressure		Cyclic Load	
		Psi	kPa	psi	kPa
Conditioning	1000	4.0	27.6	7.0	48.3
1	100	8.0	55.2	4.0	27.6
2	100	6.0	41.4	4.0	27.6
3	100	4.0	27.6	4.0	27.6
4	100	2.0	13.8	4.0	27.6
5	100	8.0	55.2	7.0	48.3
6	100	6.0	41.4	7.0	48.3
7	100	4.0	27.6	7.0	48.3
8	100	2.0	13.8	7.0	48.3
9	100	8.0	55.2	10.0	69.0
10	100	6.0	41.4	10.0	69.0
11	100	4.0	27.6	10.0	69.0
12	100	2.0	13.8	10.0	69.0
13	100	8.0	55.2	14.0	96.6
14	100	6.0	41.4	14.0	96.6
15	100	4.0	27.6	14.0	96.6
16	100	2.0	13.8	14.0	96.6

Following a conditioning cycle of 1000 repetitions, each of the above stress states is cycled 100 times, with each cycle consisting of a 0.2 second haversine load pulse followed by 0.8 seconds of rest. The resilient modulus is determined from the ratio of the cyclic axial stress to the recoverable (resilient) strain over the last five cycles for each stress state:

$$M_R = \frac{\Delta\sigma_a}{\Delta\varepsilon_a^r} \tag{3.1}$$

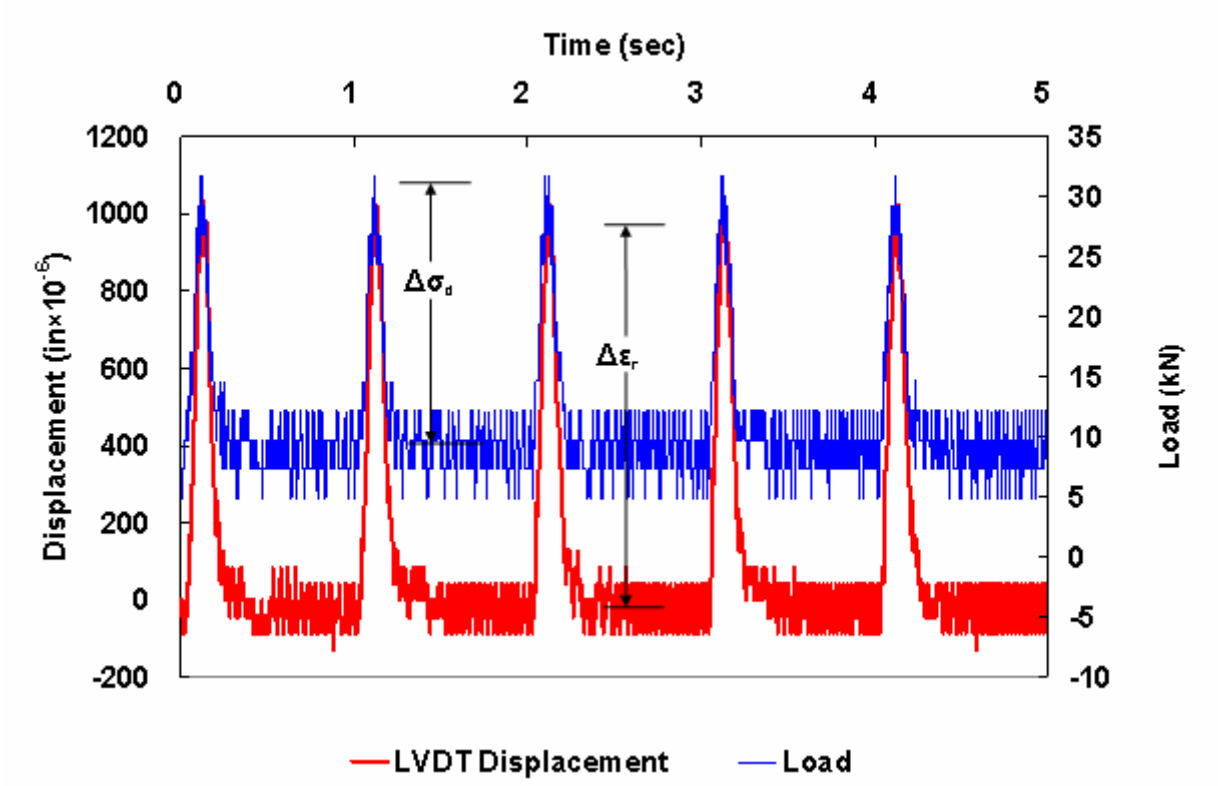

Figure 3.5. Five cycles of the resilient modulus test segment.

Standard sample preparation consists of compacting soil into a mold sized according to its grain size distribution under strict moisture and density control. For this research, however, the resilient modulus testing was performed using undisturbed samples gathered via Shelby tubes from specific depths corresponding to seismic CPT testing performed in the field. These 2.88 in. (7.3 cm) diameter samples were then cut to length to yield a length to diameter ratio of approximately 2:1. The specimens were sealed and stored in a moisture controlled environment until testing.

Prior to testing, the specimens were inserted into a latex membrane and placed between two stainless steel platens housing the bender elements – described in Section 3.2.3. The membrane was then sealed using four rubber o-rings to allow for the application of a confining pressure to the specimen. Prior to placement in the confining chamber, three LVDT's were attached to the side of the specimen using a specially sized harness to allow for measurement of axial deformation.

The specimen was then loaded into the triaxial cell allowing for the application of various confining pressures. Pressure was applied using compressed air. The axial load sequence, described previously, was applied using a closed loop, servo-hydraulic load frame manufactured by MTS Systems (Eden Prairie, MN).

A more detailed description of the specific resilient modulus testing apparatus used for this research can be found in Appendix K (Davich et al., 2004).

3.2.3 Bender Element Test

Bender element testing was performed as described by Davich et al. (2004) using bender elements manufactured in-house. The fabricated bender elements consisted of a set of 12.7 mm (0.5 inch) wide brass reinforced piezo-ceramic bending/extending actuators/sensors (Figure 3.6) by Piezo Systems, Inc.

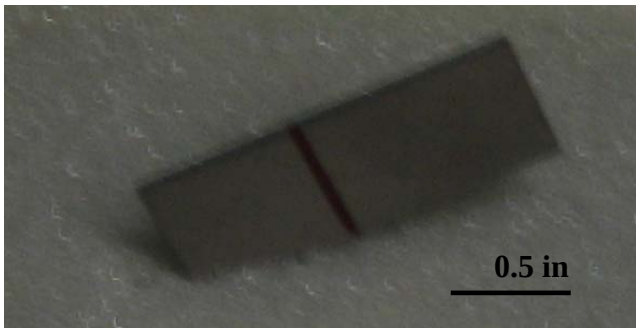

Figure 3.6. Piezo-ceramic element.

One piezo-ceramic was parallel-poled while the other was cross-poled allowing for the sending and receiving of both shear and compressive waves with one set of bender elements (Figure 3.7), as described by Lings and Greening (2001).

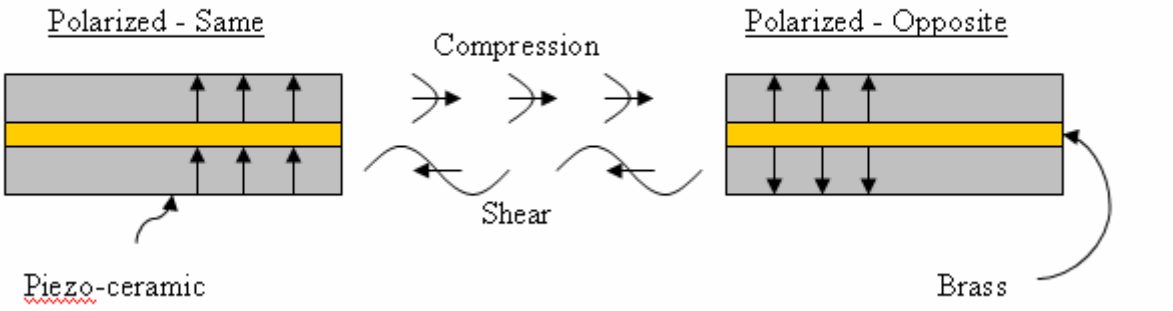

Figure 3.7. Poling of piezo-ceramics and associated waves (Lings and Greening 2001).

The elements were embedded in a stainless steel insert leaving an extension of 4 mm (0.16 in) to provide greater coupling with the soil than provided by the bender elements used by Davich et al. (2004) and Swenson et al. (2006). The elements were coated in a thin layer of epoxy using a set of brass shims and Teflon blocks to ensure even thickness (Figure 3.8).

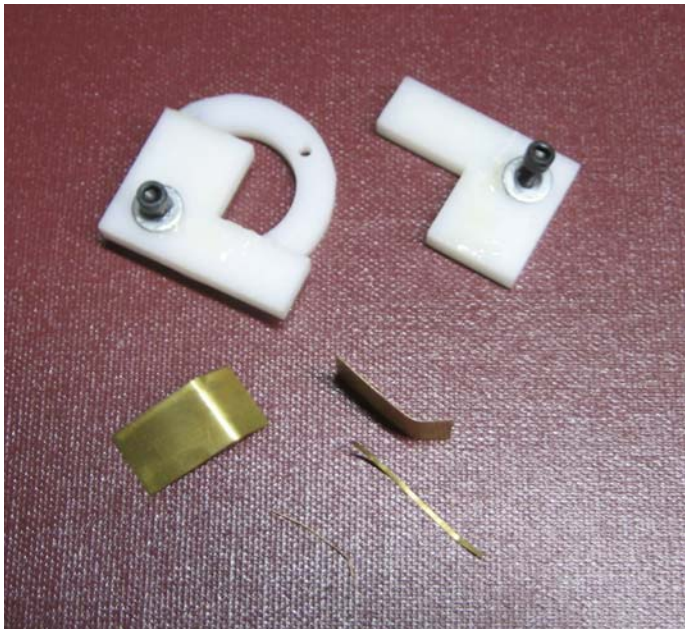

Figure 3.8. Teflon blocks and brass shims for application of flexible epoxy coating.

As shown previously in Figure 2.1, the inserts were then installed in the resilient modulus end platens and wired to work with the existing controller manufactured by GDS Instrumentation and described by Davich et al., 2004.

Davich et al. (2004) showed that the change in wave speed, as measured via bender elements, with varying wave frequency is negligible in the frequency range under which bender elements operate. The bender element testing was performed using a sine wave pulse applied at various frequencies and adjusted to produce the clearest wave form obtainable for a given specimen.

The GDS Instrumentation controller allowed for the recording and stacking of each wave individually, resulting in the selection of particularly clear wave forms over those with increased noise. The number of stacks required to obtain a clear first arrival/peak varied with the specimen and ranged from 1 – 20.

3.3 Results and Discussion

3.3.1 Data Interpretation

Cone penetration testing was performed by Mn/DOT and the raw data analyzed using their in-house program to obtain standard CPT parameters (Appendix I). Of primary interest to this research, however, was the seismic testing performed in conjunction with the CPT. The raw seismic traces (Figure 3.9) were provided by Mn/DOT in both tabular and graphic form (Appendix L).

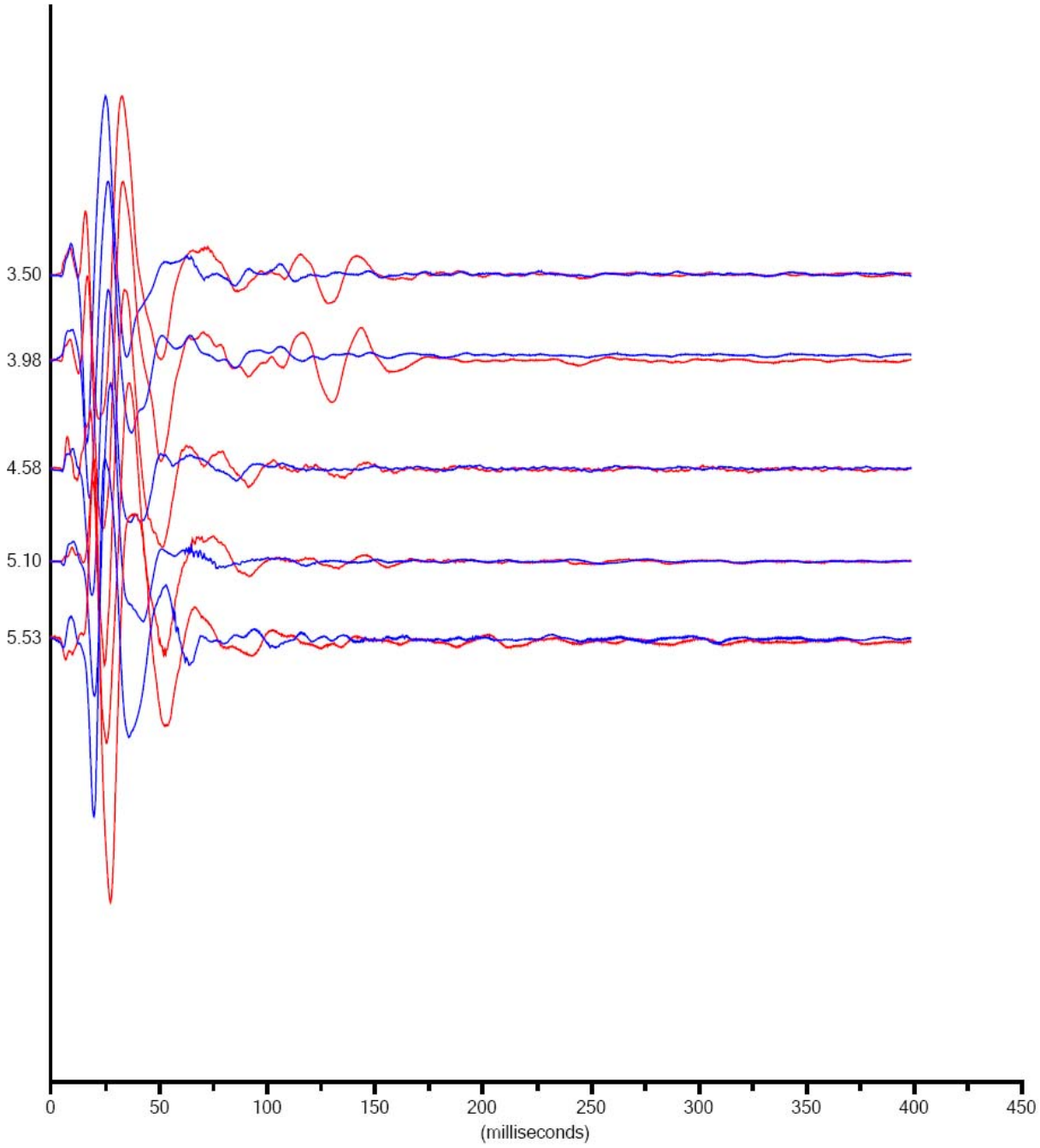

Figure 3.9. Typical CPT seismic traces with depth on y-axis (ft) (Florence 3.5-5.5 ft).

From the seismic traces, the first arrival times were selected by eye to avoid complication and possible errors due to automated picking. Using the arrival times, the shear wave velocity was determined at each location and elevation tested (Table 3.3).

Table 3.3. CPT shear wave velocities for two foot sounding spacing.

	Forest Lake 13.5-15.5	Forest Lake 18.5-20.5	Florence 8.5-10.5	Florence 13.5-15.5	Owatonna 3.5-5.5	Owatonna 8.5-10.5	Owatonna 13.5-15.5
Vs (m/s)	183	367	119	141	171	311	211
Vs (ft/s)	600	1204	390	462	561	1020	692

The shear modulus, G, was obtained from the shear wave velocity and unit weight of the soil:

$$G = \rho \cdot V_s^2 \tag{3.2}$$

yielding shear moduli ranging from 29 – 288 MPa (4,176 – 41,760 psi).

Bender element testing was performed during resilient modulus testing as described in Section 3.2.3. Compression waves are transmitted by bender elements at a much lower energy level than shear wave. Due to this and suspected poor coupling under bender element extension with the soft soils tested, only shear waves were successfully transmitted through each specimen. Figure 3.10 shows a typical compression wave recording.

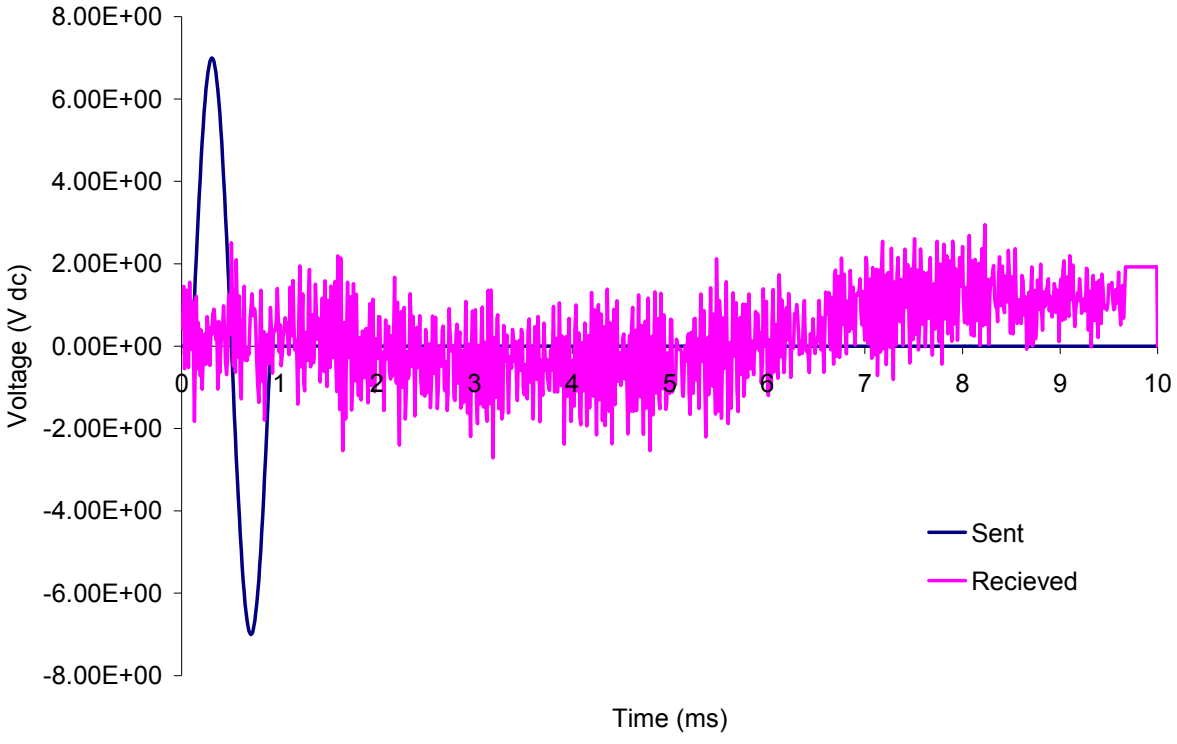

Figure 3.10. Typical bender element compression wave trace (Florence 3.5-5.5 ft).

Select compression waves were successfully transmitted (Figure 3.11).

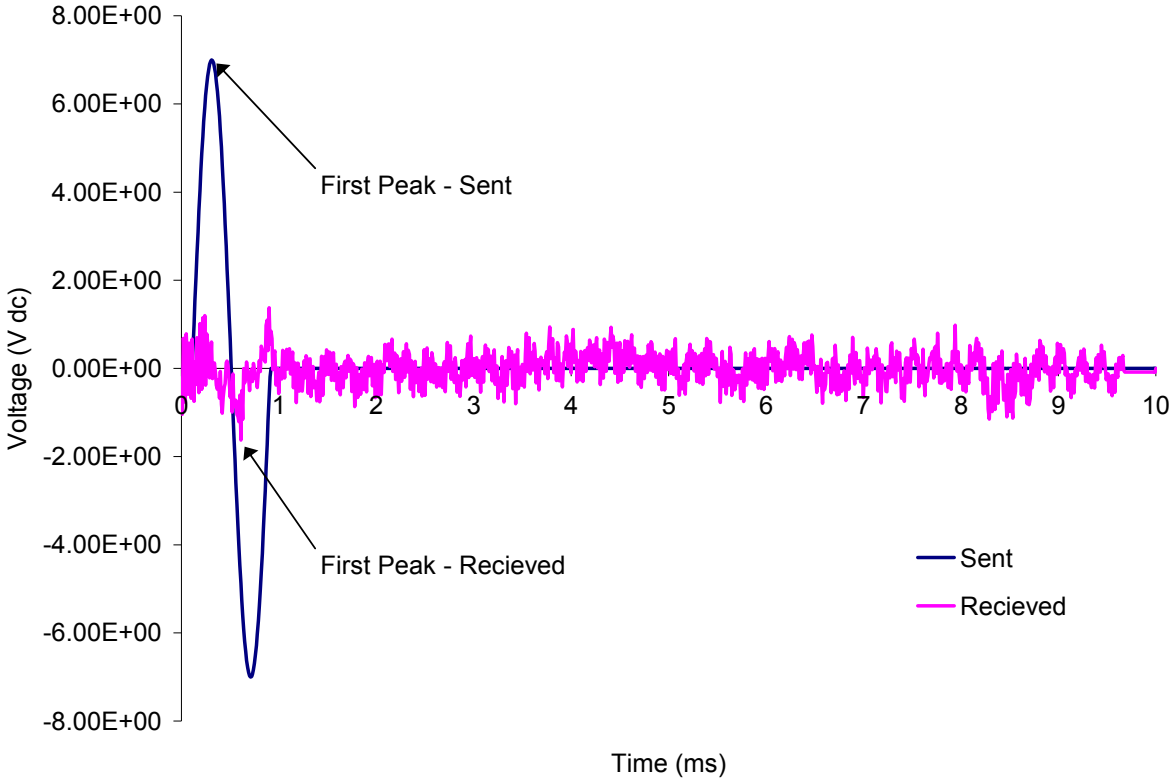

Figure 3.11. Successful bender element compression wave trace (Owatonna 13.5-15.5 ft).

Shear wave seismic traces for each bender element test were analyzed by eye to avoid complications arising from the possibility of erroneous first arrival picks via automated methods. To facilitate determination of wave arrivals in light of imprecise first arrivals, the travel time was determined by picking the first peak in both the sent and received waves. Figure 3.10 shows a typical shear wave.

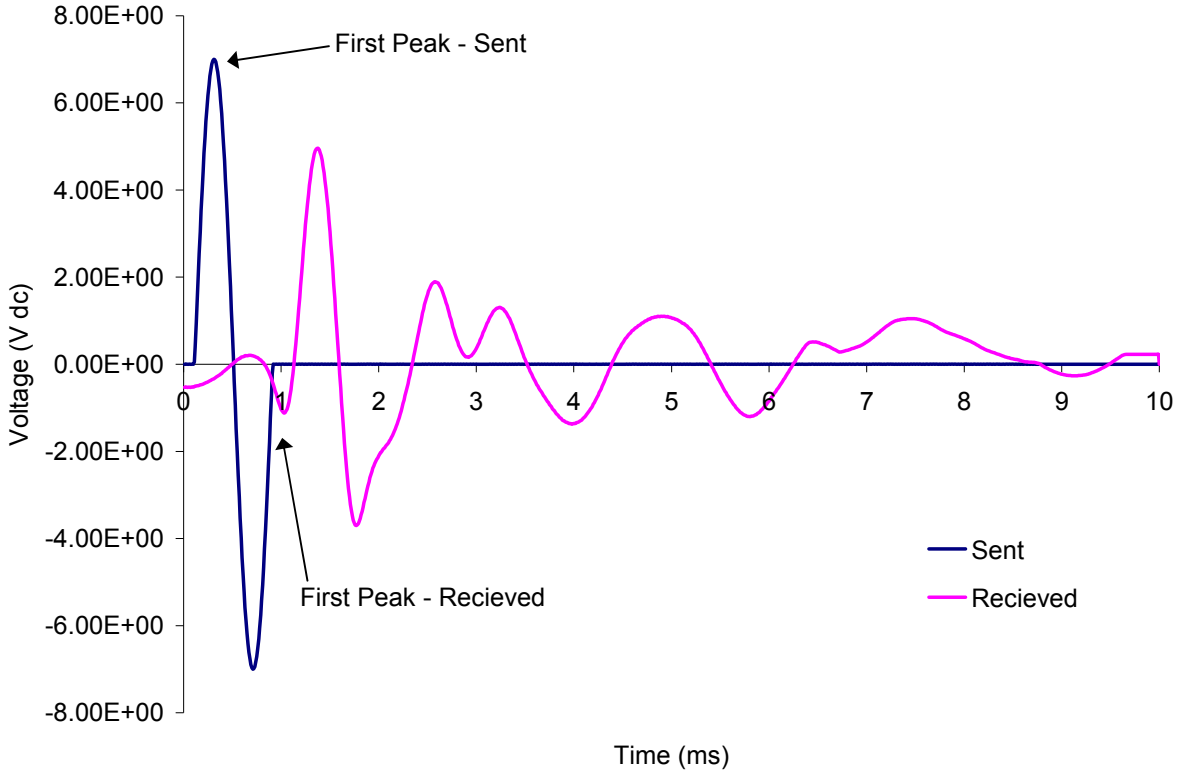

Figure 3.12. Typical bender element shear wave trace (Florence 3.5-5.5 ft).

Shear wave arrivals were determined both before and after each resilient modulus test segment to account for any plastic deformation during testing and the results averaged to determine the shear wave velocity at a given confining pressure. Opposite polarities seen in Figures 3.11 and 3.12 are due to the orientation of the bender elements with respect to each other; rotating one bender element by 180 degrees would result in traces of the same polarity. The shear modulus was again determined using Equation 3.2.

The shear modulus, as determined from both the CPT and bender element tests, were generally found to agree for moduli below 100 MPa (14,504 psi) (Table 3.4 and Figure 3.13). The outlier apparent in Figure 3.13 may be the result of significant variation in higher clay content and lower sand content as compared to the remaining, fairly consistent, samples (Table 3.1).

Table 3.4. Shear moduli as determined by both CPT and bender element testing.

	Forest Lake 13.5-15.5	Forest Lake 18.5-20.5	Florence 8.5-10.5	Florence 13.5-15.5	Owatonna 3.5-5.5	Owatonna 8.5-10.5	Owatonna 13.5-15.5
Confining Pressure (psi)	5.18	6.96	1.86	4.03	0.20	3.39	9.49
G_{scpt} (MPa)	72	288	29	43	61	198	94
G_{bender} (MPa)	79	86	30	195	38	91	61

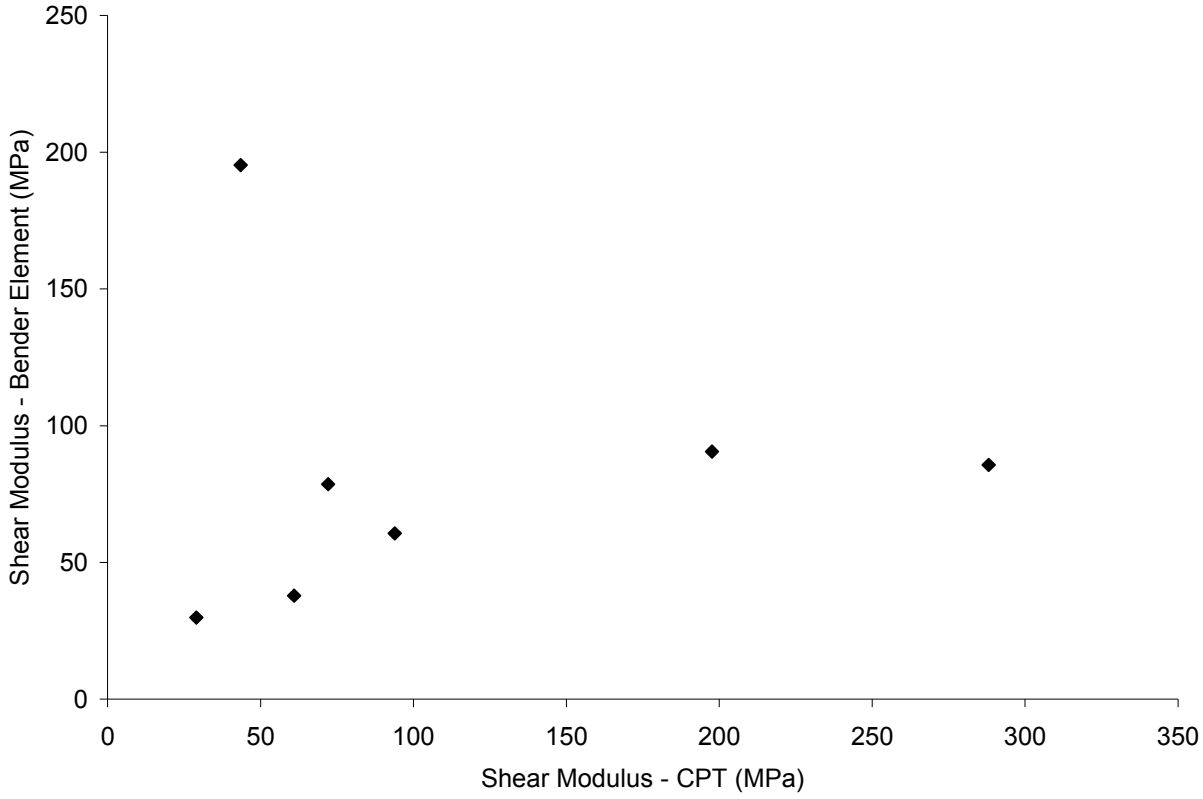

Figure 3.13. Shear moduli as determined by CPT and bender element testing.

To determine the Young's modulus from the shear modulus measured by both CPT seismic and bender element testing, the Poisson's ratio for each specimen is required. This would normally be determined using the compression wave velocities as determined via either compression wave CPT seismic soundings (using properly equipped CPT rigs) or bender element testing. However, as neither method was consistently reliable during the course of this testing, the compression wave velocity was determined using an ultrasonic bench; compression waves were sent and received via flat bender elements applied to each end of the specimen and recorded using an oscilloscope. The Poisson's ratio was calculated by:

$$\upsilon = \frac{1}{2} \cdot \frac{\left(\frac{V_p}{V_s}\right)^2 - 2}{\left(\frac{V_p}{V_s}\right)^2 - 1} \tag{3.3}$$

For those cases where compression waves were successfully transmitted via bender element testing (Figure 3.10), the velocity, as measured using that method, was used in calculating the Poisson's ratio. If no seismic method was able to provide a compression wave velocity, a value of 0.3 was assumed for Poisson's ratio. Table 3.5 shows Poisson's ratio for each specimen.

Table 3.5. Poisson's ratios (a = assumed).

Forest Lake 13.5-15.5	Forest Lake 18.5-20.5	Florence 3.5-5.5	Florence 8.5-10.5	Florence 13.5-15.5	Owatonna 3.5-5.5	Owatonna 8.5-10.5	Owatonna 13.5-15.5
0.3 (a)	0.3 (a)	0.20	0.19	0.25	0.05	0.30 (a)	0.44

From the Poisson's ratio, υ, and shear modulus, G, the Young's modulus, E, was determined:

$$E = 2G \cdot (\upsilon + 1) \tag{3.4}$$

Tables 3.6 and 3.7 show the Young's moduli for both field and laboratory seismic testing.

Table 3.6. Young's moduli as determined by field seismic testing.

	Forest Lake 13.5-15.5	Forest Lake 18.5-20.5	Florence 8.5-10.5	Florence 13.5-15.5	Owatonna 3.5-5.5	Owatonna 8.5-10.5	Owatonna 13.5-15.5
E (MPa)	187.56	749.07	69.01	108.71	128.15	513.77	270.42

Table 3.7. Young's moduli as determined by laboratory bender element testing.

Young's Modulus (MPa)								
Confining Pressure	Florence			Owatonna			Forest Lake	
(psi)	3.5-5.5	8.5-10.5	13.5-15.5	3.5-5.5	8.5-10.5	13.5-15.5	13.5-15.5	18.5-20.5
0	160.37	57.55	323.23	73.23	146.90	125.65	125.84	157.59
8	209.35	57.31	477.33	100.51	240.32	170.38	208.52	230.07
6	197.88	63.95	467.63	100.51	251.29	170.38	214.37	233.40
4	197.88	90.84	458.23	92.02	233.40	170.38	192.40	205.71
2	189.89	71.85	415.23	88.60	208.68	158.95	161.30	197.55
8	215.45	45.08	458.23	99.50	251.29	170.38	208.52	226.80
6	206.38	99.94	423.33	105.71	271.31	157.16	220.45	217.39
4	206.38	48.91	530.63	100.51	230.07	170.38	220.45	205.71
2	187.32	52.03	440.28	86.16	220.45	157.16	167.31	189.88
8	203.50	56.36	449.13	99.50	251.29	174.44	200.23	208.52
6	206.38	59.74	508.28	106.81	255.11	164.51	205.71	230.07
4	206.38	53.72	477.33	91.16	255.11	155.40	192.40	200.23
2	192.48	82.11	440.28	84.59	214.37	158.95	169.36	185.02
8	197.88	97.79	458.23	93.81	271.31	164.51	205.71	233.40
6	192.48	91.77	530.63	98.51	275.60	162.63	194.95	202.93
4	197.88	96.75	487.33	92.93	259.01	155.40	187.43	202.93
2	203.50	78.21	423.33	86.16	214.37	155.40	171.50	185.02
0	187.22	67.88	700.28	83.48	202.93	142.24	150.18	161.23

Resilient modulus testing was performed on eight specimens in accordance with the testing schedule, described in Section 3.2.2. The resulting values were analyzed with respect to the minimum quality assurance/quality control requirement for specimen rotation during testing: rotation less than 0.04°. All resilient modulus tests were found to meet the maximum rotation standard. However, the specimen collected from 8.5 – 10.5 feet below grade at TH 14 in Florence was found to undergo excessive axial yielding during the final deviator stress state of resilient modulus testing (sequences 13-16).

Figures 3.14 and 3.15 show the results of a typical resilient modulus test plotted with respect to both deviator stress and confining pressure. As can be seen, the resilient moduli of the soils tested were found to be highly dependent upon deviator stress, and not particularly dependent upon changes in confining pressure. Resilient modulus was generally found to decrease with an increase in deviator stress. The remainder of the resilient modulus plots are included in Appendix J.

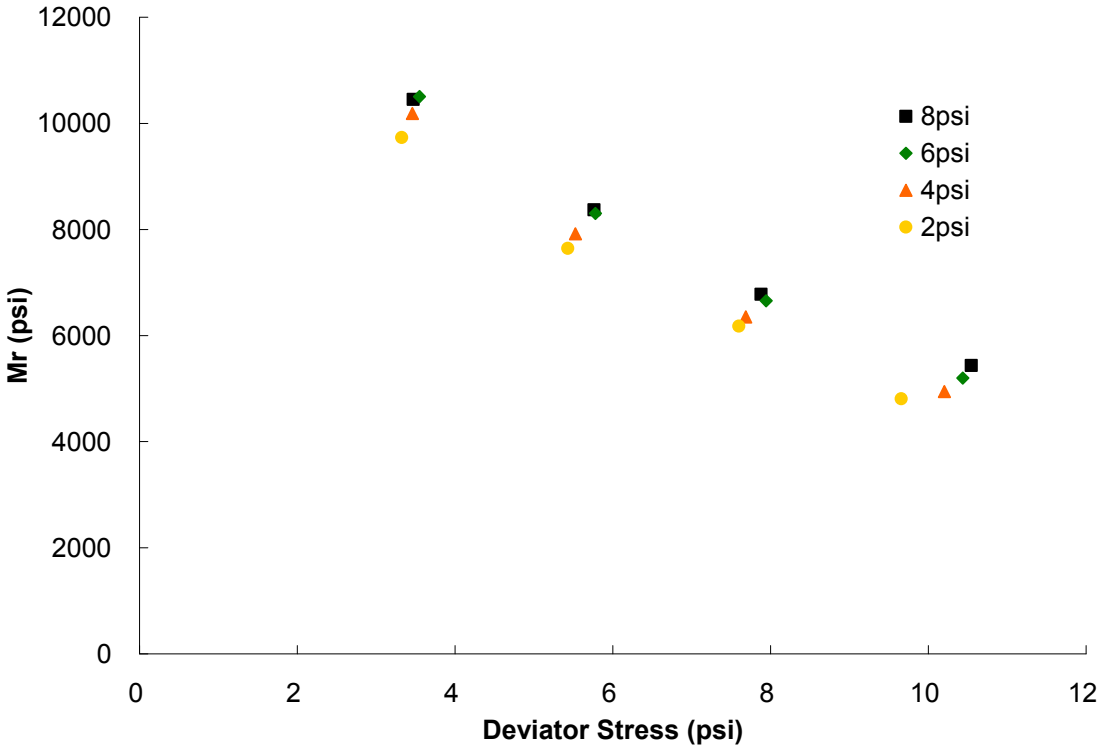

Figure 3.14. Typical plot of resilient modulus versus deviator stress (Florence 3.5-5.5 ft).

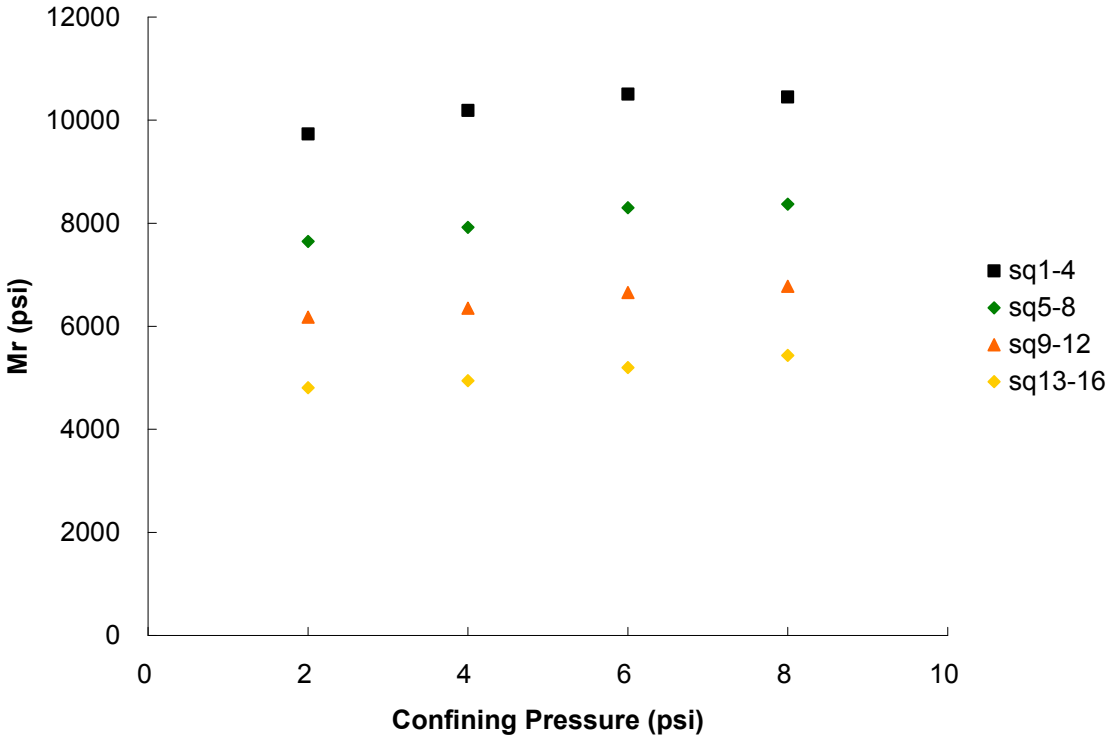

Figure 3.15. Typical plot of resilient modulus versus confining pressure (Florence 3.5-5.5 ft).

3.3.2 Correlation Analysis

The primary goal of this research was to look at the suitability of using small strain measurements of stiffness to estimate resilient modulus values of in situ soils. Accordingly, each of the three measurements of stiffness – CPT seismic (E_{scpt}), bender element (E_{bender}), and resilient modulus (M_R) – were plotted against each other to view their relationships, if any. In order to be consistent, the modulus values used should be representative of the same stress state (confining pressure and deviator stress).

Bender element testing is performed without application of axial stress, approximately at zero deviator stress. Therefore, the moduli for comparison were selected to represent the same confining stress. Each specimen was tested via both bender element and resilient modulus testing four times at each of four confining pressures (2, 4, 6, and 8 psi). The resilient modulus values were interpolated to represent the zero deviator stress state. A linear trendline was fit to each set of four resilient modulus values for a particular confining stress by least squares regression and projected to the zero deviator stress state. An example of this projection is shown in Figure 3.16. The resulting values of resilient modulus for each specimen at each of the four confining stresses is provided in Table 3.8.

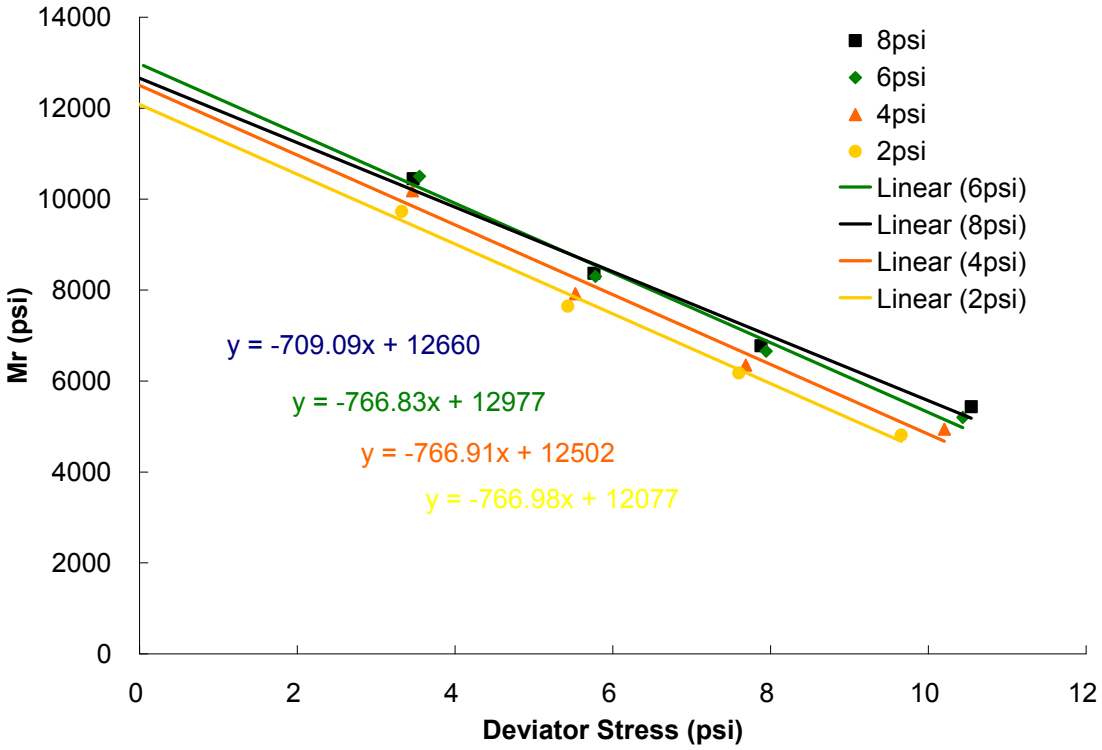

Figure 3.16. Linear projection of resilient modulus to zero deviator stress (Florence 3.5-5.5 ft).

Table 3.8. Resilient modulus values at zero deviator stress.

		Florence			Owatonna			Forest Lake	
Confining Pressure	**Depth (ft)**	**3.5-5.5**	**8.5-10.5**	**13.5-15.5**	**3.5-5.5**	**8.5-10.5**	**13.5-15.5**	**13.5-15.5**	**18.5-20.5**
8 psi	**Mr (psi)**	13287	3564	29040	4785	15583	5826	12536	10294
	Mr (MPa)	92	25	200	33	107	40	86	71
6 psi	**Mr (psi)**	13531	3013	31342	5197	11635	6430	10588	9930
	Mr (MPa)	93	21	216	36	80	44	73	68
4 psi	**Mr (psi)**	13186	3041	29898	4624	10819	5876	10241	9264
	Mr (MPa)	91	21	206	32	75	41	71	64
2 psi	**Mr (psi)**	12378	3061	28582	4786	9616	7136	8304	9812
	Mr (MPa)	85	21	197	33	66	49	57	68

Each of the resilient modulus values was plotted versus the corresponding maximum Young's modulus (Figure 3.17). The points separated from the main group are from Florence 13.5-15.5 and have a minus 10 classification of silty clay loam while the remainder are classified as only loam.

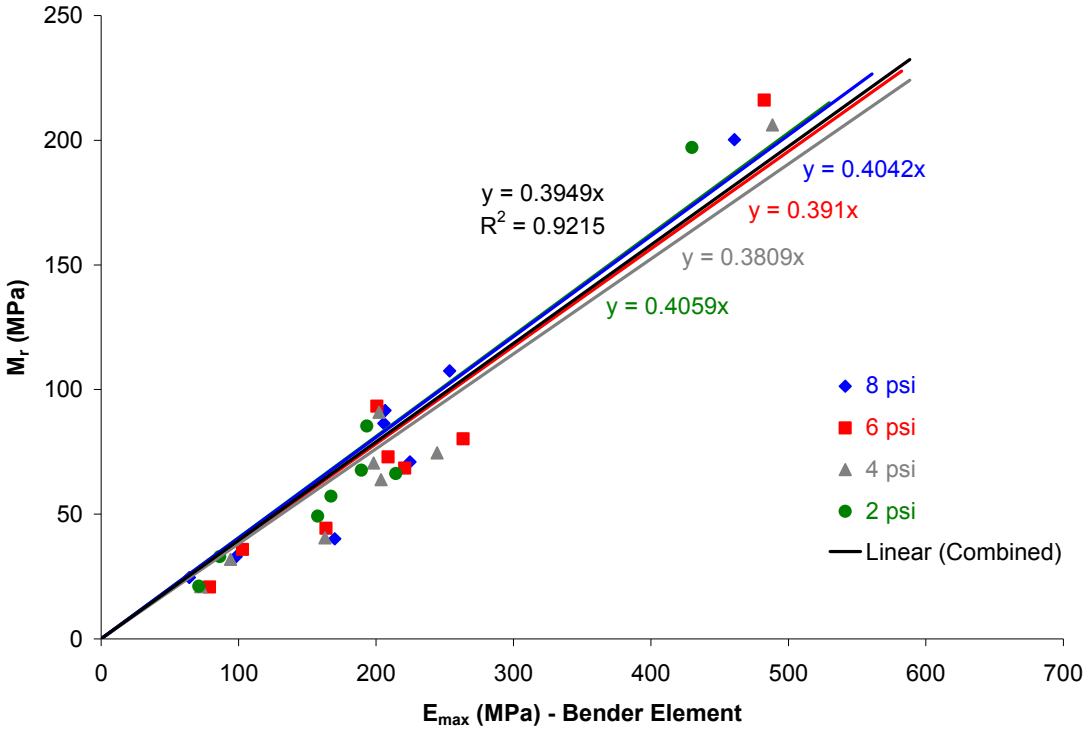

Figure 3.17. Resilient modulus versus maximum Young's modulus (bender element).

As can be seen, the resilient and Young's moduli from bender element testing appear to be related (M_R = 40%E_{max}) in a consistent manner for each of the specimens and confining pressures tested. This is in agreement with existing research by Hardin and Drnevich (1972), Prevost and Keane (1990), Shibuya et al. (1999), and Davich et al. (2004) – among others – showing that a soil's modulus generally decreases with an increase in strain during testing.

Best fit lines (in a least squares sense) show M_R as ranging from approximately 38 – 41% of the maximum Young's modulus. Combining all data points results in a best fit line showing M_R as approximately 40% of the Emax with an R^2 value of 0.92, indicating a reasonably consistent relationship between Young's modulus as determined by both bender element and resilient modulus testing. Though promising, these results may not translate well for seismic tests performed in the field.

The 40% reduction in modulus obtained above was compared to the soil modulus reduction method used by Mn/DOT from Fahey (1998) and Mayne (2006):

$$\frac{E_{reduced}}{E_{max}} = 1 - f(FS)^{-g} \tag{3.5}$$

where FS = factor of safety, f = correction factor, and g = correction factor.

Assuming f and g are equal to 1 and 0.3, respectively (Mayne 2006), the equivalent factor of safety for a reduced modulus of 40% the maximum modulus is approximately 5.5.

In comparing the maximum Young's modulus as obtained in the laboratory to that obtained in the field it was necessary to interpolate, or extrapolate as the case may be, the E_{max} as measured via bender element testing to the confining pressure of the in situ specimen. Prior to extrapolation, the in situ confining stress was determined using the relationship:

$$\sigma_c = \gamma \cdot z \cdot K_0 \tag{3.6}$$

where the unit weight of the overburden, γ, was assumed to be 120 pcf (from Mn/DOT CPT analysis software), z is the depth to the middle of the Shelby tube sample, and K_0 is defined in terms of Poisson's ratio by:

$$K_0 = \frac{\upsilon}{1 - \upsilon} \tag{3.7}$$

yielding the confining pressures and interpolated maximum Young's moduli shown in Table 3.9.

Table 3.9. In situ confining pressures and interpolated Young's moduli.

	Forest Lake 13.5-15.5	Forest Lake 18.5-20.5	Florence 8.5-10.5	Florence 13.5-15.5	Owatonna 3.5-5.5	Owatonna 8.5-10.5	Owatonna 13.5-15.5
v	0.3	0.3	0.19	0.25	0.05	0.30	0.44
K_0	0.43	0.43	0.23	0.33	0.05	0.43	0.79
σ_c (psi)	5.18	6.96	1.86	4.03	0.20	3.39	9.49
E (MPa) CPT Seismic	188	749	69	109	128	514	270
Mr (MPa) @ In Situ σ_c	38	34	12	124	24	57	45
E (MPa) Bender @ In Situ σ_c	72	70	21	206	34	72	37

The two values of E_{max} were plotted against each other (Figure 3.18).

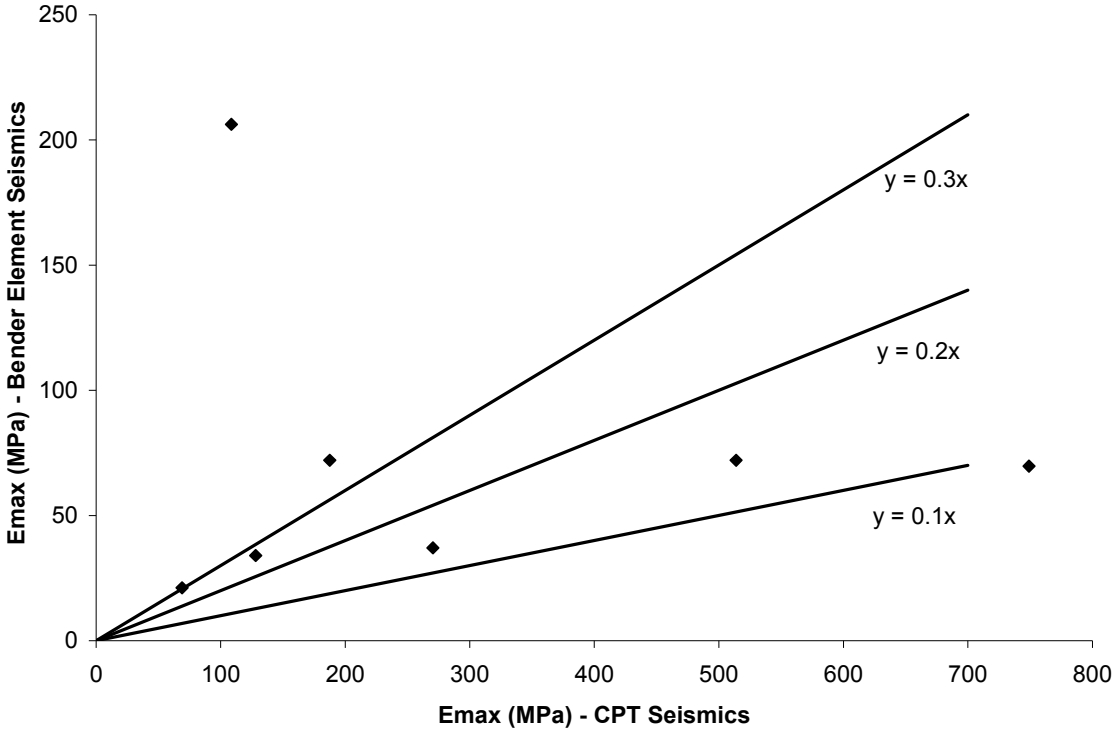

Figure 3.18. E_{bender} versus E_{scpt}.

Though both values are measured within the same range of strain (small strain seismic measurements), errors introduced in the field, likely due to inconsistencies in soil and rock distribution, resulted in poor agreement between field and laboratory values of maximum Young's modulus. Of course, this poor agreement was found to translate to the comparison of field maximum Young's modulus and laboratory resilient modulus as well (Figure 3.19).

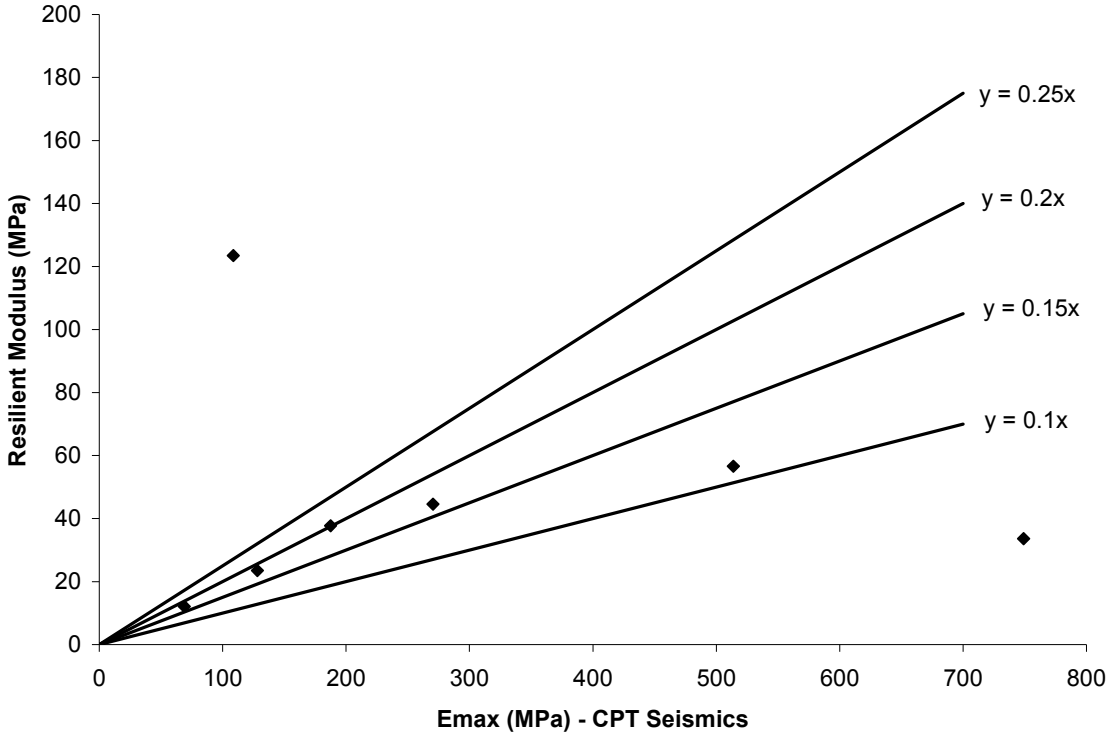

Figure 3.19. Resilient modulus versus field E_{scpt}.

As is apparent in Figure 3.19, however, there does appear to be a relationship within select data points. In addition, the reduction to approximately 20% of the maximum modulus appears to be in reasonable agreement with that obtained by the method accepted by Mn/DOT, described previously, under which a reduction to 20% would be equivalent to a factor of safety of approximately 2.1.

Chapter 4
Modelling of Organic Content

As stated in Section 1.1, two areas of CPT use where little research has been done include the prediction of resilient modulus, discussed in Chapter 3, and organic content. The existing type of CPT soil classification, based upon behavior, is not acceptable when attempting to identify soils with problematically high organic contents. In this case, actual identification of soil makeup is critical, as misinterpreting an organic soil as high plasticity clay, or vise versa, could result in large design and construction overruns. For example, the calculated settlement for a given foundation may vary significantly depending upon the possible consolidation of a highly organic soil layer. In situations such as this, it is important to know not only the soil behavior type, but the organic content.

The Minnesota Department of Transportation (Mn/DOT) has found it difficult to discern between soft clays, sensitive soils, and organic rich soils. This is shown by the disagreement between SPT Boring T20 and CPT Sounding c203a from Trunk Highway 23, provided for use in this analysis by Mn/DOT, where the CPT Sounding misidentifies the soils from 15 to 30 feet below the ground surface as consisting of clays and silt mixtures while the SPT Boring correctly identifies them as partially decomposed peat (Appendix A).

The focus of research presented in this chapter was to develop a model to assist in predicting whether or not a particular soil has a problematic organic content, defined as greater than 10% organics by Mn/DOT (Lamb 2006). The resulting model would give Mn/DOT the ability to make more informed judgments with regard to problematic soils when encountered. The analysis described in this chapter was performed on existing CPT soundings and their accompanying SPT borings, provided by Mn/DOT, using MatLAB statistical analysis software.

This analysis compares the feasibility of two model types, both of which will be described in detail in the section entitled *Statistical Analysis Background*. The first model is based upon a discriminate analysis in which the primary goal was to define a plane dividing those soils of organic content greater than 10% from those of organic content less than 10%. The second model was based upon a regression through which the goal was to predict the actual organic content of any soil and consequently whether or not the soil is above the problematic organic content threshold of 10%.

4.1 Data Preparation

Data was provided by Mn/DOT in the form of both SPT Boring logs and CPT Sounding results for Boring/Sounding pairs from across four project sites: Trunk Highways 19 (Scott/Le Sueur Co.), 23 (Kandiyohi Co.), 169 (Faribault Co.), and 241 (Wright Co.). From these sites the data from Trunk Highway 169 was set aside for use as a secondary model verification data set. The remaining data set was narrowed down to eleven adjacent SPT boring/CPT sounding pairs. Within each pair the data set was further refined by creating one datum point for each organic content test performed, resulting in 65 data points:

Table 4.1. Data set as provided by Mn/DOT consisting of 65 uncorrected data points where % Org is the organic content, qc the uncorrected tip resistance, qt the corrected tip resistance, f_s the uncorrected sleeve friction, u_2 the measured pore water pressure, σ_{vo} the overburden stress, and σ'_{vo} the effective overburden stress.

Project	SPT Boring #	Boring Depth (ft)	Primary Classification	% Org	CPT Sounding #	CPT Depth (ft)	q_c (psi)	f_s (psi)	q_t (psi)	u_2 (psi)	σ_{vo} (psi)	σ'_{vo} (psi)
TH 19	T23	14 - 16	slorg CL	3.2	C36	14 - 16	208.835	12.632	208.446	-1.930	12.494	5.996
TH19	T23	41.5 - 43.5	horg slpl SiL	16.1	C36	41.5 - 43.5	137.274	6.931	143.817	32.340	35.419	17.002
TH19	T23	51 - 53	horg slpl SiL	26.1	C36	51 - 53	117.008	5.088	126.004	44.397	43.322	20.794
TH19	T23	59 - 61	org Silt	9.5	C36	59 - 61	98.636	3.009	109.380	52.885	50.024	24.011
TH19	T23	61 - 63	org Silt	10.4	C36	61 - 63	108.550	3.261	119.654	54.896	51.649	24.790
TH19	T35	36.7 - 37.4	org L	7.5	C113	36.7 - 37.4	271.280	11.249	272.760	7.273	30.854	14.811
TH19	T35	41.4 - 42.4	horg pl L	39.3	C113	41.4 - 42.4	220.279	14.359	222.550	11.217	34.964	16.784
TH23	T132	8.8 - 10.5	marly org CL	6	C32	9.9 - 11.6	67.258	0.106	70.384	15.396	8.978	4.309
TH23	T132	13.8 - 14.5	marl w/ org slpl SiL	6.7	C32	14.9 - 15.6	285.914	0.094	287.914	9.923	12.726	6.108
TH23	T132	14.5 - 15.5	marl w/ slorg Silt	5.5	C32	15.6 - 16.6	659.450	0.938	660.208	3.785	13.433	6.448
TH23	T19	11.0 - 13.0	slorg pl SiL	5.6	C307	11.0 - 13.0	135.579	4.901	141.571	29.567	9.961	4.782
TH23	T19	13.5 - 15.5	slorg pl SiL	2.5	C307	13.5 - 15.5	84.830	2.700	90.752	29.227	12.070	5.794
TH23	T19	16 - 18	slorg SiCL	3	C307	16 - 18	95.229	3.556	102.571	36.311	14.150	6.791
TH23	T19	18.5 - 20.5	slorg SiCL	3.5	C307	18.5 - 20.5	49.279	2.912	52.254	14.693	16.259	7.804
TH23	T21	28.5 - 30.5	Well decomposed peat	8.9	C204	28.5 - 30.5	418.352	0.909	422.236	19.186	24.563	11.789
TH23	T33	18.7 - 20.0	marly org SiCL	9.9	C19	18.4 - 19.7	90.073	2.513	96.107	29.842	15.889	7.627
TH23	T33	22 - 23	horg slpl SiL	20.5	C19	21.7 - 22.7	139.664	9.106	142.818	15.457	18.516	8.888
TH23	T33	23.5 - 25.5	horg slpl SiL	10.6	C19	23.2 - 25.2	138.884	8.981	142.500	17.787	20.148	9.671
TH241	B1	1.0 - 2.0	horg slpl SiL	24.6	C04	1.0 - 2.0	209.375	1.481	211.494	10.504	1.218	0.585
TH241	B1	2 - 3.5	horg slpl SiL	15.7	C04	2 - 3.5	-2.304	1.784	-2.513	-0.791	2.279	1.094
TH241	B1	4.5 - 6	horg slpl SiL	22.7	C04	4.5 - 6	6.043	3.339	7.017	4.811	4.353	2.089
TH241	B1	7.0 - 9.0	horg slpl SiL	22.1	C04	7.0 - 9.0	19.310	5.053	20.548	6.020	6.621	3.178
TH241	B1	9.5 - 10	Well decompsed peat	30	C04	9.5 - 10	12.250	4.190	13.913	8.041	8.109	3.892
TH241	B1	10 - 11.0	horg slpl SiL	21.5	C04	10 - 11.0	11.200	3.491	13.373	10.629	8.739	4.195
TH241	B1	12.0 - 14	horg slpl SiL	17.4	C04	12.0 - 14	9.114	2.720	11.817	13.463	10.845	5.205
TH241	B1	14.5 - 16	horg slpl SiL	11.9	C04	14.5 - 16	10.260	2.330	13.645	16.839	12.725	6.108
TH241	B1	17 - 19	horg slpl SiL	11.5	C04	17 - 19	6.634	2.077	10.431	18.819	14.964	7.183
TH241	B1	19.5 - 21	horg slpl SiL	9.1	C04	19.5 - 21	2.381	1.852	6.619	21.081	16.862	8.094
TH241	B1	22 - 24	horg slpl SiL	10.4	C04	22 - 24	7.667	2.302	12.633	24.601	19.179	9.206
TH241	B1	24.5 - 26	horg slpl SiL	9.7	C04	24.5 - 26	9.511	2.162	15.222	28.304	21.082	10.119
TH241	B1	27 - 29	horg slpl SiL	8	C04	27 - 29	8.043	2.043	14.532	32.020	23.336	11.201
TH241	B1	29.5 - 31	org pl SiL	9.6	C04	29.5 - 31	4.505	2.250	11.481	34.349	25.207	12.100
TH241	B1	32 - 34	org pl SiL	8.2	C04	32 - 34	17.133	2.338	24.303	35.444	27.500	13.200
TH241	B1	34.5 - 36	org pl SiL	7.3	C04	34.5 - 36	12.824	2.246	20.924	39.937	29.381	14.103
TH241	B1	39.5 - 41	org pl SiL	7.1	C04	39.5 - 41	23.938	2.376	32.833	43.844	33.505	16.082
TH241	B1	49.5 - 51	mixed slorg SiCL & CL	5.2	C04	49.5 - 51	938.700	4.585	942.360	18.157	41.870	20.098
TH241	B1	52 - 52.5	mixed slorg SiCL & CL	4.7	C04	52 - 52.5	721.389	3.479	725.600	20.746	43.537	20.898
TH241	B2	7.0 - 9.0	org C	4.9	C76	7.0 - 9.0	50.950	0.695	50.819	-0.565	6.614	3.175
TH241	B2	9.5 - 11	org C	3.6	C76	9.5 - 11	61.741	1.682	62.047	1.594	8.503	4.081
TH241	B2	12.0 - 14.0	org C	12	C76	12.0 - 14.0	56.168	1.498	57.008	4.302	10.827	5.197
TH241	B2	14.5 - 16	org C	10.7	C76	14.5 - 16	57.095	1.226	58.747	8.307	12.723	6.107
TH241	B2	17.0 - 19.0	org C	9.3	C76	17.0 - 19.0	59.782	1.097	62.755	15.581	15.061	7.230
TH241	B2	19.5 - 21	org C	11.8	C76	19.5 - 21	58.659	0.667	62.829	21.769	16.833	8.080
TH241	B2	22.0 - 24	org C	3.5	C76	22.0 - 24	111.732	0.545	115.424	19.134	19.146	9.190
TH241	B2	24.5 - 26.5	pl SL	1.9	C76	24.5 - 26.5	67.552	0.608	73.784	32.367	21.246	10.198
TH241	B2	29.5 - 31	C	5.2	C76	29.5 - 31	1459.916	5.582	1461.853	10.086	25.181	12.087
TH241	T1	24.5 - 26	horg pl SiL	17.7	C11	23.8 - 25.3	101.265	3.948	109.890	42.476	20.488	9.834
TH241	T1	29 - 31	horg marly slpl SiL	15.3	C11	28.3 - 30.3	112.900	5.557	120.597	37.854	24.431	11.727
TH241	T1	34 - 36	horg marly slpl SiL	11.5	C11	33.3 - 35.3	98.500	3.945	107.350	43.650	28.556	13.707
TH241	T1	39 - 41	org marly slpl SiL	7	C11	38.3 - 40.3	95.510	2.807	105.945	51.692	32.772	15.730
TH241	T1	44 - 46	slorg slpl SiL	4	C11	43.3 - 45.3	96.550	2.405	107.667	54.854	36.943	17.733
TH241	T2	1.6 - 2	org to slorg pl L	6.7	C77	1.6 - 2	142.233	6.950	142.317	0.403	1.502	0.721
TH241	T2	3.5 - 5.5	org to slorg pl L	6.6	C77	3.5 - 5.5	61.275	2.439	61.750	2.417	3.763	1.806
TH241	T2	5.5 - 7	org to slorg pl L	3.5	C77	5.5 - 7	48.286	1.265	48.959	3.323	5.215	2.503
TH241	T2	8.5 - 10.5	org lplp & pl SiL	8.2	C77	8.5 - 10.5	59.886	1.492	61.482	8.300	7.917	3.800
TH241	T2	11.0 - 13.0	org lplp & pl SiL	10.3	C77	11.0 - 13.0	64.737	2.185	66.844	10.842	9.909	4.756
TH241	T2	13.5 - 15.5	org lplp & pl SiL	11.3	C77	13.5 - 15.5	60.720	1.668	63.635	14.981	12.083	5.800
TH241	T2	16 - 18	org lplp & pl SiL	9.7	C77	16 - 18	62.818	1.503	66.486	18.928	14.155	6.794
TH241	T2	18.5 - 20.5	org lplp & pl SiL	4.6	C77	18.5 - 20.5	65.813	1.280	70.565	24.492	16.241	7.796
TH241	T2	21 - 23	org lplp & pl SiL	3.3	C77	21 - 23	75.214	0.563	80.582	27.772	18.412	8.838
TH241	T3	4.1 - 6	slorg slpl & pl SL & L	3.1	C78	4.1 - 6	60.836	2.920	60.843	0.033	4.195	2.014
TH241	T3	7.0 - 8.5	org pl & slpl SiL	5.5	C78	7.0 - 8.5	39.204	1.619	40.004	4.239	6.445	3.094
TH241	T3	9.0 - 11.0	org pl & slpl SiL	8.5	C78	9.0 - 11.0	61.400	2.593	62.178	4.033	8.292	3.980
TH241	T3	11.5 - 13.5	org pl & slpl SiL	7.8	C78	11.5 - 13.5	46.768	1.762	48.441	8.820	10.434	5.009
TH241	T3	14.0 - 16.0	LS	0.7	C78	14.0 - 16.0	238.077	2.012	240.569	12.964	12.569	6.033

For each datum point the organic content provided on the SPT Boring log was assumed to be the truth. The primary data provided by the CPT Sounding consisted of uncorrected tip resistance,

q_c, uncorrected sleeve friction, f_s, and measured pore water pressure, u_2. From this primary data the corrected tip resistance, q_t, was calculated:

$$q_t = q_c + (1 - a)u_2 \tag{4.1}$$

where the value of "a" is dependent upon the specific cone design (Robertson 1990).

Secondary data consisted of both the overburden stress, σ_{vo}, and the effective overburden stress σ'_{vo}. These secondary data are based entirely upon two assumptions resulting in stress values that do not necessarily represent the true in situ state of the soil:

i. overlying soils have a density (unit weight) of 1922 kg/m^3 (120 pcf)

ii. water table is at the soil surface (all soil is fully saturated)

Measuring the true unit weight of the entire soil column is not feasible and the assumption of 1922 kg/m^3 (120 pcf) is reasonable for most soils, not including organics. Therefore this assumption is valid if the organic soil of interest is not overlain by other organic soils. Measurement of the actual water table, however, is possible and was provided on the SPT boring logs. Accordingly, the data set was refined using the true water table to define u_0, the initial pore water pressure prior to intrusion:

Table 4.2. Data set as provided by Mn/DOT consisting of 65 data points corrected for initial pore water pressure, u_o, as determined from water table provided on SPT Boring logs.

Project	Boring #	Boring Depth (ft)	Primary Classification	CPT #	CPT Depth (ft)	CPT Mid-Depth (ft)	Water Table (ft)	%Org	q_c (psi)	f_s (psi)	q_t (psi)	u_o (psi)	u_2 (psi)	σ_{vo} (psi)	σ'_{vo} (psi)
TH 19	T23	14 - 16	slorg CL	C36	14 - 16	15.000	14.000	3.200	208.835	12.632	208.446	0.433	-1.930	12.500	12.067
TH19	T23	41.5 - 43.5	horg slpl SiL	C36	41.5 - 43.5	42.500	14.000	16.100	137.274	6.931	143.817	12.350	32.340	35.417	23.067
TH19	T23	51 - 53	horg slpl SiL	C36	51 - 53	52.000	14.000	26.100	117.008	5.088	126.004	16.467	44.397	43.333	26.867
TH19	T23	59 - 61	org Silt	C36	59 - 61	60.000	14.000	9.500	98.636	3.009	109.380	19.933	52.885	50.000	30.067
TH19	T23	61 - 63	org Silt	C36	61 - 63	62.000	14.000	10.400	108.550	3.261	119.654	20.800	54.896	51.667	30.867
TH19	T35	34.8 - 35.5	org L	C113	36.7 - 37.4	37.050	None	7.500	271.280	11.249	272.760	0.000	7.273	30.875	30.875
TH19	T35	39.5 - 40.5	horg pl L	C113	41.4 - 42.4	41.900	None	39.300	220.279	14.359	222.550	0.000	11.217	34.917	34.917
TH23	T132	8.8 - 10.5	marly org CL	C32	9.9 - 11.6	10.750	9.100	6.000	67.258	0.106	70.384	0.715	15.396	8.958	8.243
TH23	T132	13.8 - 14.5	marl w/ org slpl SiL	C32	14.9 - 15.6	15.250	9.100	6.700	285.914	0.094	287.914	2.665	9.923	12.708	10.043
TH23	T132	14.5 - 15.5	marl w/ slorg Silt	C32	15.6 - 16.6	16.100	9.100	5.500	659.450	0.938	660.208	3.033	3.785	13.417	10.383
TH23	T19	11.0 - 13.0	slorg pl SiL	C307	11.0 - 13.0	12.000	None	5.600	135.579	4.901	141.571	0.000	29.567	10.000	10.000
TH23	T19	13.5 - 15.5	slorg pl SiL	C307	13.5 - 15.5	14.500	None	2.500	84.830	2.700	90.752	0.000	29.227	12.083	12.083
TH23	T19	16 - 18	slorg SiCL	C307	16 - 18	17.000	None	3.000	95.229	3.556	102.571	0.000	36.311	14.167	14.167
TH23	T19	18.5 - 20.5	slorg SiCL	C307	18.5 - 20.5	19.500	None	3.500	49.279	2.912	52.254	0.000	14.693	16.250	16.250
TH23	T21	28.5 - 30.5	Well decomposed peat	C204	28.5 - 30.5	29.500	8.500	8.900	418.352	0.909	422.236	9.100	19.186	24.583	15.483
TH23	T33	18.7 - 20.0	marly org SiCL	C19	18.4 - 19.7	19.050	11.200	9.900	90.073	2.513	96.107	3.402	29.842	15.875	12.473
TH23	T33	22 - 23	horg slpl SiL	C19	21.7 - 22.7	22.200	11.200	20.500	139.664	9.106	142.818	4.767	15.457	18.500	13.733
TH23	T33	23.5 - 25.5	horg slpl SiL	C19	23.2 - 25.2	24.200	11.200	10.600	138.884	8.981	142.500	5.633	17.787	20.167	14.533
TH241	B1	1.0 - 2.0	horg slpl SiL	C04	1.0 - 2.0	1.500	11.800	24.600	209.375	1.481	211.494	0.000	10.504	1.250	1.250
TH241	B1	2 - 3.5	horg slpl SiL	C04	2 - 3.5	2.750	11.800	15.700	-2.304	1.784	-2.513	0.000	-0.791	2.292	2.292
TH241	B1	4.5 - 6	horg slpl SiL	C04	4.5 - 6	5.250	11.800	22.700	6.043	3.339	7.017	0.000	4.811	4.375	4.375
TH241	B1	7.0 - 9.0	horg slpl SiL	C04	7.0 - 9.0	8.000	11.800	22.100	19.310	5.053	20.548	0.000	6.020	6.667	6.667
TH241	B1	9.5 - 10	Well decompsed peat	C04	9.5 - 10	9.750	11.800	30.000	12.250	4.190	13.913	0.000	8.041	8.125	8.125
TH241	B1	10 - 11.0	horg slpl SiL	C04	10 - 11.0	10.500	11.800	21.500	11.200	3.491	13.373	0.000	10.629	8.750	8.750
TH241	B1	12.0 - 14	horg slpl SiL	C04	12.0 - 14	13.000	11.800	17.400	9.114	2.720	11.817	0.520	13.463	10.833	10.313
TH241	B1	14.5 - 16	horg slpl SiL	C04	14.5 - 16	15.250	11.800	11.900	10.260	2.330	13.645	1.495	16.839	12.708	11.213
TH241	B1	17 - 19	horg slpl SiL	C04	17 - 19	18.000	11.800	11.500	6.634	2.077	10.431	2.687	18.819	15.000	12.313
TH241	B1	19.5 - 21	horg slpl SiL	C04	19.5 - 21	20.250	11.800	9.100	2.381	1.852	6.619	3.662	21.081	16.875	13.213
TH241	B1	22 - 24	horg slpl SiL	C04	22 - 24	23.000	11.800	10.400	7.667	2.302	12.633	4.853	24.601	19.167	14.313
TH241	B1	24.5 - 26	horg slpl SiL	C04	24.5 - 26	25.250	11.800	9.700	9.511	2.162	15.222	5.828	28.304	21.042	15.213
TH241	B1	27 - 29	horg slpl SiL	C04	27 - 29	28.000	11.800	8.000	8.043	2.043	14.532	7.020	32.020	23.333	16.313
TH241	B1	29.5 - 31	org pl SiL	C04	29.5 - 31	30.250	11.800	9.600	4.505	2.250	11.481	7.995	34.349	25.208	17.213
TH241	B1	32 - 34	org pl SiL	C04	32 - 34	33.000	11.800	8.200	17.133	2.338	24.303	9.187	35.444	27.500	18.313
TH241	B1	34.5 - 36	org pl SiL	C04	34.5 - 36	35.250	11.800	7.300	12.824	2.246	20.924	10.162	39.937	29.375	19.213
TH241	B1	39.5 - 41	org pl SiL	C04	39.5 - 41	40.250	11.800	7.100	23.938	2.376	32.833	12.328	43.844	33.542	21.213
TH241	B1	49.5 - 51	mixed slorg SiCL & CL	C04	49.5 - 51	50.250	11.800	5.200	938.700	4.585	942.360	16.662	18.157	41.875	25.213
TH241	B1	52 - 52.5	mixed slorg SiCL & CL	C04	52 - 52.5	52.250	11.800	4.700	721.389	3.479	725.600	17.528	20.746	43.542	26.013
TH241	B2	7.0 - 9.0	org C	C76	7.0 - 9.0	8.000	21.500	4.900	50.950	0.695	50.819	0.000	-0.565	6.667	6.667
TH241	B2	9.5 - 11	org C	C76	9.5 - 11	10.250	21.500	3.600	61.741	1.682	62.047	0.000	1.594	8.542	8.542
TH241	B2	12.0 - 14.0	org C	C76	12.0 - 14.0	13.000	21.500	12.000	56.168	1.498	57.008	0.000	4.302	10.833	10.833
TH241	B2	14.5 - 16	org C	C76	14.5 - 16	15.250	21.500	10.700	57.095	1.226	58.747	0.000	8.307	12.708	12.708
TH241	B2	17.0 - 19.0	org C	C76	17.0 - 19.0	18.000	21.500	9.300	59.782	1.097	62.755	0.000	15.581	15.000	15.000
TH241	B2	19.5 - 21	org C	C76	19.5 - 21	20.250	21.500	11.800	58.659	0.667	62.829	0.000	21.769	16.875	16.875
TH241	B2	22.0 - 24	org C	C76	22.0 - 24	23.000	21.500	3.500	111.732	0.545	115.424	0.650	19.134	19.167	18.517
TH241	B2	24.5 - 26.5	pl SL	C76	24.5 - 26.5	25.500	21.500	1.900	67.552	0.608	73.784	1.733	32.367	21.250	19.517
TH241	B2	29.5 - 31	C	C76	29.5 - 31	30.250	21.500	5.200	1459.916	5.582	1461.853	3.792	10.086	25.208	21.417
TH241	T1	24.5 - 26	horg pl SiL	C11	23.8 - 25.3	24.550	13.800	17.700	101.265	3.948	109.890	4.658	42.476	20.458	15.800
TH241	T1	29 - 31	horg marly slpl SiL	C11	28.3 - 30.3	29.300	13.800	15.300	112.900	5.557	120.597	6.717	37.854	24.417	17.700
TH241	T1	34 - 36	horg marly slpl SiL	C11	33.3 - 35.3	34.300	13.800	11.500	98.500	3.945	107.350	8.883	43.650	28.583	19.700
TH241	T1	39 - 41	org marly slpl SiL	C11	38.3 - 40.3	39.300	13.800	7.000	95.510	2.807	105.945	11.050	51.692	32.750	21.700
TH241	T1	44 - 46	slorg slpl SiL	C11	43.3 - 45.3	44.300	13.800	4.000	96.550	2.405	107.667	13.217	54.854	36.917	23.700
TH241	T2	1.6 - 2	org to slorg pl L	C77	1.6 - 2	1.800	12.700	6.700	142.233	6.950	142.317	0.000	0.403	1.500	1.500
TH241	T2	3.5 - 5.5	org to slorg pl L	C77	3.5 - 5.5	4.500	12.700	6.600	61.275	2.439	61.750	0.000	2.417	3.750	3.750
TH241	T2	5.5 - 7	org to slorg pl L	C77	5.5 - 7	6.250	12.700	3.500	48.286	1.265	48.959	0.000	3.323	5.208	5.208
TH241	T2	8.5 - 10.5	org lplp & pl SiL	C77	8.5 - 10.5	9.500	12.700	8.200	59.886	1.492	61.482	0.000	8.300	7.917	7.917
TH241	T2	11.0 - 13.0	org lplp & pl SiL	C77	11.0 - 13.0	12.000	12.700	10.300	64.737	2.185	66.844	0.000	10.842	10.000	10.000
TH241	T2	13.5 - 15.5	org lplp & pl SiL	C77	13.5 - 15.5	14.500	12.700	11.300	60.720	1.668	63.635	0.780	14.981	12.083	11.303
TH241	T2	16 - 18	org lplp & pl SiL	C77	16 - 18	17.000	12.700	9.700	62.818	1.503	66.486	1.863	18.928	14.167	12.303
TH241	T2	18.5 - 20.5	org lplp & pl SiL	C77	18.5 - 20.5	19.500	12.700	4.600	65.813	1.280	70.565	2.947	24.492	16.250	13.303
TH241	T2	21 - 23	org lplp & pl SiL	C77	21 - 23	22.000	12.700	3.300	75.214	0.563	80.582	4.030	27.772	18.333	14.303
TH241	T3	4.1 - 6	slorg slpl & pl SL & L	C78	4.1 - 6	5.050	10.300	3.100	60.836	2.920	60.843	0.000	0.033	4.208	4.208
TH241	T3	7.0 - 8.5	org pl & slpl SiL	C78	7.0 - 8.5	7.750	10.300	5.500	39.204	1.619	40.004	0.000	4.239	6.458	6.458
TH241	T3	9.0 - 11.0	org pl & slpl SiL	C78	9.0 - 11.0	10.000	10.300	8.500	61.400	2.593	62.178	0.000	4.033	8.333	8.333
TH241	T3	11.5 - 13.5	org pl & slpl SiL	C78	11.5 - 13.5	12.500	10.300	7.800	46.768	1.762	48.441	0.953	8.820	10.417	9.463
TH241	T3	14.0 - 16.0	LS	C78	14.0 - 16.0	15.000	10.300	0.700	238.077	2.012	240.569	2.037	12.964	12.500	10.463

Existing CPT/soil behavior type correlations are based upon three parameters: the corrected friction ratio, R_f, pore pressure ratio, B_q, and normalized cone resistance, Q_t, defined by Equations 4.2 – 4.4 (Robertson 1990):

$$R_f = \frac{f_s}{q_t - \sigma_{vo}} \cdot 100\% \tag{4.2}$$

$$B_q = \frac{u_2 - u_0}{q_t - \sigma_{vo}} \tag{4.3}$$

$$Q_t = \frac{q_t - \sigma_{vo}}{\sigma'_{vo}} \tag{4.4}$$

As these parameters have already been found to accurately classify soil behavior type based upon CPT data, shown by wide acceptance in the engineering community, it made sense to include them as possible parameters for the models. The remainder of the possible parameters included each of the parameters previously defined – q_c, f_s, q_t, u_o, u_2, σ_{vo}, and σ'_{vo} – as well as du:

$$du = u_2 - u_0 \tag{4.5}$$

Although both principal component and correlation analyses were performed, the process of narrowing down the parameters was highly guided by physical meaning.

The results of the principal component analysis of the z-score of the possible parameters – normalized parameters achieved by subtracting the mean and dividing by the standard deviation (MathWorks 2000) – indicated that the spread of the data could be accounted for by using a combination of independent variables representing three physical characteristics: confining pressure, end bearing, and a combination of sleeve friction and pore water pressure (Table 4.3).

Each column of numbers in Table 4.3 (principal component) represents the multiplier for the corresponding parameter (column 1). If multiplied out, the principal components approximate some form of the three physical conditions listed above. For the given data set any model should be able to adequately predict organic content using only three parameters, provided they are the correct parameters.

Table 4.3. Principal component analysis of the z-scores of the possible parameters.

	(PC1)	(PC2)	(PC3)	(PC4)	(PC5)	(PC6)	(PC7)	(PC8)	(PC9)	(PC10)	(PC11)
q_c (psi)	-0.0909	0.5726	0.0384	0.1401	-0.1784	-0.2884	0.1647	0.0009	-0.7076	-0.0000	-0.0000
f_s (psi)	-0.0778	0.2169	-0.1629	-0.7812	0.4505	-0.0456	0.3131	0.0835	-0.0001	0.0000	0.0000
q_t (psi)	-0.0966	0.5708	0.0371	0.1435	-0.1756	-0.2906	0.1682	0.0012	0.7066	0.0000	0.0000
R_f	0.2046	0.0510	-0.6593	0.1196	0.0186	0.0735	0.1397	-0.6937	-0.0001	0.0000	0.0000
u_o (psi)	-0.4250	0.0748	-0.0500	0.1514	-0.0980	0.6447	0.4024	0.1005	-0.0019	-0.2652	-0.3474
u_2 (psi)	-0.4270	-0.1955	-0.1003	0.2433	0.2278	-0.1511	0.2257	0.0325	-0.0039	0.7619	-0.0545
du (psi)	-0.3524	-0.2873	-0.1061	0.2432	0.3399	-0.4964	0.1031	-0.0050	-0.0042	-0.5903	0.0423
B_q	0.1934	0.0899	-0.6550	0.1710	0.0262	0.0149	-0.1474	0.6882	0.0001	0.0000	0.0000
σ_{vo} (psi)	-0.4627	0.1044	-0.1299	-0.0677	-0.1050	0.2394	-0.2272	-0.0402	-0.0006	-0.0233	0.7946
σ'_{vo} (psi)	-0.4292	0.1126	-0.1721	-0.2219	-0.0962	-0.0943	-0.6658	-0.1396	0.0005	0.0145	-0.4930
Q_t	0.1073	0.3724	0.1913	0.3329	0.7322	0.2713	-0.2948	-0.0764	0.0000	0.0000	-0.0000

The correlation analysis provided less insight, as the results showed primarily that the q_c and q_t as well as the σ_{vo} and σ'_{vo} parameter pairs were, as expected, highly correlated and redundant (represented by correlation values close to 1 in Table 4.4). Since both u_o and σ'_{vo} are independent of the soil type at the location of interest (they depend entirely upon the unit weight of the overlying soil and the location of the water table) they were removed from the list of possible parameters.

Table 4.4. Correlation analysis of the possible parameters, with percent organic content.

	q_c (psi)	f_s (psi)	q_t (psi)	u_2 (psi)	R_f	u_o (psi)	B_q	σ_{vo} (psi)	σ'_{vo} (psi)	Q_t	%Org
q_c (psi)	1.0000	0.1984	0.9999	-0.1124	-0.0316	0.2470	0.0380	0.2973	0.2952	0.4712	-0.1562
f_s (psi)	0.1984	1.0000	0.1979	-0.0663	0.0562	0.0530	0.0365	0.2566	0.3741	0.0466	0.3960
q_t (psi)	0.9999	0.1979	1.0000	-0.0993	-0.0349	0.2571	0.0349	0.3075	0.3042	0.4685	-0.1569
u_2 (psi)	-0.1124	-0.0663	-0.0993	1.0000	-0.2457	0.7330	-0.2363	0.7393	0.6457	-0.2538	-0.0409
R_f	-0.0316	0.0562	-0.0349	-0.2457	1.0000	-0.2570	0.9007	-0.2403	-0.1960	-0.0183	0.2515
u_o (psi)	0.2470	0.0530	0.2571	0.7330	-0.2570	1.0000	-0.2444	0.8966	0.7004	-0.0792	-0.0291
B_q	0.0380	0.0365	0.0349	-0.2363	0.9007	-0.2444	1.0000	-0.2120	-0.1598	0.0381	0.1221
σ_{vo} (psi)	0.2973	0.2566	0.3075	0.7393	-0.2403	0.8966	-0.2120	1.0000	0.9441	-0.1832	0.0365
σ'_{vo} (psi)	0.2952	0.3741	0.3042	0.6457	-0.1960	0.7004	-0.1598	0.9441	1.0000	-0.2363	0.0805
Q_t	0.4712	0.0466	0.4685	-0.2538	-0.0183	-0.0792	0.0381	-0.1832	-0.2363	1.0000	0.0408
%Org	-0.1562	0.3960	-0.1569	-0.0409	0.2515	-0.0291	0.1221	0.0365	0.0805	0.0408	1.0000

As was stated by both Olsen (1994) and Robertson (1990), the normalization of each of the raw CPT parameters, f_s, q_t, and d_u, with respect to the vertical effective stress is important as each of the three parameters increase with increasing depth. In addition, friction and bearing values should be corrected for pore water pressure when available, especially when penetrating fine grained soils that have the ability to generate high pore pressures without quick dissipation (Robertson and Campanella 1983). Based upon these statements, the normalized representations of the sleeve friction, end bearing, and pore water pressure (the corrected friction ratio R_f, the normalized cone resistance, Q_t, and the pore pressure ratio, B_q) were selected from the six remaining possible parameters, f_s, q_t, d_u, R_f, Q_t, and B_q, to be used as model parameters. One bonus resulting from this choice is that the normalized parameters are also dimensionless.

4.2 Statistical Analysis Background

As was stated previously, two types of analyses were performed: discriminate and linear regression. In a discriminate analysis a set of parameters are used to define a plane in space. This plane serves the purpose of dividing a data set into two groups based upon a value of interest, organic content, such that data points above a certain value are in one and those below are in the other. This value is defined as the threshold value. Linear regression is the traditional analysis method used to create basic predictive models. As with a discriminate analysis a set of parameters are used to define a line or plane in space. In this case, however, the line/plane defines the value of interest, organic content, for each data point as opposed to dividing the data set into groups. For example, a discriminate analysis model would predict whether or not a soil contained problematic organic contents; a regression analysis model would simply predict the actual organic content of each soil sample, based upon the independent variables.

More specifically, a discriminate analysis is used to determine an N-1 dimensional discriminating plane of the form:

$$y = a_1 + a_2 x_1 + a_3 x_2 + \ldots + a_N x_{N-1} \tag{4.6}$$

where the analysis returns the values, a_i. This plane, by definition, provides the most accurate classification of a single dependent variable with N-1 independent variables as either above or below a threshold value. In this case the three independent variables – x_1, x_2, and x_3 – were B_q,

R_f, and Q_t, respectively, while the dependent variable threshold was 10% organic content, yielding:

$$y = a_1 + a_2 B_q + a_3 R_f + a_4 Q_t \tag{4.7}$$

Again, regression analysis is considered the standard method of modeling both linear and non-linear data sets and produces a set of parameters used to predict the dependent variable, as opposed to the discriminate analysis which attempts to predict classification on one side of a threshold or another. The resultant least squares regression is therefore of the form:

$$y = b_1 x_1 + b_2 x_2 + \ldots + b_N x_N + b_{N+1} \tag{4.8}$$

where the analysis returns the values, b_i, for the prediction of a single dependant variable using N independent variables, x_i. As with the previous model the three independent variables – x_1, x_2, and x_3 – were B_q, R_f, and Q_t, respectively, while in this model the predicted dependent variable was organic content. By using the predicted values of organic content those soils with organic contents greater than 10% could be identified directly using:

$$y = b_1 B_q + b_2 R_f + b_3 Q_t + b_4 \tag{4.9}$$

4.3 Results & Discussion

The discriminate analysis was performed using the MatLAB function file DiscAn, Appendix B, that relies primarily upon the MatLAB function fmincon found in the MatLAB Optimization Toolbox. "fmincon finds the constrained minimum of a scalar function of several variables starting at an initial estimate" (Coleman et al. 1999). The scalar function to be minimized is described in the function file DiscOb (Appendix C) and is subject to two variables: theta and S_i:

$$\sum_{i=1}^{\text{datapoints}} \left(1 - e^{-\theta S_i}\right) \tag{4.10}$$

S_i is defined as the slack and is related to the number of misclassifications resulting from the calculated discriminating plane and is the variable minimized for a given value of theta (Barnes 2006):

$$\sum_{j=0}^{\text{parameters}} a_j y_i x_{ij} + S_i \geq 0 \qquad \forall_i = 1 \rightarrow \text{datapoints} \tag{4.11}$$

The optimum parameters were determined by running fmincon for multiple values of theta and selecting the theta that resulted in the minimum number of misclassifications.

The complete output of the discriminate analysis of the three parameters can be found in Appendix E. The results of the analysis indicated that the model provides accurate classification of organic soils as either greater or less than 10% organics approximately 72.3 % of the time with model parameters:

a_1 = -1.3814
a_2 = -0.4277
a_3 = 0.0710
a_4 = -0.0082

The range of the misclassified organic contents was from 10.4 % to 39.3 % indicating that the model, when wrong, underestimates the organic content (Figure 4.1). Note that if one simply assumed all soils had organic contents less than 10% they would be correct 63% of the time with this data set.

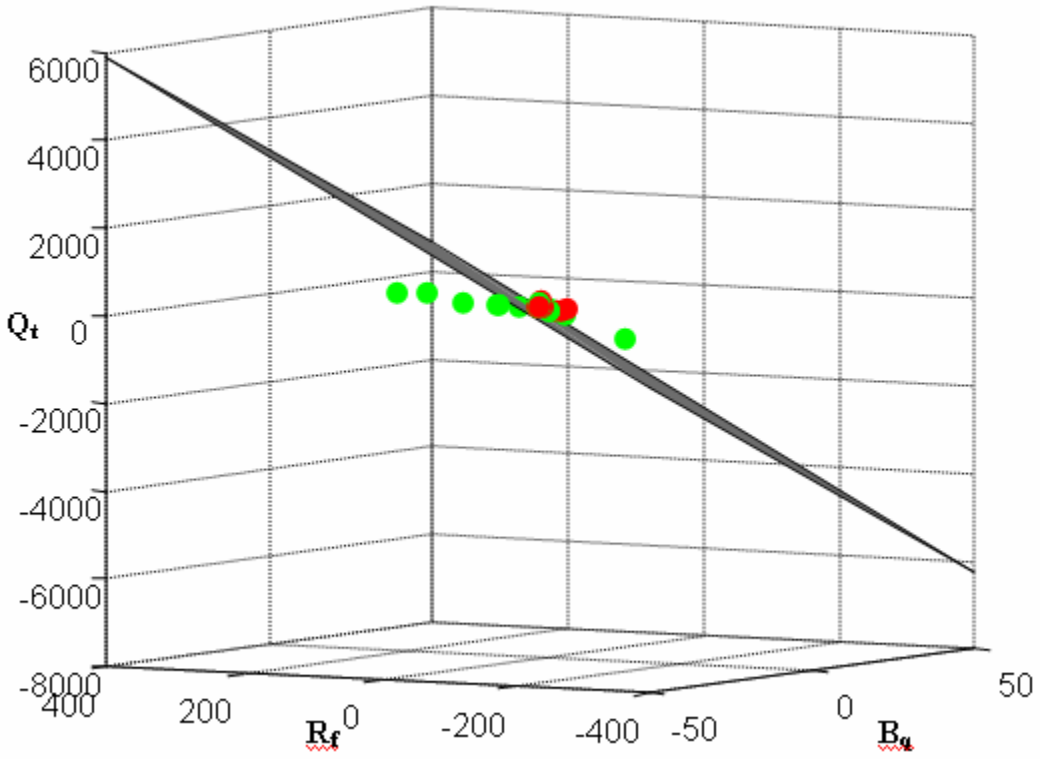

Figure 4.1. 3D plot of the discriminate model depicting the discriminating plane and each data point with green (light grey) points for correctly classified organic contents and red (dark grey) points for incorrectly classified organic contents.

The regression analysis is much simpler than the discriminate analysis and was performed using the standard MatLAB function file for non-linear regression, nlinfit, found in the MatLAB Statistics Toolbox (The Math Works 2000). The complete output of the non-linear regression can be found in Appendix F. The results of the analysis indicated that the model provides accurate classification of organic soils as either greater or less than 10% organics approximately 66.2 % of the time with model parameters:

$$b_1 = -0.6634$$
$$b_2 = 0.0833$$
$$b_3 = 0.0218$$
$$b_4 = 9.1605$$

In this case the range of the misclassified organic contents was found to be from 3.2 % to 39.3 %. However, only 4 of the 22 misclassifications were the result of overestimation of the organic content.

As shown by the percent correct classification above, 72.3 versus 66.2 percent, the discriminate model does a better job of predicting problematic organic content levels than the regression model for this primary data set. Testing this model with the secondary data set (Appendix G), set aside previously, however, does not yield the same results as the original data set with respect to the percent correctly classified. In this case, the model classified all of the data points as having organic contents less than 10%, and was only 57% correct. As before, note that if one assumed all soils had organic contents less than 10% they would be correct 57% of the time with this second data set.

The results of the secondary analysis indicate that the primary discriminate model proposed does not result in an advantage over guessing, and the decrease in misclassification for the first data set is due simply to the model being based upon that data set. This shows that the current model is not truly grounded in the underlying mechanical properties of the organic content in soil and as such is of no advantage. This result is most likely due to the limited size of the primary data set, and increasing the data set size would likely yield a more robust model. Though adding the primary and secondary data sets together and using the discriminate analysis tools to identify a new model would likely create a better model, it is not advantageous at this time as there is not currently any additional data available to test the resulting model. More data must first be collected.

In addition, is should be restated that it was assumed that in future explorations the true water table could be identified from the CPT data (possibly through analysis of either changes in pore water pressure or wave speed measurements), as using the previous assumption – of the water table at the soil surface – would likely result in a less representative model. One other source of error is the assumption of the unit weight of overlying soils being constant at 1922 kg/m^3 (120 pcf). Future models should address both of these issues through either direct measurement, development of correlations to values measurable by CPT, or, in the case of the unit weight, assumption of unit weights based upon the soil behavior type provided by existing CPT analysis tools.

The models proposed in this paper are based entirely upon identifying parameters that have some relationship with the underlying mechanical properties of the organic soil content. As such, identifying additional parameters that may better model the organic content should be a priority. Possible parameters that should be tested include the soils shear wave velocity and rate of pore water pressure dissipation (Robertson 1990).

Overall the analysis presented here shows that at this point the model identified using the discriminate analysis method is not currently sufficient to use in practice for identifying problematic organic soils. The 10% increase in correctly classified soils, however, holds promise for the future, and the introduction of additional independent parameters within a significantly larger data set can be easily analyzed using the methods and tools presented here.

Chapter 5
Summary

Through a combination of resilient modulus and bender element testing, it was shown that the use of small strain (seismic) measurements of material stiffness to estimate resilient modulus is feasible for the soil samples tested in the laboratory. The relationship between Young's modulus as determined by bender element testing (E_{bender}) and that determined by resilient modulus (M_R) testing was well described by $M_R = 40\%E_{bender}$. However, this relationship did not hold for field-based seismic measurements of stiffness. The cone penetration testing (CPT) seismic estimates of resilient modulus required a 10 – 20% reduction of E_{max}. Further work is needed to suggest an appropriate modulus reduction factor for CPT soundings.

Nonetheless, this simple method of predicting resilient modulus through seismic testing appears well grounded in existing research showing the possibility of estimating resilient modulus from small strain laboratory testing, and due to the simplicity of the model, further studies, on a larger scale, are recommended.

The analysis presented with respect to the identification of highly organic soils via CPT testing shows that at this point the model identified using the discriminate analysis method is not currently sufficient to use in practice. The 10% increase in correctly classified soils, however, holds promise for the future, and the introduction of additional independent parameters within a significantly larger data set can be easily analyzed using the methods and tools presented here.

References

Baig, S. and Nazarian, S. (1995), "Determination of Resilient Modulus of Subgrades Using Bender Elements," *Transportation Research Record* 1504, Washington, DC, 79-86.

Barnes, R. (2006), *CE 8361 – Engineering Model Fitting – Class Notes,* Minneapolis, MN: University of Minnesota, Department of Civil Engineering.

Barnes, R. (2006), Personal Communication, Minneapolis, MN: University of Minnesota, Department of Civil Engineering.

Coleman, T., Branch, M.A., and Grace, A. (1999), *Optimization Toolbox Users Guide, For Use with MatLAB, Version 2,* Natick, MA: The Math Works, Inc.

Davich, P., Labuz, J.F., Guzina, B., and Drescher, A. (2004), *Small Strain and Resilient Modulus Testing of Granular Soils,* Final Report 2004-39*,* St. Paul, MN: Minnesota Department of Transportation.

Duncan, J.M. and Buchignani, A.L. (1976), *An Engineering Manual for Settlement Studies,* Berkeley CA: University of California.

Egorov, K.E. (1965), "Calculation of Bed for Foundation with Ring Footing," *Proc. 6th Int. Conf. Soil Mechanics and Foundation Engineering*, vol. 2, 41-45.

Fahey, M. (1998), "Deformation and In Situ Stress Measurement," *Geotechnical Site Characterization*, P.K. Robertson and P. Mayne, eds., Balkema, Rotterdam, 49-68.

George, K.P. (2004), *Prediction of Resilient Modulus from Soil Index Properties*, *Final Report,* Jackson, Mississippi: Mississippi Department of Transportation.

Gudishala, R. (2004), *Development of Resilient Modulus Prediction Models for Base and Subgrade Pavement Layers From In Situ Devices Test Results, M.S. Thesis,* Louisiana State University and Agricultural and Mechanical College Department of Civil Engineering.

Hardin, B.O., and Richart, F.E., Jr. (1963), "Elastic Wave Velocities in Granular Soils," *Journal of the Soil Mechanics and Foundations Division, ASCE*, vol. 89, no. SM1, 33-65.

Hardin, B.O. and Drnevich, V.P. (1972), "Shear Modulus and Damping in Soils," *Journal of Soil Mechanics and Foundations Division, ASCE*, vol. 98, 603-624.

Harr, M.E. (1966), *Foundation of Theoretical Soil Mechanics,* McGraw-Hill.

Heukelom, W. and Klomp, A.J.G. (1962), "Dynamic Testing as a Means of Controlling Pavement during and after Construction, *Proc. 1st International Conference on the Structural Design of Asphalt Pavement*, Ann Arbor, MI: University of Michigan.

Lamb, R. (2006), Personal Communication, St. Paul, MN: Minnesota Department of Transportation.

Lings, M.L. and Greening, P.D. (2001), "A Novel Bender/Extender Element for Soil Testing," *Geotechnique*, vol. 51, no. 8, 713-717.

Mayne, P.W. (2006), *Enhanced In-Situ Testing for Geotechnical Site Characterization – Short Course Presentation*, Atlanta, GA: GT Global Learning Center.

Mohammad, L.N., Titi, H.H., and Herath, A. (2000), "Evaluation of Resilient Modulus of Subgrade Soil by Cone Penetration Test," *Transportation Research Record*, 1652, 236-245.

Olsen, R.S. (1994), *Normalization and Prediction of Geotechnical Properties Using the Cone Penetrometer Test (CPT),* U.S. Army Corps of Engineers Technical Report GL-94-29.

Powell, W.D., Potter, J.F., Mayhew, H.C., and Nunn, M.E. (1984), *The Structural Design of Bituminous Roads*, TRRL Report LR 1132.

Prevost, J.H. and Keane, C.M. (1990), "Shear Stress-Strain Curve Generation from Simple Material Parameters," *Journal of Geotechnical Engineering, ASCE*, vol. 116, no. 8, 1255-1263.

Robertson, P.K. (1990), "Soil Classification Using the Cone Penetration Test," *Canadian Geotechnical Journal*, vol. 27, 151-158.

Robertson, P.K. and Campanella, R.G. (1983), "Interpretation of Cone Penetration Tests – Part I (Sand)," *Canadian Geotechnical Journal*, vol. 20, no. 4, 718-733.

Robertson, P.K. and Campanella, R.G. (1983), "Interpretation of Cone Penetration Tests – Part II (Clay)," *Canadian Geotechnical Journal*, vol. 20, no. 4, 734-745.

Seed, H.B., Chan, C.K., and Lee, C.E. (1962), "Resilience Characteristics of Subgrade Soils and their Relation to Fatigue Failures in Asphalt Pavements, *Proc. 1st Int. Conf. Structural Design of Asphalt Pavement*, Ann Arbor, MI: University of Michigan.

Shibuya, S. (1998), "Characterizing Stiffness and Strength of Soft Bangkok Clay from In-Situ and Laboratory Tests," *Geotechnical Site Characterization*, P.K. Robertson and P. Mayne, eds., Balkema, Rotterdam, 1361-1366.

Shirley, D.J. and Hampton, L.D. (1978), "Shear-Wave Measurements in Laboratory Sediments," *Journal of the Acoustical Society of America*, vol. 63, no. 2, 607-613.

Siekmeier, J.A., Young, D., and Beberg, D. (1999), "Comparison of the Dynamic Cone Penetrometer with other Tests during Subgrade and Granular Base Characterization in Minnesota," *Nondestructive Testing of Pavements and Backcalculation of Moduli*, 3rd vol, ASTM STP 1375, West Conshonocken, PA, ASTM.

Swenson, J.N., Guzina, B.B., Labuz, J.F., and Drescher, A. (2006), *Moisture Effects on PVD and DCP Measurements,* Final Report 2006-26, St. Paul, MN: Minnesota Department of Transportation.

The Math Works (2000), *Statistics Toolbox Users Guide, For Use with MatLAB, Version 3* Natick, MA: The Math Works, Inc.

Thompson, M.R. and Robnett, Q.L. (1979, "Resilient Properties of Subgrade Soils," *Journal of Transportation Engineering*, *ASCE*, vol. 105, no. 1, 71-89.

Webster, S.L., Brown, R.W., and Porter, J.R. (1994), *Force Projection Site Evaluation Using the Electric Cone Penetrometer and the Dynamic Cone Penetrometer,* Technical Report GL-94-17, U.S. Waterways Experimental Station.

Witczak, M. (2002), *Recommended Standard Method for Routine Resilient Modulus Testing of Unbound Granular Base/Subbase Materials and Subgrade Soils*. National Cooperative Highway Research Program (NCHRP) Protocol 1-28A.

Appendix A

Boring Log T20 & Sounding Log c203a

Minnesota Trunk Highway 23 SPT Boring Log No. T20 and CPT Sounding Log c203a (Provided by Mn/DOT).

MINNESOTA DEPARTMENT OF TRANSPORTATION - GEOTECHNICAL SECTION
LABORATORY LOG & TEST RESULTS - SUBSURFACE EXPLORATION

UNIQUE NUMBER 58681

U.S. Customary Units

State Project	Bridge No. or Job Desc.	Trunk Highway/Location	Boring No.	Ground Elevation
3413-22	Roadway	23	T20	1166.1 (Survey)

Location: TH 23 EB,7987+94.6, 21.0,RT
Co. Coordinate: X=451068 Y=223710 (ft.)
Latitude (North)=45°13'49.83" Longitude (West)=94°56'23.68"

Drill Machine: 91286 CME 850 Track
Hammer: CME Automatic Calibrated
SHEET 1 of 2
Drilling Completed: 6/26/01

DEPTH	Depth / Elev.	Lithology	Classification	Drilling Operation	SPT N_{60} / REC (%)	MC (%) / RQD (%)	COH (psf) / ACL (ft)	γ (pcf) / Core Breaks	Soil / Rock	Other Tests Or Remarks / Formation or Member
	0		LS & G w/ CL seams, brn w/ dk brn, moist			18				
	3.8 / 1162.3									
	4.8 / 1161.3		pl SL, lt brn & moist			20				
5			slpl SL w/ pl L layer, seam slorg slpl L w/ a few pebbles; brn w/ dk brn, blk; moist		8	14				
	8.0 / 1158.1									
			LS & G, lt gray & wet		6	20				
10	11.5 / 1154.6				8	114				
						66	500	82		3 consolidation tests
15			partially decomposed Peat w/ shells, seam of semi-fibrous Peat @ 25.0'; gray-brn to gray; wet			68	690	81		3 consolidation tests
						61	610	89		3 consolidation tests
20						71	590	87		
						60	660	85		3 consolidation tests
25	25.0									

Index Sheet Code 3.0 (Continued Next Page)

Soil Class:DSB Rock Class: Edit: DMS Date: 4/4/06
G:\GEOTECH\GINTW\PROJECTS\3413B.GPJ

MINNESOTA DEPARTMENT OF TRANSPORTATION - GEOTECHNICAL SECTION
LABORATORY LOG & TEST RESULTS - SUBSURFACE EXPLORATION

UNIQUE NUMBER 58681

U.S. Customary Units

Mn/DOT GEOTECHNICAL SECTION - LOG & TEST RESULTS — *SHEET 2 of 2*

State Project	Bridge No. or Job Desc.	Trunk Highway/Location	Boring No.	Ground Elevation
3413-22	Roadway	23	T20	1166.1 (Survey)

DEPTH	Depth / Elev.	Lithology	Classification	Drilling Operation	SPT N_{60} / REC (%)	MC (%) / RQD (%)	COH (psf) / ACL (ft)	γ (pcf) / Core Breaks	Soil / Rock	Other Tests Or Remarks / Formation or Member
	1141.1									
			Well-decomposed Peat w/ few shells, dk gray & wet			62	820	85		
	28.5 / 1137.6									
			Well-decomposed Peat, lt grays & wet			57	920	88		
30	30.0 / 1136.1		horg SiCL w/ some partially-decomposed Peat & roots mixed in; lt grays w/ dk brn; wet							3.5' heave @ 30.5'
	32.0 / 1134.1			PD						
					11	NSR				
35				PD						
					11	16				
			S & G, a few stone pieces; lt gray & sat	PD						
40										
					12	15				
	41.5 / 1124.6									

Bottom of Hole - 41.5'
Water measured at 14.2' while sampling and/or drilling

Soil Class:DSB Rock Class: Edit: DMS Date: 4/4/06
G:\GEOTECH\GINTW\PROJECTS\3413B.GPJ

MINNESOTA DEPARTMENT OF TRANSPORTATION - GEOTECHNICAL SECTION

CONE PENETRATION TEST RESULTS

UNIQUE NUMBER 59526

U.S. Customary Units

State Project	Bridge No. or Job Desc.	Trunk Highway/Location	Sounding No.	Ground Elevation
3413-22	nb shoulder	23	c203a	1166.2 (CPT-GPS)

Location	CPT Machine	SHEET 1 of 2
TH 23 EB, 7987+88.9, 22.4'RT	99649	
Co. Coordinate: X=451068 Y=223705 (ft.)	CPT Operator: D. Brady	Date Completed
Latitude (North)=45°13'49.77" Longitude (West)=94°56'23.68"	Cone #: 2560001304	12/12/01

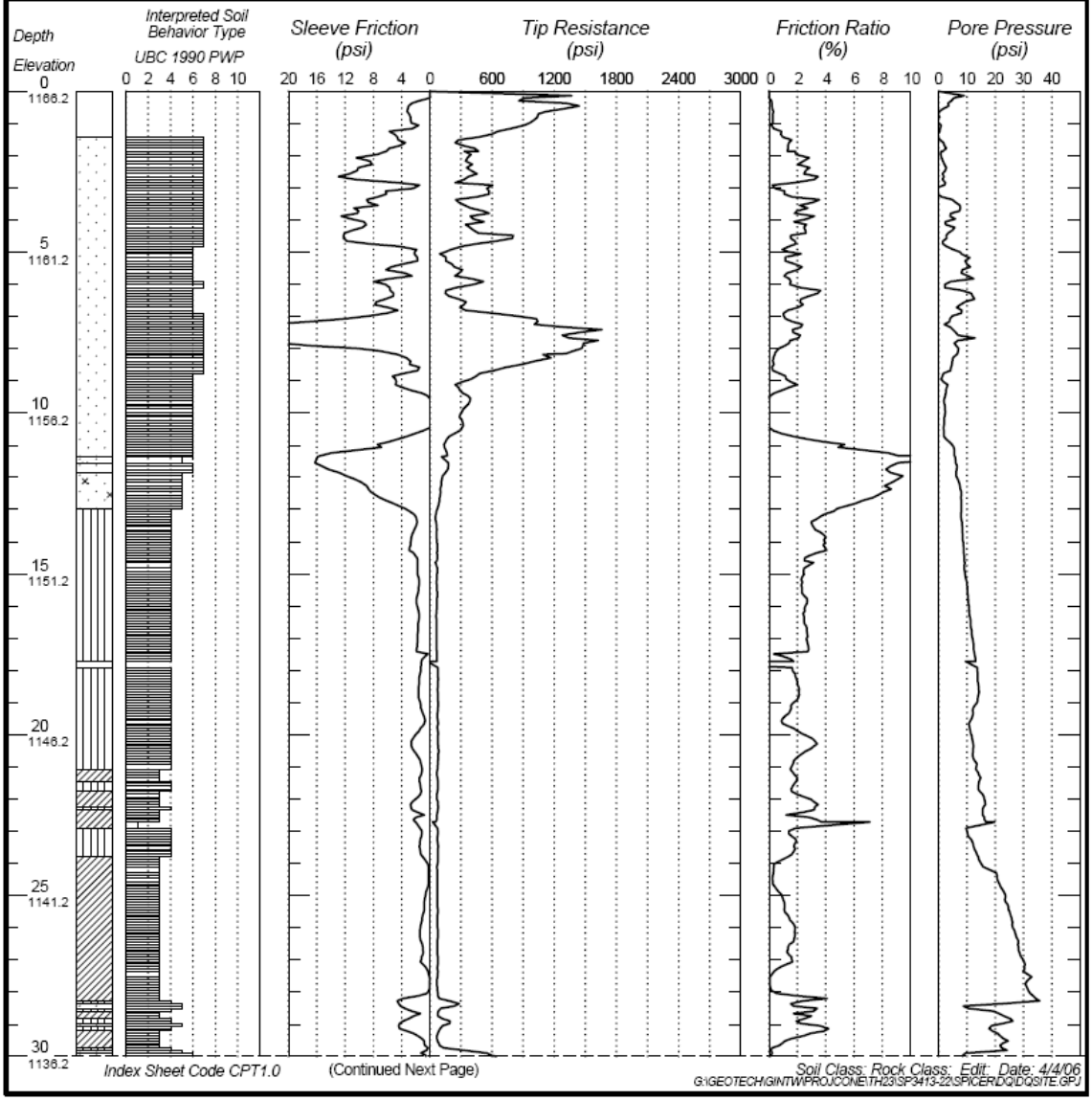

MINNESOTA DEPARTMENT OF TRANSPORTATION - GEOTECHNICAL SECTION

CONE PENETRATION TEST RESULTS

UNIQUE NUMBER 59526

U.S. Customary Units

State Project	Bridge No. or Job Desc.	Trunk Highway/Location	Sounding No.	Ground Elevation
3413-22	**nb shoulder**	**23**	**c203a**	**1166.2** *(CPT-GPS)*

Mn/DOT GEOTECHNICAL SECTION - CONE PENETRATION TEST RESULTS — *SHEET 2 of 2*

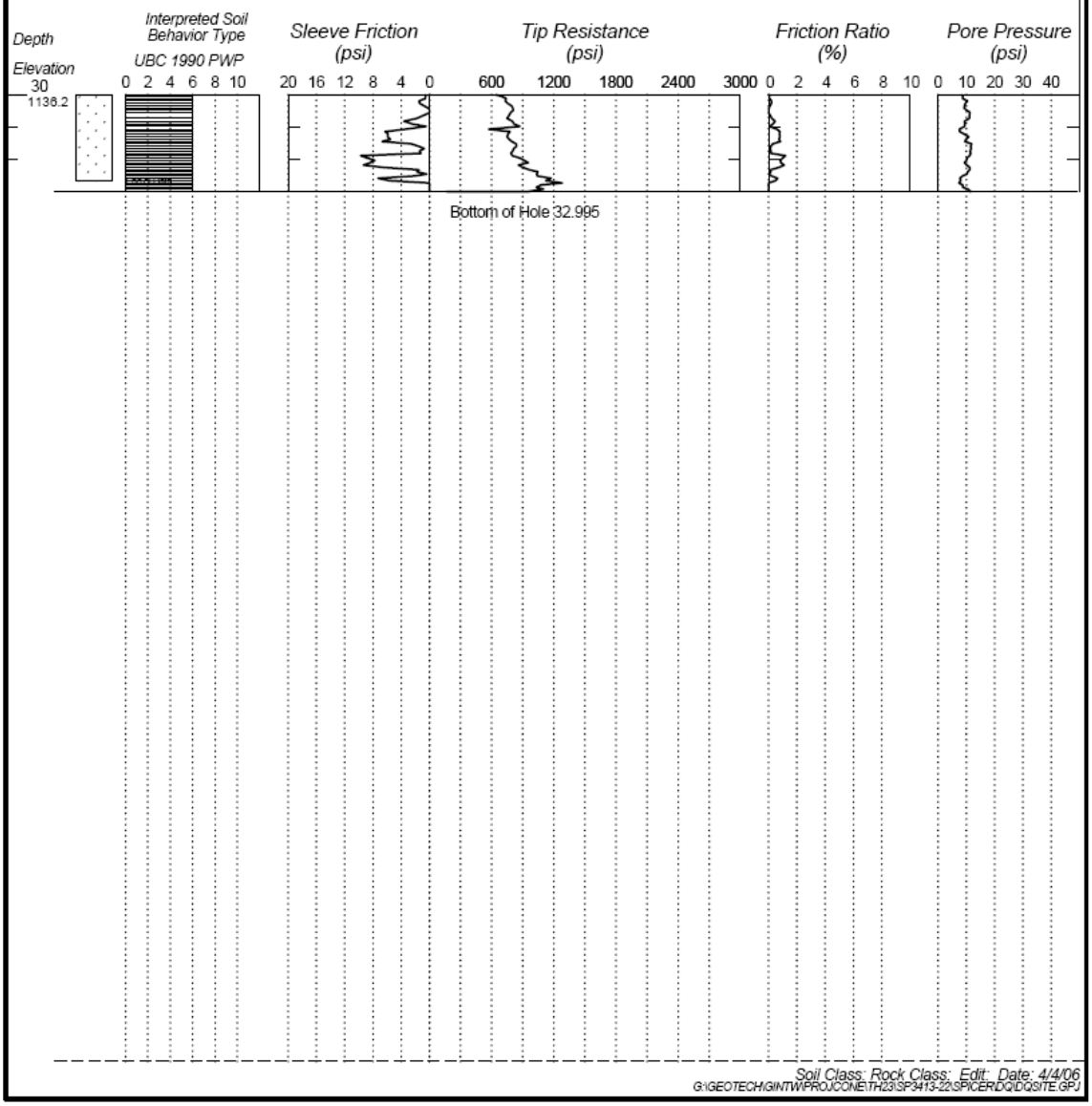

Appendix B

MatLAB Function DiscAn

```
function DiscAn

%------------------------------------------------------------------------
%
%DISCRIMINATE ANALYSIS - DiscAn.m - VERSION 4/21/2006
%
%WILLIAM DEHLER, E.I.T. - U OF MN, DEPT. OF CE
%
%WRITTEN USING MATLAB VERSION 7.0.4.365 (R14) SERVICE PACK 2
%
%THE PURPOSE OF THIS TOOLPACK IS TO PERFORM A DISCRIMINATE ANALYSIS
%OF A SINGLE DEPENDANT VARIABLE SUBJECT TO A SET OF N-1 INDEPENDANT
%VARIABLES AND RETURN AN OPTIMUM SET OF PARAMETERS (a) FOR AN N-1
%DIMENSIONAL DICRIMINATING PLANE OF THE FORM:
%
%       y = a(1) + a(2)x(1) + a(3)x(2) + ... + a(N)x(N-1)
%
%THIS TOOLPACK USES STANDARD FUNCTIONS PROVIDED IN MATLAB VERSION
%7.0.4.365 (R14) SERVICE PACK 2 - COPYRIGHT 2005, THE MATHWORKS, INC. AS
%WELL AS THE MATLAB OPTIMIZATION TOOLPACK AND THE .m FUNCTION FILES
%GetData.m AND DiscOb.m BY WILLIAM DEHLER, E.I.T. - U OF MN, DEPT. OF CE
%
```

```
%PLEASE NOTE THAT THE DATA MUST BE ARRANGED IN A DELIMITED .DAT FILE
%WITH THE FINAL COLUMN CONSISTING OF THE DEPENDANT VARIABLE AND
%EACH ROW REPRESENTING A SEPERATE DATA POINT
%
%THIS TOOLPACK IS BASED UPON THE PROGRAMS trypro.m AND object.m
%PROVIDED BY HUINA XUAN, U OF MN, DEPT. OF CE, AND WAS WRITTEN WITH
%ASSISTANCE BY PROF. R. BARNES, U OF MN, DEPT. OF CE
%
%--------------------------------------------------------------------------

clear all

% Load data table
Data = GetData;

% Number of data points and parameters
global M
global N
[M,N] = size(Data);     %M = data points
                        %N = parameters (N-1 independent parameters)

% Define Threshold Value (T)
T = input('Threshold Value:');
```

```
% Data point above or below threshold value
y = sign(Data(:,N)-T);


% Initialize matrices
x = [ones(M,1),Data(:,1:N-1)];
A = zeros(M,M+N);
for i = 1:M
   for j = 1:N
      A(i,j) = y(i)*x(i,j);
   end
end
A(:,N+1:M+N)=eye(M);
A = -A;
b = -1*ones(M,1);
lb = zeros(M+N,1);
lb(1:N,1) = -1e6*ones(N,1);


%Initialize the parameters
p0 = x\y;
p0 = [p0;zeros(M,1)];


%Initialize the optimization matrices
```

```
% Define Number of Loops (nloops)
nloops = input('Number of Loops Allowed:');
MAX = zeros(nloops,2);
PC = zeros(M,1);

%Redefine the standard optimization options (Maximum # Evals and Display)
options = optimset('fmincon');

%Define Maximum Number of fmincon.m Function Evaluations (MFE)
MFE = input('Maximum Number of fmincon.m Function Evaluations:');
options = optimset(options,'Display','off','MaxFunEvals',MFE);


%Determine the parameters and percent correct for various theta
for i = (1:nloops)
   global theta;
   theta = (T/20)*i;   %Initialize theta
   loop = i
   p = fmincon(@DiscOb,p0,A,b,[],[],lb,[],[],options);       %Initialize p
   for j = (1:M)
      if abs(p(N+j))<0.00001
         PC(j,1)=1;
      else
```

```
            PC(j,1)=0;
        end
    end
    MAX(i,1) = (sum(PC)/M)*100;
    MAX(i,2) = theta;
end

%sort the results
[s, i] = sort (MAX(:, 1));
SORTED = MAX (i,:);

%Define the optimum theta
theta = SORTED(nloops,2);

%Return the optimum results (using the optimum theta)
p = fmincon(@DiscOb,p0,A,b,[],[],lb,[]);

%Output

percent_correct_vs_theta = SORTED
max_percent_correct = SORTED(nloops,1)
parameters = p(1:N)
```

Appendix C

MatLAB Function DiscOb

```
function [f] = DiscOb(p, M, N, theta);

%-------------------------------------------------------------------------
%
%DISCRIMINATE ANALYSIS OBJECT FUNCTION - DiscOb.m - VERSION 4/18/2006
%
%WILLIAM DEHLER, E.I.T. - U OF MN, DEPT. OF CE
%
%WRITTEN USING MATLAB VERSION 7.0.4.365 (R14) SERVICE PACK 2
%
%THE PURPOSE OF THIS TOOLPACK IS TO DEFINE THE DISCRIMINATE ANALYSIS
%SCALAR FUNCTION, AND IS TO BE USED IN CONJUNCTION WITH STANDARD
%FUNCTIONS PROVIDED IN MATLAB VERSION 7.0.4.365 (R14) SERVICE PACK 2 -
%COPYRIGHT 2005, THE MATHWORKS, INC. AS WELL AS THE MATLAB
%OPTIMIZATION TOOLPACK AND IS PRIMARILY FOR USE AS A FUNCTION FILE
%FOR DiscAn.m BY WILLIAM DEHLER, E.I.T. - U OF MN, DEPT. OF CE
%
%THIS TOOLPACK IS BASED UPON THE PROGRAM object.m PROVIDED BY HUINA
%XUAN, U OF MN, DEPT. OF CE, AND WAS WRITTEN WITH ASSISTANCE BY PROF.
%R. BARNES, U OF MN, DEPT. OF CE
%
%-------------------------------------------------------------------------
```

```
global M

global N

global theta


% Define Slack (S)

S = p(N+1:M+N,1);


% Return result

f = M - sum(exp(-theta.*S));
```

Appendix D

MatLAB Function GetData

```
function [Data] = GetData;

%-------------------------------------------------------------------------
%
%RETRIEVE DATA FROM AN EXTERNAL SOURCE - GetData.m - VERSION 4/13/2006
%
%WILLIAM DEHLER, E.I.T. - U OF MN, DEPT. OF CE
%
%WRITTEN USING MATLAB VERSION 7.0.4.365 (R14) SERVICE PACK 2
%
%THE PURPOSE OF THIS TOOLPACK IS TO IMPORT DATA FROM A DELIMITED
%DATA FILE ASSUMING THE DATA IS ARRANGED IN COLUMNS WITH NO
%HEADERS.
%
%THIS TOOLPACK USES STANDARD FUNCTIONS PROVIDED IN: MATLAB VERSION
%7.0.4.365 (R14) SERVICE PACK 2 - COPYRIGHT 2005, THE MATHWORKS, INC.
%
%THIS TOOLPACK IS BASED UPON THE PROGRAM GETINPUT.M BY PROF. R.
%BARNES, U OF MN, DEPT. OF CE
%
%-------------------------------------------------------------------------
```

```
%PROMPT USER TO ENTER DATA FILE NAME
while(exist('Data')~=1)
   try
      name = input('Data File Name (with .dat extension):', 's');
      Data = load(name);
   catch
      fprintf('Unable to open and read file %s \n\n',  name);
      clear Data;
   end
end.
```

Appendix E

Discriminate Analysis

Discriminate analysis.

>> DiscAn

Data File Name (with .dat extension):BFQ_c.dat

Threshold Value:10

Number of Loops Allowed:50

Maximum Number of fmincon.m Function Evaluations:1000000

percent_correct_vs_theta =

60.0000	0.5000
69.2308	1.0000
70.7692	8.5000
70.7692	9.0000
70.7692	9.5000
70.7692	10.0000
70.7692	10.5000
70.7692	11.0000
70.7692	11.5000
70.7692	12.0000
70.7692	12.5000
70.7692	13.0000
70.7692	13.5000
70.7692	14.0000
70.7692	14.5000
70.7692	15.0000
70.7692	15.5000
70.7692	16.0000
70.7692	16.5000
70.7692	17.0000
70.7692	17.5000
70.7692	18.0000
70.7692	18.5000
70.7692	19.0000
70.7692	19.5000
70.7692	20.0000
70.7692	20.5000

```
   70.7692   21.0000
   70.7692   21.5000
   70.7692   22.0000
   70.7692   22.5000
   70.7692   23.0000
   70.7692   23.5000
   70.7692   24.0000
   70.7692   24.5000
   70.7692   25.0000
   72.3077    1.5000
   72.3077    2.0000
   72.3077    2.5000
   72.3077    3.0000
   72.3077    3.5000
   72.3077    4.0000
   72.3077    4.5000
   72.3077    5.0000
   72.3077    5.5000
   72.3077    6.0000
   72.3077    6.5000
   72.3077    7.0000
   72.3077    7.5000
   72.3077    8.0000

max_percent_correct =

   72.3077

parameters =

   -1.3814
   -0.4277
    0.0710
   -0.0082
```

Appendix F

Regression Analysis

Regression analysis with function definition.

x =

-0.0121	6.4466	16.2386
0.1844	6.3941	4.6995
0.3378	6.1550	3.0771
0.5549	5.0677	1.9749
0.5015	4.7967	2.2026
0.0301	4.6506	7.8343
0.0598	7.6528	5.3737
0.2390	0.1731	7.4516
0.0264	0.0343	27.4019
0.0012	0.1451	62.2913
0.2247	3.7252	13.1571
0.3715	3.4321	6.5105
0.4107	4.0222	6.2403
0.4081	8.0870	2.2156
0.0254	0.2286	25.6826
0.3295	3.1326	6.4323
0.0860	7.3250	9.0523
0.0993	7.3413	8.4174
0.0500	0.7042	168.1950
0.1646	-37.1292	-2.0964
1.8206	126.3513	0.6040
0.4336	36.3989	2.0822
1.3894	72.3974	0.7123
2.2989	75.5011	0.5284
13.1551	276.4836	0.0954
16.3810	248.7544	0.0835
-3.5308	-45.4491	-0.3711
-1.6985	-18.0615	-0.7762
-3.0226	-35.2347	-0.4565
-3.8621	-37.1456	-0.3825
-2.8405	-23.2111	-0.5395
-1.9198	-16.3941	-0.7975
-8.2140	-73.1491	-0.1746
-3.5232	-26.5784	-0.4399
-44.4931	-335.3950	-0.0334
0.0017	0.5092	35.7146
0.0047	0.5101	26.2196
-0.0128	1.5741	6.6229
0.0298	3.1443	6.2640
0.0932	3.2442	4.2623
0.1804	2.6636	3.6227
0.3263	2.2977	3.1836

```
    0.4737    1.4516    2.7232
    0.1920    0.5664    5.1984
    0.5831    1.1566    2.6918
    0.0044    0.3885   67.0807
    0.4229    4.4145    5.6602
    0.3237    5.7777    5.4339
    0.4414    5.0085    3.9983
    0.5553    3.8355    3.3730
    0.5885    3.3993    2.9852
    0.0029    4.9355   93.8778
    0.0417    4.2044   15.4667
    0.0759    2.8914    8.4001
    0.1550    2.7850    6.7662
    0.1907    3.8435    5.6844
    0.2755    3.2356    4.5607
    0.3262    2.8722    4.2525
    0.3967    2.3574    4.0828
    0.3814    0.9040    4.3520
    0.0006    5.1565   13.4577
    0.1264    4.8253    5.1942
    0.0749    4.8158    6.4614
    0.2069    4.6346    4.0181
    0.0479    0.8820   21.7970

y =

   3.2000
  16.1000
  26.1000
   9.5000
  10.4000
   7.5000
  39.3000
   6.0000
   6.7000
   5.5000
   5.6000
   2.5000
   3.0000
   3.5000
   8.9000
   9.9000
  20.5000
  10.6000
  24.6000
  15.7000
```

22.7000
22.1000
30.0000
21.5000
17.4000
11.9000
11.5000
9.1000
10.4000
9.7000
8.0000
9.6000
8.2000
7.3000
7.1000
5.2000
4.7000
4.9000
3.6000
12.0000
10.7000
9.3000
11.8000
3.5000
1.9000
5.2000
17.7000
15.3000
11.5000
7.0000
4.0000
6.7000
6.6000
3.5000
8.2000
10.3000
11.3000
9.7000
4.6000
3.3000
3.1000
5.5000
8.5000
7.8000
0.7000

```
beta =

     0
     0
     0
     0

>> beta = nlinfit(x , y , @mymodel , beta)

beta =

   -0.6634
    0.0833
    0.0218
    9.1605
```

```
function yhat = mymodel(beta, x)
        yhat = beta(1)*x(:,1) + beta(2)*x(:,2) + beta(3)*x(:,3) + beta(4);
```

Appendix G

Secondary Data Set

Secondary data set provided by Mn/DOT.

Project	CPT #	CPT Depth (ft)	CPT Mid-Depth (ft)	Water Table (ft)	q_c (psi)	f_s (psi)	q_t (psi)	u_o (psi)	u_2 (psi)	σ_{vo} (psi)	σ'_{vo} (psi)	B_q	F_r	Q_t	%Org
TH169	cs04	25 - 27	26.0	0.0	69.342	2.472	75.742	11.267	33.188	21.667	10.400	0.405	4.571	5.200	7.7
TH169	cs04	34 - 36	35.0	0.0	112.342	5.193	120.416	15.167	41.830	29.167	14.000	0.292	5.691	6.518	15.7
TH169	cs05	23 - 25	24.0	0.0	116.604	7.019	123.615	10.400	36.273	20.000	9.600	0.250	6.774	10.793	32.6
TH169	cs05	26 - 28	27.0	0.0	124.959	7.947	133.052	11.700	41.912	22.500	10.800	0.273	7.188	10.236	51.2
TH169	cs06	9.0 - 11.0	10.0	0.0	99.108	9.147	99.750	4.333	3.308	8.333	4.000	-0.011	10.005	22.854	0.8
TH169	cs06	15 - 17	16.0	0.0	113.176	8.220	114.968	6.933	9.229	13.333	6.400	0.023	8.087	15.880	54.7
TH169	cs06	22 - 24	23.0	0.0	145.309	3.773	149.196	9.967	20.077	19.167	9.200	0.078	2.901	14.134	5.0
TH169	cs12	7.0 - 8.0	7.5	0.0	131.323	3.843	133.792	3.250	12.772	6.250	3.000	0.075	3.013	42.514	1.4
TH169	cs19	11.0 - 13.0	12.0	0.0	58.969	4.799	59.804	5.200	4.400	10.000	4.800	-0.016	9.635	10.376	8.9
TH169	cs19	17 - 19	18.0	0.0	113.397	5.860	120.848	7.800	38.606	15.000	7.200	0.291	5.537	14.701	33.6
TH169	cs19	20.3 - 21	20.7	0.0	126.500	7.638	134.656	8.948	42.162	17.208	8.260	0.283	6.503	14.219	34.3
TH169	cs19	24 - 26	25.0	0.0	220.004	2.178	223.367	10.833	17.455	20.833	10.000	0.033	1.075	20.253	1.3
TH169	cs19	30 - 31	30.5	0.0	129.507	2.814	135.986	13.217	33.546	25.417	12.200	0.184	2.545	9.063	4.9
TH169	cs19	31 - 32	31.5	0.0	128.923	1.845	136.462	13.650	39.132	26.250	12.600	0.231	1.674	8.747	4.8
TH169	cs25	11.0 - 12.0	11.5	0.0	125.883	7.457	128.000	4.983	10.956	9.583	4.600	0.050	6.297	25.743	4.2
TH169	cs25	22 - 24	23.0	0.0	95.669	6.358	104.038	9.967	43.356	19.167	9.200	0.393	7.491	9.225	26.9
TH169	cs25	30 - 31	30.5	0.0	93.486	3.858	103.421	13.217	51.349	25.417	12.200	0.489	4.946	6.394	7.3
TH169	csv20	10.0 - 12.0	11.0	0.0	114.700	10.470	116.158	4.767	7.575	9.167	4.400	0.026	9.785	24.316	8.2
TH169	csv20	18 - 20	19.0	0.0	85.992	2.787	92.356	8.233	32.958	15.833	7.600	0.323	3.642	10.069	6.4
TH169	csv20	31 - 33	32.0	0.0	120.553	6.345	129.173	13.867	44.605	26.667	12.800	0.300	6.190	8.008	51.0
TH169	csv32	25 - 27	26.0	0.0	109.048	3.346	116.948	11.267	40.867	21.667	10.400	0.311	3.511	9.162	10.8

Appendix H

Index Property Laboratory Results

Laboratory test results for index property testing performed and provided by Mn/DOT.

Minnesota Department Of Transportation

TEST REPORT ON SAMPLE OF SUBSOIL

Office of Materials
1400 Gervais Avenue
Maplewood, MN 55109

Sample ID:	**CO-FS06-0028**	Depth:	**8.5' - 10.5'**
Project No.:	**Various**	Field ID:	
Source:		Field Classification:	
Submitted By:	**Dave Borys**	Date Sampled:	
Proj. Eng.:		Date Received:	
Point Number:		Report Approved:	**11/22/2006 07:17**
Tests Required:	**ORG, HYDRO**	Boring No:	**UT04**
Sample Taken From:			

Sieves

Sieve Size	*Percent Passing*
2" (50 mm)	100.0
1" (25.0 mm)	100.0
3/4" (19.0 mm)	100.0
3/8" (9.5 mm)	100.0
#4 (4.75 mm)	100.0
#10 (2.00 mm)	98.1
#20 (850 um)	94.4
#40 (425 um)	88.7
#60 (250 um)	80.6
#100 (150 um)	71.8
#200 (75 um)	62.4

Other Soil Tests

Test	*Result*
Clay (%)	15.8
Silt (%)	46.6
Mn/DOT Class (Entire Sample)	L
Mn/DOT Class (Minus 10)	L
Percent Organic (%)	2.4

Test Procedures: AASHTO T87, T88, T89, T90, T99 Method "C"(M), T100, T190 (M), T-265 M = Mn/DOT Modified

Comments: Florence Bridge

Charge Out: 1038, 1150

Copies To:
Dave Borys

Rod Patrus

REVIEWED BY

Minnesota Department Of Transportation

TEST REPORT ON SAMPLE OF SUBSOIL

Office of Materials
1400 Gervais Avenue
Maplewood, MN 55109

Sample ID:	**CO-FS06-0029**	Depth:	**13.5' - 15.5'**
Project No.:	**Various**	Field ID:	
Source:		Field Classification:	
Submitted By:	**Dave Borys**	Date Sampled:	
Proj. Eng.:		Date Received:	
Point Number:		Report Approved:	**11/22/2006 07:18**
Tests Required:	**ORG, HYDRO**	Boring No:	**UT04**
Sample Taken From:			

Sieves

Sieve Size	*Percent Passing*
2" (50 mm)	100.0
1" (25.0 mm)	100.0
3/4" (19.0 mm)	100.0
3/8" (9.5 mm)	99.9
#4 (4.75 mm)	89.6
#10 (2.00 mm)	88.1
#20 (850 um)	86.4
#40 (425 um)	83.9
#60 (250 um)	81.2
#100 (150 um)	77.8
#200 (75 um)	74.1

Other Soil Tests

Test	*Result*
Clay (%)	26.3
Silt (%)	47.8
Mn/DOT Class (Entire Sample)	CL
Mn/DOT Class (Minus 10)	SiCL
Percent Organic (%)	4.8

Test Procedures: AASHTO T87, T88, T89, T90, T99 Method "C"(M), T100, T190 (M), T-265 M = Mn/DOT Modified

Comments: Florence Bridge

Charge Out: 1038, 1150

Copies To:
Dave Borys

Rod Patrum
REVIEWED BY

Minnesota Department Of Transportation

TEST REPORT ON SAMPLE OF SUBSOIL

Office of Materials
1400 Gervais Avenue
Maplewood, MN 55109

Sample ID:	**CO-FS06-0030**	Depth:	**13.5' - 15.5'**
Project No.:	**Various**	Field ID:	
Source:		Field Classification:	
Submitted By:	**Dave Borys**	Date Sampled:	
Proj. Eng.:		Date Received:	
Point Number:		Report Approved:	**11/22/2006 07:18**
Tests Required:	**ORG, HYDRO**	Boring No:	**T1-2**
Sample Taken From:			

Sieves

Sieve Size	*Percent Passing*
2" (50 mm)	100.0
1" (25.0 mm)	100.0
3/4" (19.0 mm)	95.9
3/8" (9.5 mm)	95.9
#4 (4.75 mm)	93.8
#10 (2.00 mm)	92.2
#20 (850 um)	87.5
#40 (425 um)	80.2
#60 (250 um)	70.8
#100 (150 um)	61.2
#200 (75 um)	51.0

Other Soil Tests

Test	*Result*
Clay (%)	14.4
Silt (%)	36.6
Mn/DOT Class (Entire Sample)	L
Mn/DOT Class (Minus 10)	L
Percent Organic (%)	2.6

Test Procedures: AASHTO T87, T88, T89, T90, T99 Method "C"(M), T100, T190 (M), T-265 M = Mn/DOT Modified

Comments: 8207-54 culvert distress

Charge Out: 1038, 1150

Copies To:
Dave Borys

Rod Patrus
REVIEWED BY

Minnesota Department Of Transportation

TEST REPORT ON SAMPLE OF SUBSOIL

Office of Materials
1400 Gervais Avenue
Maplewood, MN 55109

Sample ID:	**CO-FS06-0031**	Depth:	**18.5' - 20.5'**
Project No.:	**Various**	Field ID:	
Source:		Field Classification:	
Submitted By:	**Dave Borys**	Date Sampled:	
Proj. Eng.:		Date Received:	
Point Number:		Report Approved:	**11/22/2006 07:18**
Tests Required:	**ORG, HYDRO**	Boring No:	**T1-3**
Sample Taken From:			

Sieves

Sieve Size	*Percent Passing*
2" (50 mm)	100.0
1" (25.0 mm)	100.0
3/4" (19.0 mm)	97.6
3/8" (9.5 mm)	96.8
#4 (4.75 mm)	90.7
#10 (2.00 mm)	88.5
#20 (850 um)	84.1
#40 (425 um)	77.4
#60 (250 um)	68.9
#100 (150 um)	59.5
#200 (75 um)	49.0

Other Soil Tests

Test	*Result*
Clay (%)	12.5
Silt (%)	36.5
Mn/DOT Class (Entire Sample)	SL
Mn/DOT Class (Minus 10)	L
Percent Organic (%)	2.3

Test Procedures: AASHTO T87, T88, T89, T90, T99 Method "C"(M), T100, T190 (M), T-265 M = Mn/DOT Modified

Comments: 8207-54 culvert distress

Charge Out: 1038, 1150

Copies To:

Dave Borys

Rod Patrus

REVIEWED BY

Minnesota Department Of Transportation

TEST REPORT ON SAMPLE OF SUBSOIL

Office of Materials
1400 Gervais Avenue
Maplewood, MN 55109

Sample ID:	**CO-FS06-0032**	Depth:	**3.5' - 5.5'**
Project No.:	**Various**	Field ID:	
Source:		Field Classification:	
Submitted By:	**Dave Borys**	Date Sampled:	
Proj. Eng.:		Date Received:	
Point Number:		Report Approved:	**11/22/2006 07:19**
Tests Required:	**ORG, HYDRO**	Boring No:	**U6-1**
Sample Taken From:			

Sieves

Sieve Size	*Percent Passing*
2" (50 mm)	100.0
1" (25.0 mm)	100.0
3/4" (19.0 mm)	100.0
3/8" (9.5 mm)	99.4
#4 (4.75 mm)	93.7
#10 (2.00 mm)	90.5
#20 (850 um)	86.4
#40 (425 um)	81.2
#60 (250 um)	74.4
#100 (150 um)	64.8
#200 (75 um)	52.7

Other Soil Tests

Test	*Result*
Clay (%)	11.5
Silt (%)	41.2
Mn/DOT Class (Entire Sample)	L
Mn/DOT Class (Minus 10)	L
Percent Organic (%)	2.9

Test Procedures: AASHTO T87, T88, T89, T90, T99 Method "C"(M), T100, T190 (M), T-265 M = Mn/DOT Modified

Comments: 7401-34 research boring

Charge Out: 1038, 1150

Copies To:
Dave Borys

Rod Patrun
REVIEWED BY

Minnesota Department Of Transportation

TEST REPORT ON SAMPLE OF SUBSOIL

Office of Materials
1400 Gervais Avenue
Maplewood, MN 55109

Sample ID:	**CO-FS06-0033**	Depth:	**8.5' - 10.5'**
Project No.:	**Various**	Field ID:	
Source:		Field Classification:	
Submitted By:	**Dave Borys**	Date Sampled:	
Proj. Eng.:		Date Received:	
Point Number:		Report Approved:	**11/22/2006 07:19**
Tests Required:	**ORG, HYDRO**	Boring No:	**U5-2**
Sample Taken From:			

Sieves

Sieve Size	*Percent Passing*
2" (50 mm)	100.0
1" (25.0 mm)	100.0
3/4" (19.0 mm)	100.0
3/8" (9.5 mm)	99.6
#4 (4.75 mm)	90.2
#10 (2.00 mm)	85.5
#20 (850 um)	81.0
#40 (425 um)	75.9
#60 (250 um)	69.9
#100 (150 um)	60.4
#200 (75 um)	50.1

Other Soil Tests

Test	*Result*
Clay (%)	13.8
Silt (%)	36.3
Mn/DOT Class (Entire Sample)	L
Mn/DOT Class (Minus 10)	L
Percent Organic (%)	2.8

Test Procedures: AASHTO T87, T88, T89, T90, T99 Method "C"(M), T100, T190 (M), T-265 M = Mn/DOT Modified

Comments: 7401-34 research boring

Charge Out: 1038, 1150

Copies To:
Dave Borys

REVIEWED BY

Minnesota Department Of Transportation

TEST REPORT ON SAMPLE OF SUBSOIL

Office of Materials
1400 Gervais Avenue
Maplewood, MN 55109

Sample ID:	**CO-FS06-0034**	Depth:	**13.5' - 15.5'**
Project No.:	**Various**	Field ID:	
Source:		Field Classification:	
Submitted By:	**Dave Borys**	Date Sampled:	
Proj. Eng.:		Date Received:	
Point Number:		Report Approved:	**11/22/2006 07:19**
Tests Required:	**ORG, HYDRO**	Boring No:	**U5-3**
Sample Taken From:			

Sieves

Sieve Size	*Percent Passing*
2" (50 mm)	100.0
1" (25.0 mm)	100.0
3/4" (19.0 mm)	100.0
3/8" (9.5 mm)	100.0
#4 (4.75 mm)	96.3
#10 (2.00 mm)	93.6
#20 (850 um)	87.4
#40 (425 um)	81.3
#60 (250 um)	73.5
#100 (150 um)	64.6
#200 (75 um)	54.2

Other Soil Tests

Test	*Result*
Clay (%)	14.3
Silt (%)	39.9
Mn/DOT Class (Entire Sample)	L
Mn/DOT Class (Minus 10)	L
Percent Organic (%)	2.3

Test Procedures: AASHTO T87, T88, T89, T90, T99 Method "C"(M), T100, T190 (M), T-265 M = Mn/DOT Modified

Comments: 7401-34 research boring

Charge Out: 1038, 1150

Copies To:
Dave Borys

REVIEWED BY

Minnesota Department Of Transportation

SubSoil Sample Worksheet

Sample ID:	CO-FS06-0028	Submitted By:	Dave Borys
Project No.:	Various	Source:	
Date Sampled:		Date Received:	

Hydrometer Analysis

Time	Temp	Read	Size (mm)	% Finer
2 min	71.0	32.0	0.03244	51.7
5 min	71.0	26.5	0.02184	40.7
15 min	71.0	21.0	0.01304	29.6
30 min	71.0	20.0	0.00874	27.6
60 min	69.0	18.0	0.00664	22.7
250 mi	70.0	15.5	0.00326	18.1
24 hr	72.0	13.0	0.00136	14.0

Liquid Limit

Type	Weight 1	Weight 2

Particle Size

%	Particle	Size (mm)
37.6	Total Sand	
46.6	Silt	.075-.002
15.8	Clay	<.002

Hygroscopic Moisture

Content Type	Weight
Air Dry + Can	24.02
Oven Dry + Can	23.79
Can	14.42
Corr. Factor	0.975%

Plastic Limit

Type	Weight 1	Weight 2

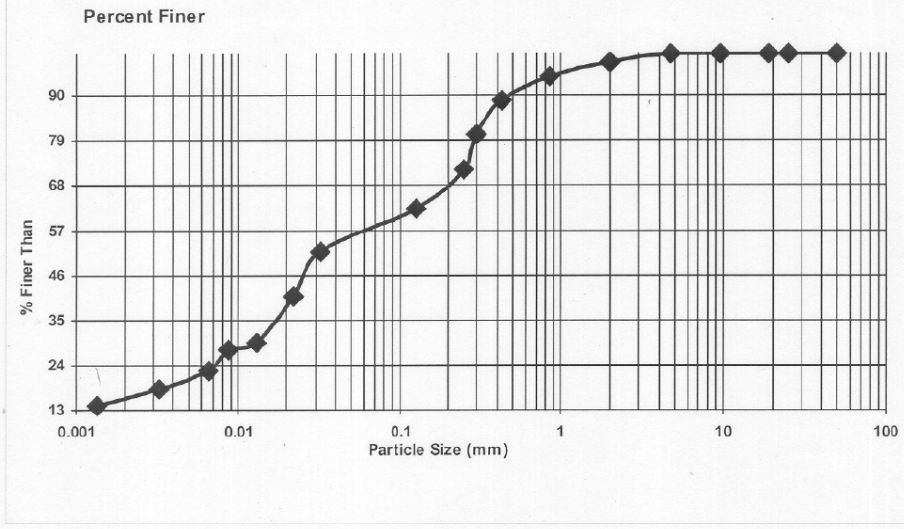

Minnesota Department Of Transportation

SubSoil Sample Worksheet

Sample ID:	**CO-FS06-0029**	Submitted By:	**Dave Borys**
Project No.:	**Various**	Source:	
Date Sampled:		Date Received:	

Hydrometer Analysis

Time	Temp	Read	Size (mm)	% Finer
2 min	71.0	42.0	0.03032	63.1
5 min	71.0	37.0	0.02040	54.2
15 min	71.0	32.5	0.01212	46.3
30 min	71.0	31.0	0.00816	43.6
60 min	69.0	29.0	0.00620	39.3
250 mi	70.0	24.0	0.00309	30.9
24 hr	70.0	19.0	0.00133	22.1

Liquid Limit

Type	Weight 1	Weight 2

Particle Size

%	Particle	Size (mm)
25.9	Total Sand	
47.8	Silt	.075-.002
26.3	Clay	<.002

Hygroscopic Moisture

Content Type	Weight
Air Dry + Can	28.40
Oven Dry + Can	28.37
Can	14.41
Corr. Factor	0.998%

Plastic Limit

Type	Weight 1	Weight 2

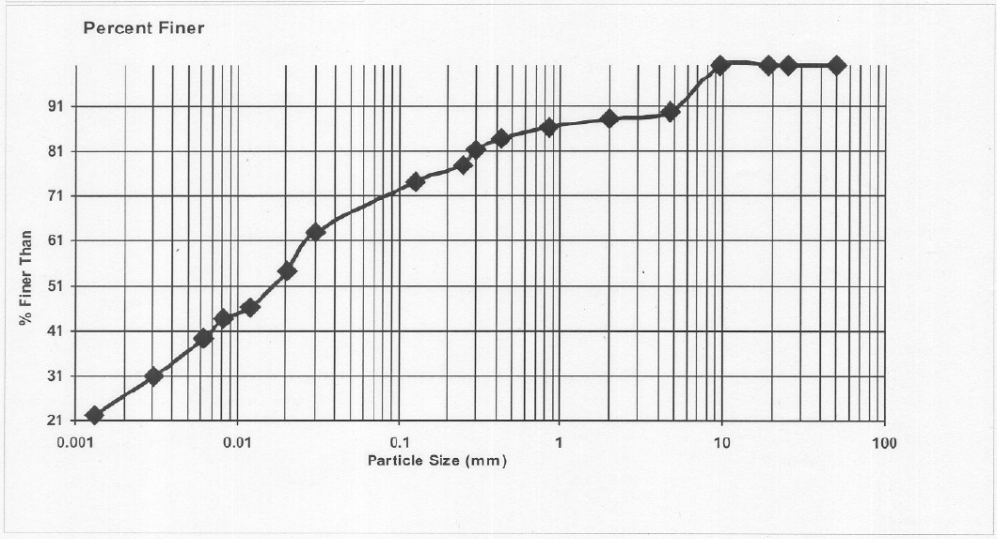

Minnesota Department Of Transportation

SubSoil Sample Worksheet

Sample ID:	**CO-FS06-0030**	Submitted By:	**Dave Borys**
Project No.:	**Various**	Source:	
Date Sampled:		Date Received:	

Hydrometer Analysis

Time	Temp	Read	Size (mm)	% Finer
2 min	71.0	30.0	0.03286	43.7
5 min	71.0	25.0	0.02205	34.5
15 min	71.0	21.0	0.01304	27.1
30 min	71.0	20.0	0.00874	25.3
60 min	69.0	19.0	0.00660	22.6
250 mi	70.0	16.0	0.00325	17.5
24 hr	72.0	12.5	0.00136	11.9

Liquid Limit

Type	Weight 1	Weight 2

Particle Size

%	Particle	Size (mm)
49.0	Total Sand	
36.6	Silt	.075-.002
14.4	Clay	<.002

Hygroscopic Moisture

Content Type	Weight
Air Dry + Can	29.50
Oven Dry + Can	29.50
Can	14.36
Corr. Factor	1.000%

Plastic Limit

Type	Weight 1	Weight 2

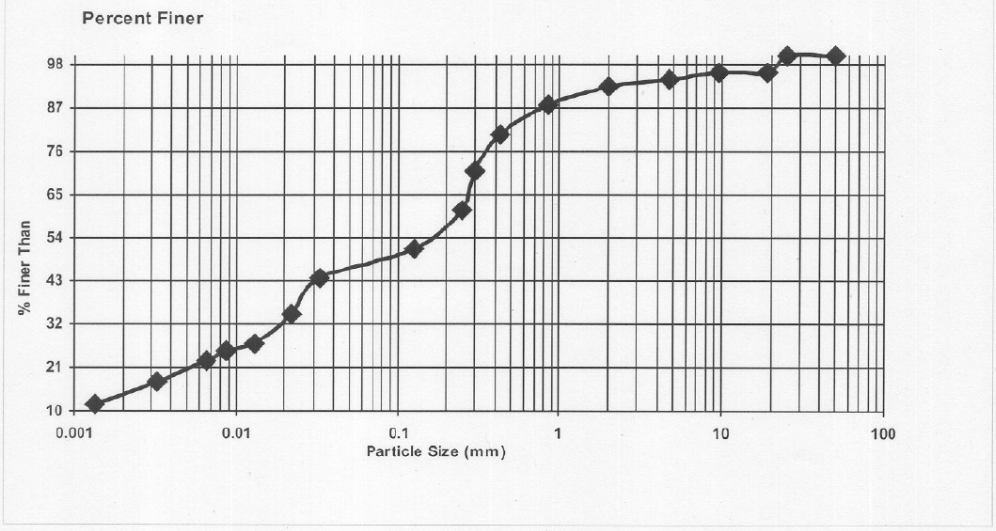

Minnesota Department Of Transportation

SubSoil Sample Worksheet

Sample ID:	**CO-FS06-0031**	Submitted By:	**Dave Borys**
Project No.:	**Various**	Source:	
Date Sampled:		Date Received:	

Hydrometer Analysis

Time	Temp	Read	Size (mm)	% Finer
2 min	71.0	27.0	0.03350	36.7
5 min	71.0	24.0	0.02219	31.4
15 min	71.0	20.0	0.01312	24.3
30 min	71.0	19.0	0.00880	22.5
60 min	69.0	18.0	0.00664	20.0
250 mi	70.0	15.0	0.00326	15.1
24 hr	72.0	12.0	0.00137	10.5

Liquid Limit

Type	Weight 1	Weight 2

Particle Size

%	Particle	Size (mm)
51.0	Total Sand	
36.5	Silt	.075-.002
12.5	Clay	<.002

Hygroscopic Moisture

Content Type	Weight
Air Dry + Can	33.01
Oven Dry + Can	33.00
Can	14.29
Corr. Factor	0.999%

Plastic Limit

Type	Weight 1	Weight 2

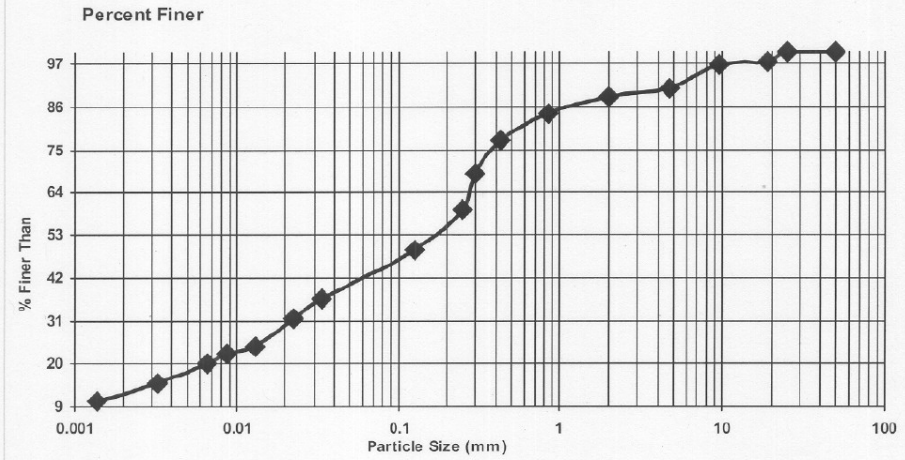

Minnesota Department Of Transportation

SubSoil Sample Worksheet

Sample ID:	**CO-FS06-0032**	Submitted By:	**Dave Borys**
Project No.:	**Various**	Source:	
Date Sampled:		Date Received:	

Hydrometer Analysis

Time	Temp	Read	Size (mm)	% Finer
2 min	71.0	29.0	0.03307	41.3
5 min	71.0	25.0	0.02205	34.0
15 min	71.0	21.0	0.01304	28.7
30 min	71.0	19.0	0.00880	23.1
60 min	69.0	18.0	0.00664	20.5
250 mi	70.0	14.0	0.00328	13.6
24 hr	72.0	11.5	0.00137	9.9

Liquid Limit

Type	Weight 1	Weight 2

Particle Size

%	Particle	Size (mm)
47.3	Total Sand	
41.2	Silt	.075-.002
11.5	Clay	<.002

Hygroscopic Moisture

Content Type	Weight
Air Dry + Can	27.29
Oven Dry + Can	27.25
Can	14.41
Corr. Factor	0.997%

Plastic Limit

Type	Weight 1	Weight 2

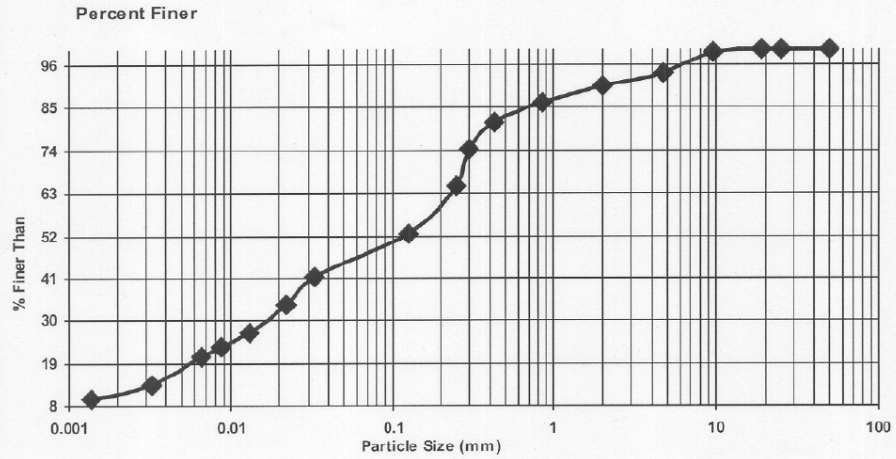

Minnesota Department Of Transportation

SubSoil Sample Worksheet

Sample ID:	CO-FS06-0033	Submitted By:	Dave Borys
Project No.:	Various	Source:	
Date Sampled:		Date Received:	

Hydrometer Analysis

Time	Temp	Read	Size (mm)	% Finer
2 min	71.0	28.0	0.03328	37.2
5 min	71.0	25.0	0.02205	32.0
15 min	71.0	21.0	0.01304	25.2
30 min	71.0	20.0	0.00874	23.5
60 min	69.0	18.0	0.00664	19.3
250 mi	70.0	16.0	0.00325	16.3
24 hr	72.0	13.0	0.00136	11.9

Liquid Limit

Type	Weight 1	Weight 2

Particle Size

%	Particle	Size (mm)
49.9	Total Sand	
36.3	Silt	.075-.002
13.8	Clay	<.002

Hygroscopic Moisture

Content Type	Weight
Air Dry + Can	28.36
Oven Dry + Can	28.36
Can	14.43
Corr. Factor	1.000%

Plastic Limit

Type	Weight 1	Weight 2

Percent Finer

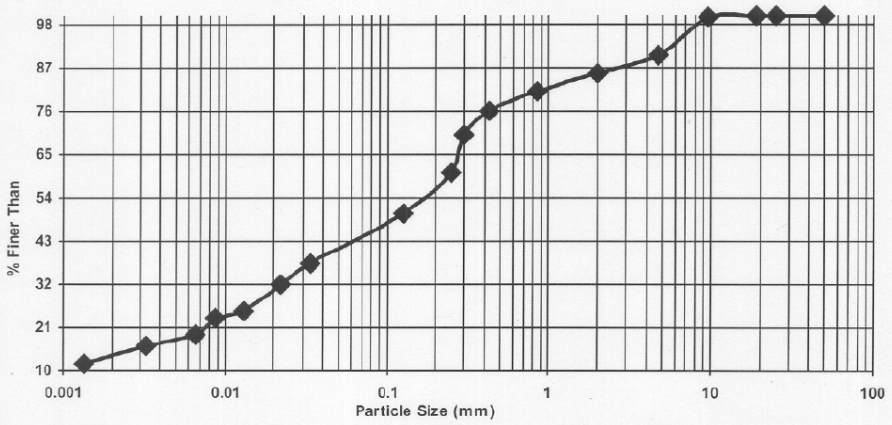

Minnesota Department Of Transportation

SubSoil Sample Worksheet

Sample ID:	**CO-FS06-0034**	Submitted By:	**Dave Borys**
Project No.:	**Various**	Source:	
Date Sampled:		Date Received:	

Hydrometer Analysis

Time	Temp	Read	Size (mm)	% Finer
2 min	71.0	28.0	0.03328	40.7
5 min	71.0	26.0	0.02191	36.9
15 min	71.0	21.0	0.01304	27.6
30 min	71.0	20.0	0.00874	25.7
60 min	69.0	18.0	0.00664	21.1
250 mi	70.0	15.0	0.00326	15.9
24 hr	72.0	13.0	0.00136	13.0

Liquid Limit

Type	Weight 1	Weight 2

Particle Size

%	Particle	Size (mm)
45.8	Total Sand	
39.9	Silt	.075-.002
14.3	Clay	<.002

Hygroscopic Moisture

Content Type	Weight
Air Dry + Can	31.91
Oven Dry + Can	31.90
Can	14.52
Corr. Factor	0.999%

Plastic Limit

Type	Weight 1	Weight 2

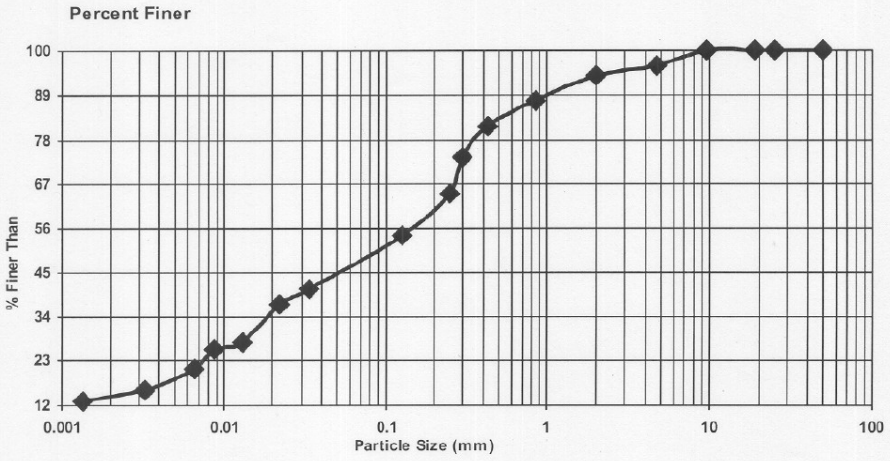

Appendix I

Mn/DOT CPT Logs

CPT sounding logs for Owatonna (US3), Florence (UT04), and Forest Lake (US31) sites (Provided by Mn/DOT).

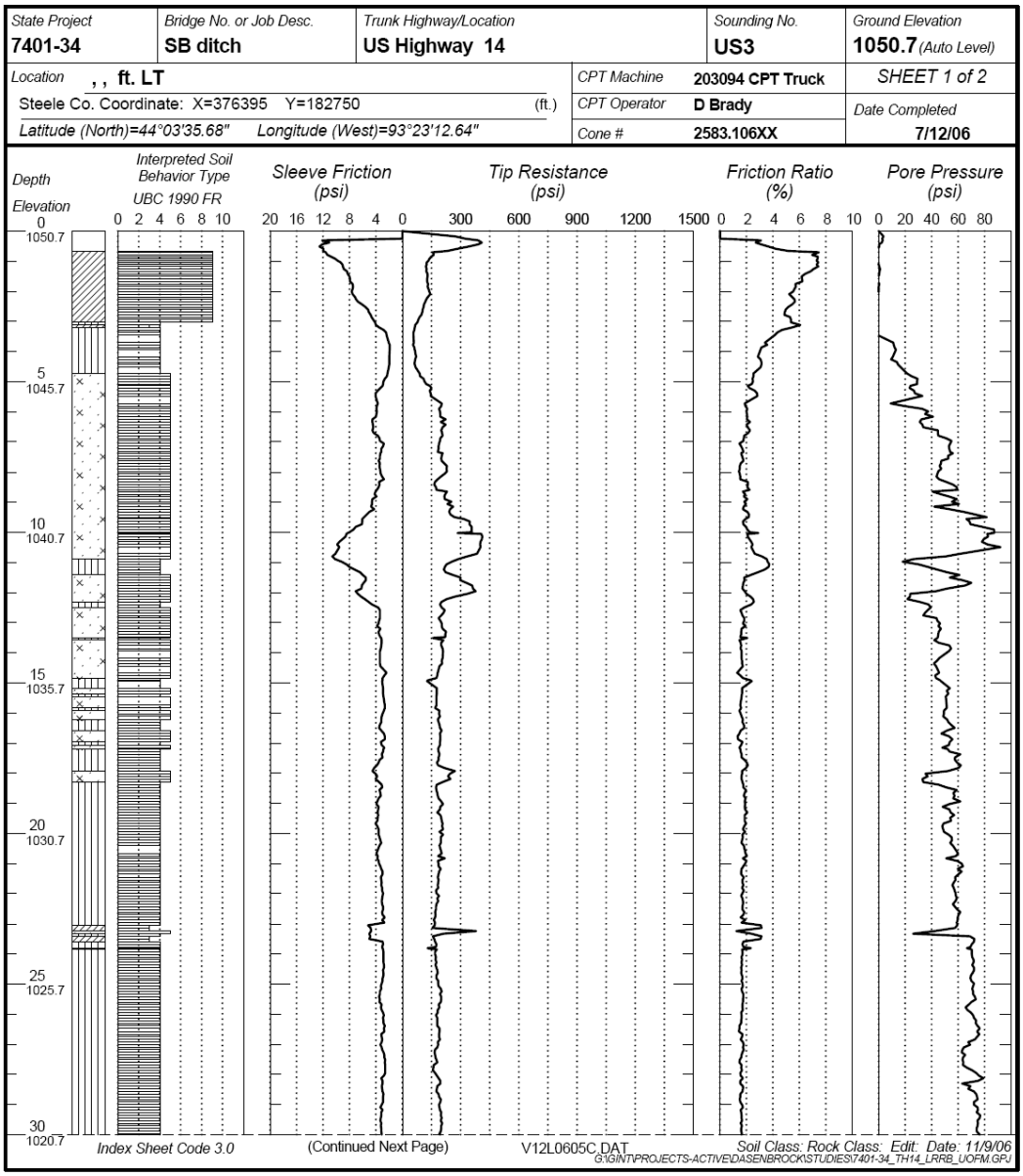

MINNESOTA DEPARTMENT OF TRANSPORTATION - GEOTECHNICAL SECTION

CONE PENETRATION TEST RESULTS

UNIQUE NUMBER 68209

U.S. Customary Units

State Project	Bridge No. or Job Desc.	Trunk Highway/Location	Sounding No.	Ground Elevation
7401-34	**SB ditch**	**US Highway 14**	**US3**	**1050.7** *(Auto Level)*

Mn/DOT GEOTECHNICAL SECTION - CONE PENETRATION TEST RESULTS — *SHEET 2 of 2*

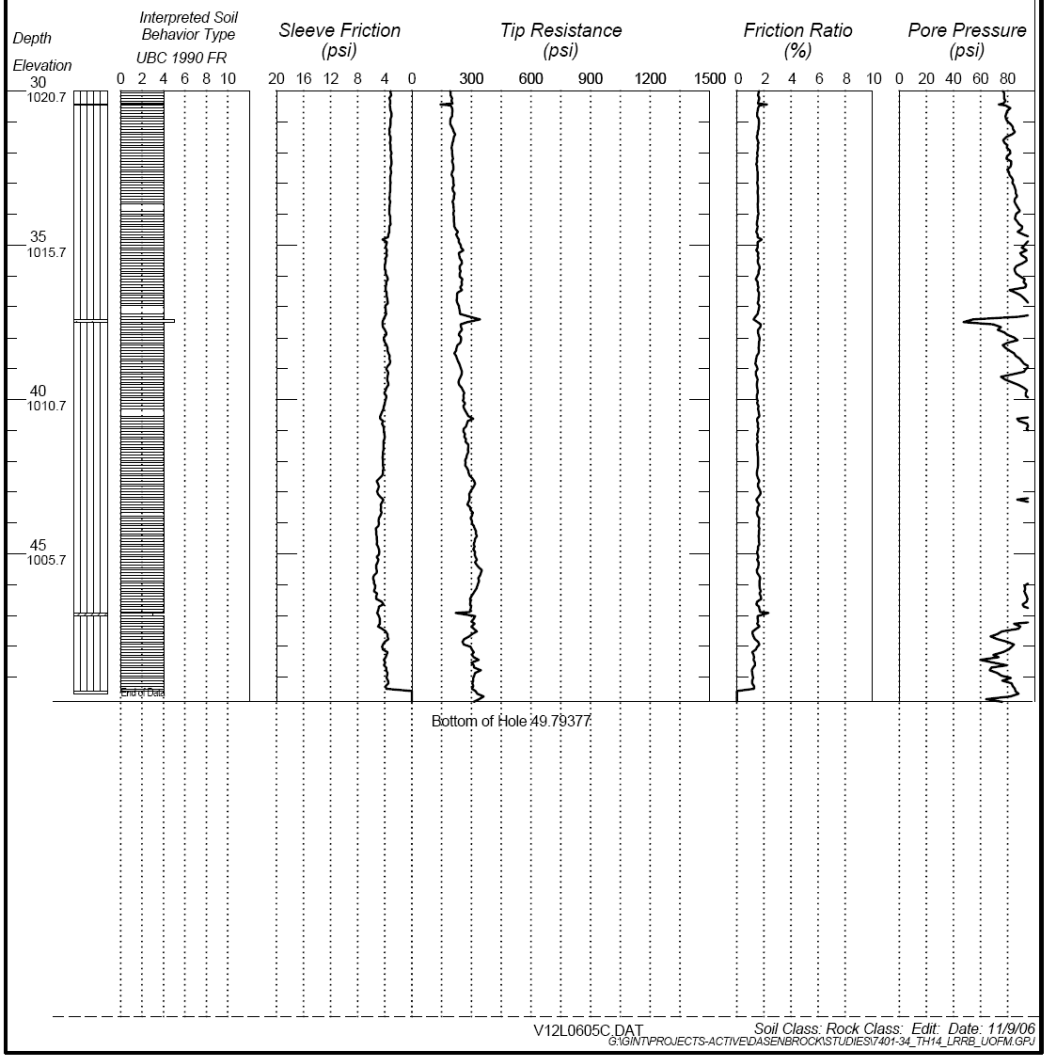

MINNESOTA DEPARTMENT OF TRANSPORTATION - GEOTECHNICAL SECTION

LABORATORY LOG & TEST RESULTS - SUBSURFACE EXPLORATION

UNIQUE NUMBER 68100

U.S. Customary Units

State Project	Bridge No. or Job Desc.	Trunk Highway/Location	Boring No.	Ground Elevation
4201	42013	US Highway 14	UT04	1710.8 (survey)

Location , , ft. LT

Lyon Co. Coordinate: X=448308 Y=116612 (ft.)

Latitude (North)=44°14'27.42" Longitude (West)=96°02'50.02"

Drill Machine 205120

Hammer CME Automatic Calibrated

SHEET 1 of 3

Drilling Completed 7/27/06

DEPTH	Depth / Elev.	Lithology	Classification	Drilling Operation	SPT N_{60}	MC (%)	COH (psf)	γ (pcf)	Soil / Rock	Other Tests Or Remarks / Formation or Member
					REC (%)	RQD (%)	ACL (ft)	Core Breaks		
5			CL w/ a few pebbles, layer C, org on top; brns, lt grays & gray-brns w/ blk; moist							
10										
15	14.5 / 1696.3			PD	13	19				
20			mixed SCL & SC w/ pebbles, gray & moist	PD	24	17 18	2170	136		
25				PD		16				

Index Sheet Code 3.0 (Continued Next Page)

Soil Class:DSB Rock Class: Edit: Date: 11/9/06

G:\GINT\PROJECTS-ACTIVE\DASENBROCK\STUDIES\4201_BR42013-TH14.GPJ

MINNESOTA DEPARTMENT OF TRANSPORTATION - GEOTECHNICAL SECTION
LABORATORY LOG & TEST RESULTS - SUBSURFACE EXPLORATION

UNIQUE NUMBER 68100

U.S. Customary Units

Mn/DOT GEOTECHNICAL SECTION - LOG & TEST RESULTS — *SHEET 2 of 3*

State Project	Bridge No. or Job Desc.	Trunk Highway/Location	Boring No.	Ground Elevation
4201	42013	US Highway 14	UT04	1710.8 (survey)

DEPTH	Depth / Elev.	Lithology	Classification	Drilling Operation	SPT N_{60} (%)	MC (%)	COH (psf)	γ (pcf)	Soil / Rock	Other Tests Or Remarks / Formation or Member
					REC (%)	RQD (%)	ACL (ft)	Core Breaks		
					24	18				
				PD						
					27	NSR				
30				PD						
					22	17				
				PD						
						MUD				
35					34	18				
			mixed SCL & SC w/ pebbles, gray & moist *(continued)*	PD						
						16	2550	135		
40					33	16				
				PD						
						14	1980	139		
45					26	15				
				PD						
						15				
50										

(Continued Next Page)

Soil Class:DSB Rock Class: Edit: Date: 11/9/06
G:\GINT\PROJECTS-ACTIVE\DASENBROCK\STUDIES\4201_BR42013-TH14.GPJ

MINNESOTA DEPARTMENT OF TRANSPORTATION - GEOTECHNICAL SECTION
LABORATORY LOG & TEST RESULTS - SUBSURFACE EXPLORATION

UNIQUE NUMBER 68100

U.S. Customary Units

Mn/DOT GEOTECHNICAL SECTION - LOG & TEST RESULTS — *SHEET 3 of 3*

State Project	Bridge No. or Job Desc.	Trunk Highway/Location	Boring No.	Ground Elevation
4201	42013	US Highway 14	UT04	1710.8 (survey)

DEPTH	Depth / Elev.	Lithology	Classification	Drilling Operation	SPT N_{60} (%)	MC (%)	COH (psf)	γ (pcf)	Soil / Rock	Other Tests Or Remarks / Formation or Member
					REC (%)	RQD (%)	ACL (ft)	Core Breaks		
			mixed SCL & SC w/ pebbles, gray & moist *(continued)*	PD	22	14				
						18				
55	55.5 / 1655.3				40/.5 50/.35	12				
			LS & G, gray & wet	PD						
60										
					59	10				
65	65.0 / 1645.8									

Bottom of Hole - 65.0'
No water encountered or measured during drilling

Soil Class:DSB Rock Class: Edit: Date: 11/9/06
G:\GINT\PROJECTS-ACTIVE\DASEN\BROCK\STUDIES\4201_BR42013-TH14.GPJ

MINNESOTA DEPARTMENT OF TRANSPORTATION - GEOTECHNICAL SECTION

CONE PENETRATION TEST RESULTS

UNIQUE NUMBER 68099

U.S. Customary Units

State Project	Bridge No. or Job Desc.	Trunk Highway/Location	Sounding No.	Ground Elevation
8207-57	NB shoudler	US Highway 61	US31	836.0 (from Plan)

Location			
, , ft. LT	CPT Machine	203094 CPT Truck	SHEET 1 of 1
Washington Co. Coordinate: X=461074 Y=283457 (ft.)	CPT Operator	D Brady	Date Completed
Latitude (North)=45°14'55.93" Longitude (West)=92°59'04.34"	Cone #	2583.106XX	9/12/06

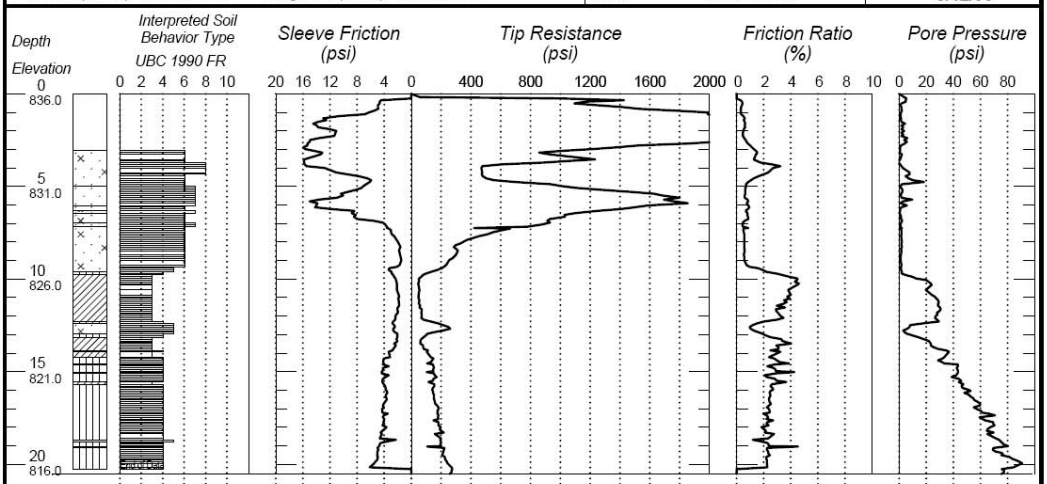

Index Sheet Code CPT1.0 V12S0603C.DAT Soil Class: Rock Class: Edit: Date: 11/9/06

G:\GINT\PROJECTS-ACTIVE\DASENBROCK\6207-57_TH61_CULVERT_DISTRESS.GPJ

Appendix J

Resilient Modulus Plots

Florence 3.5-5.5 feet:

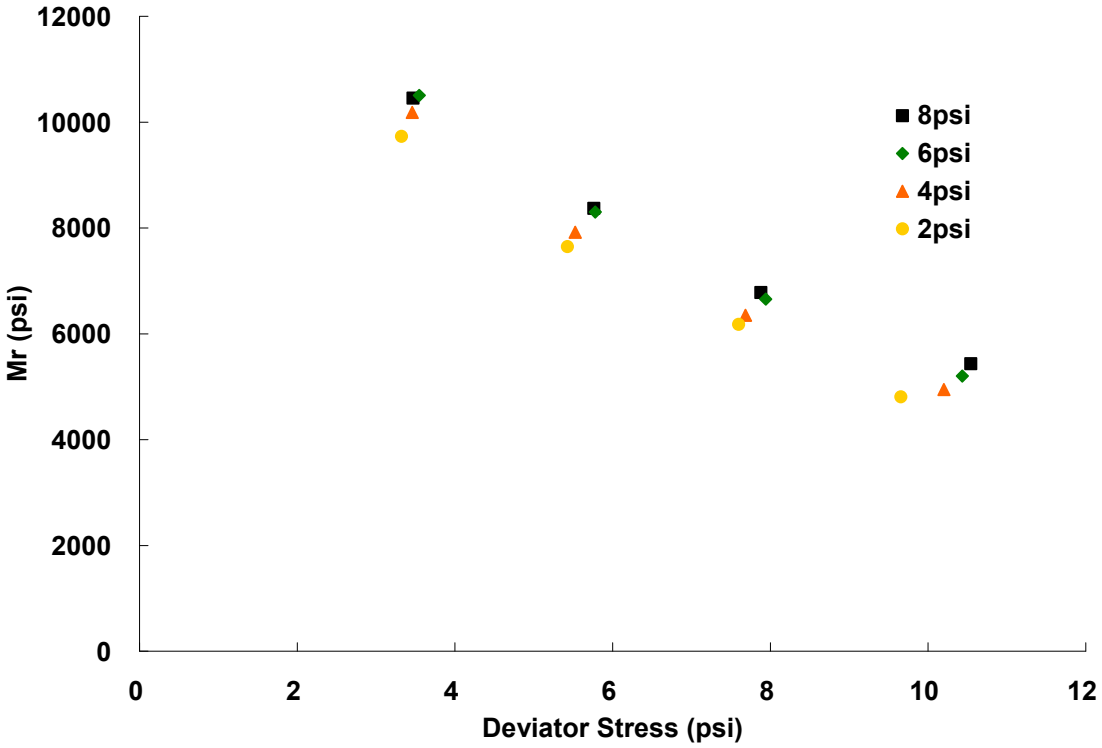

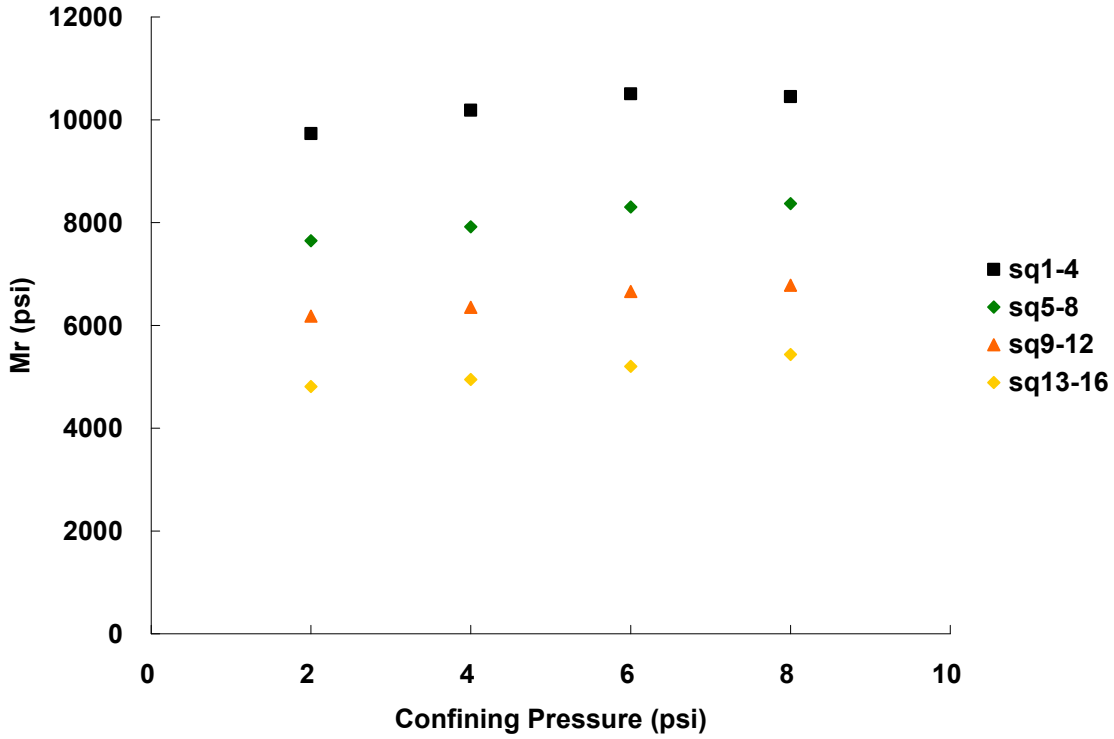

Florence 8.5-10.5 feet:

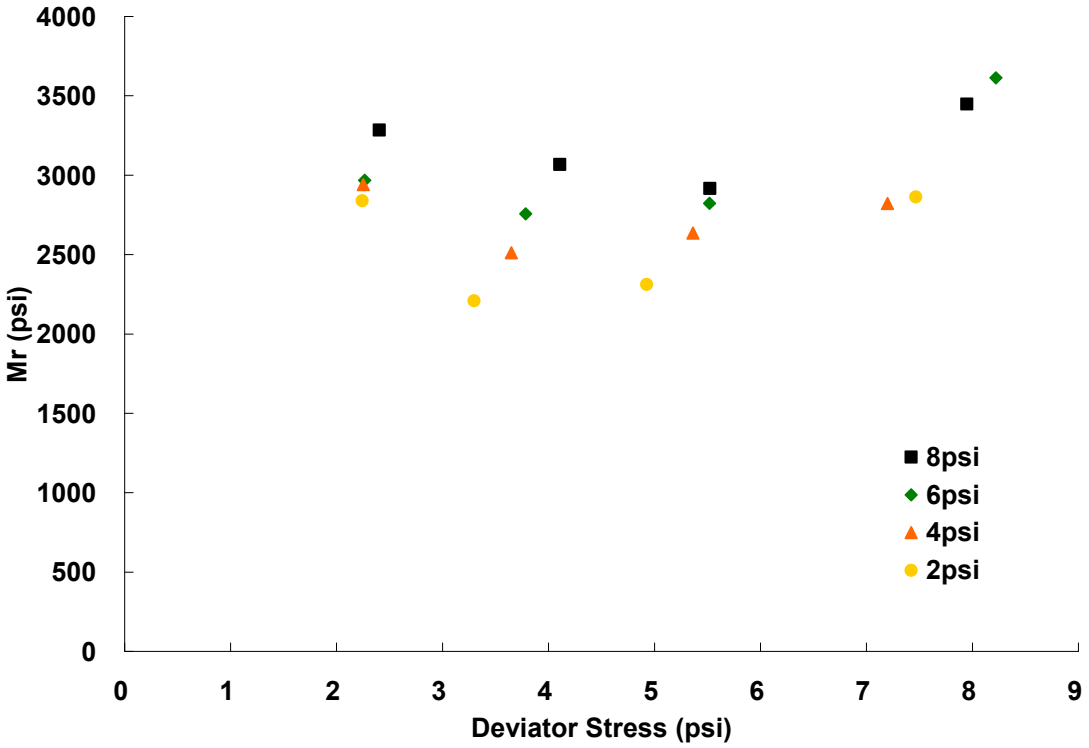

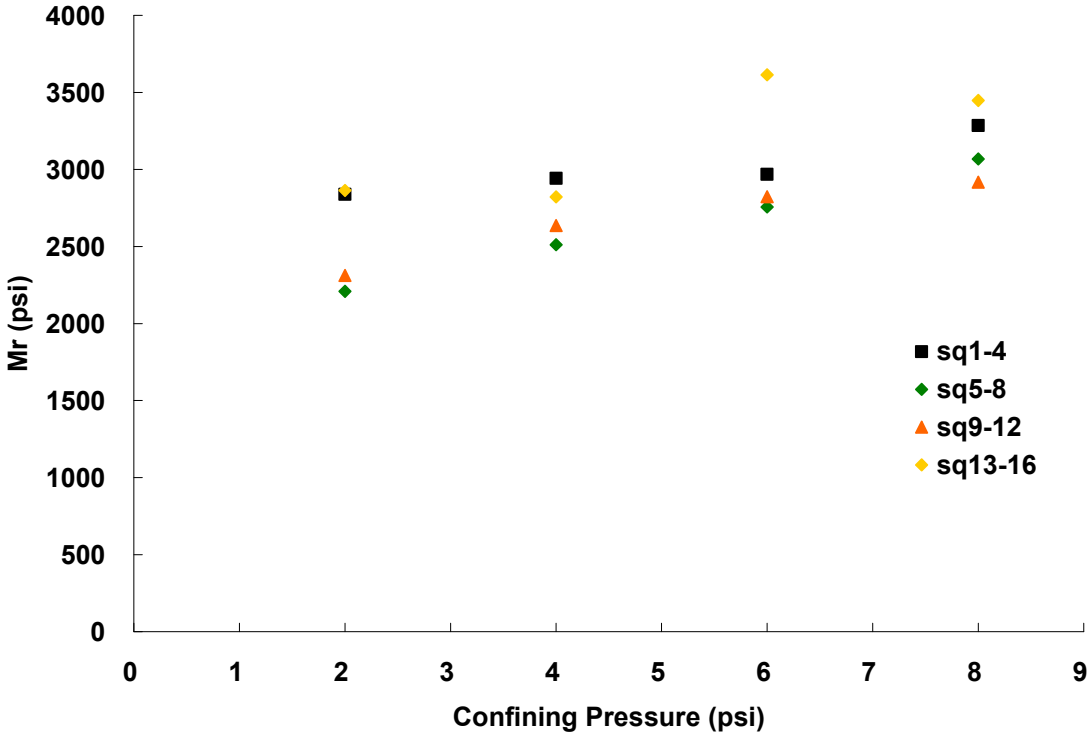

Florence 13.5-15.5 feet:

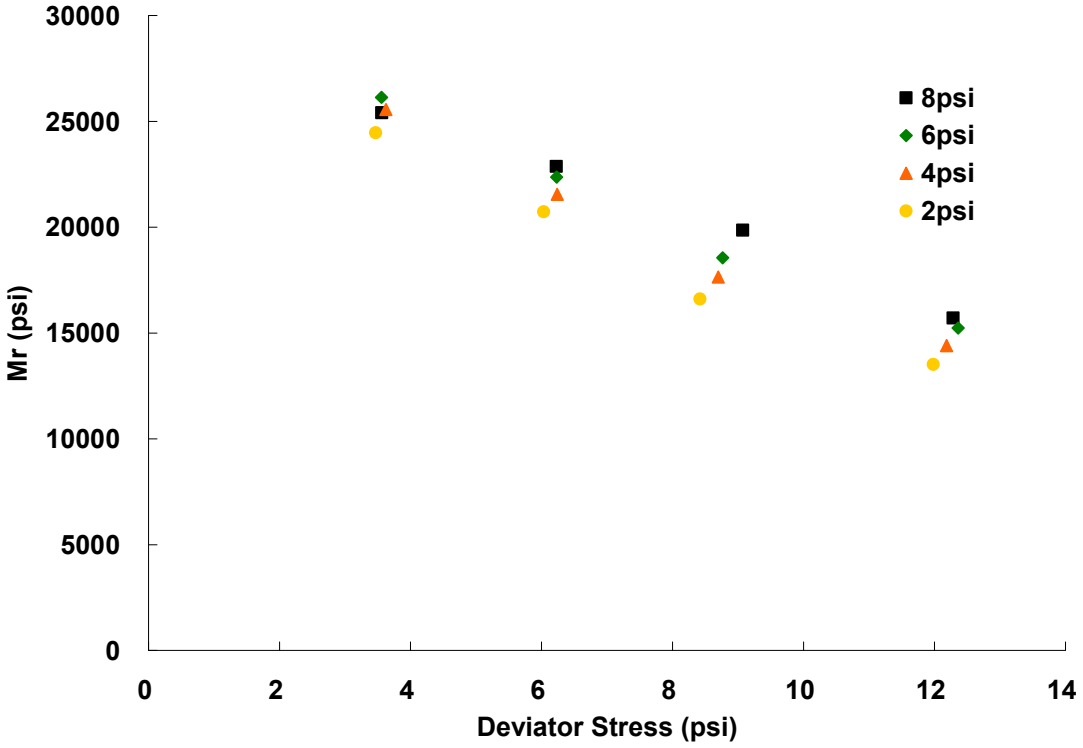

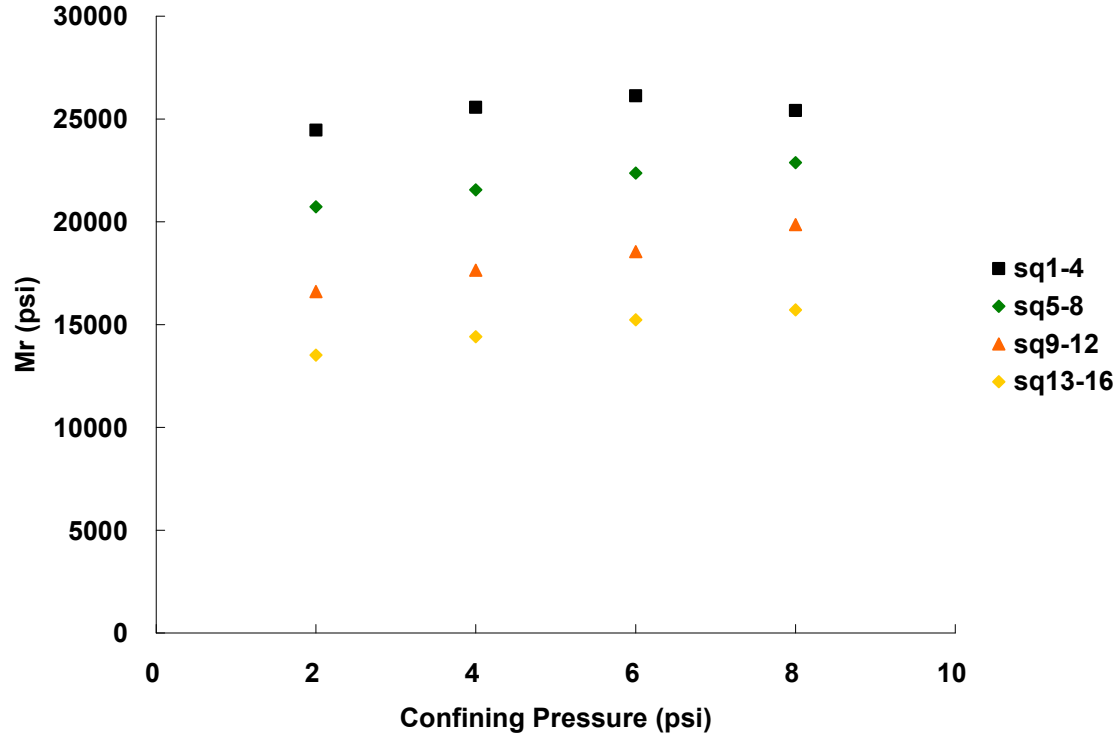

Owatonna 3.5-5.5 feet:

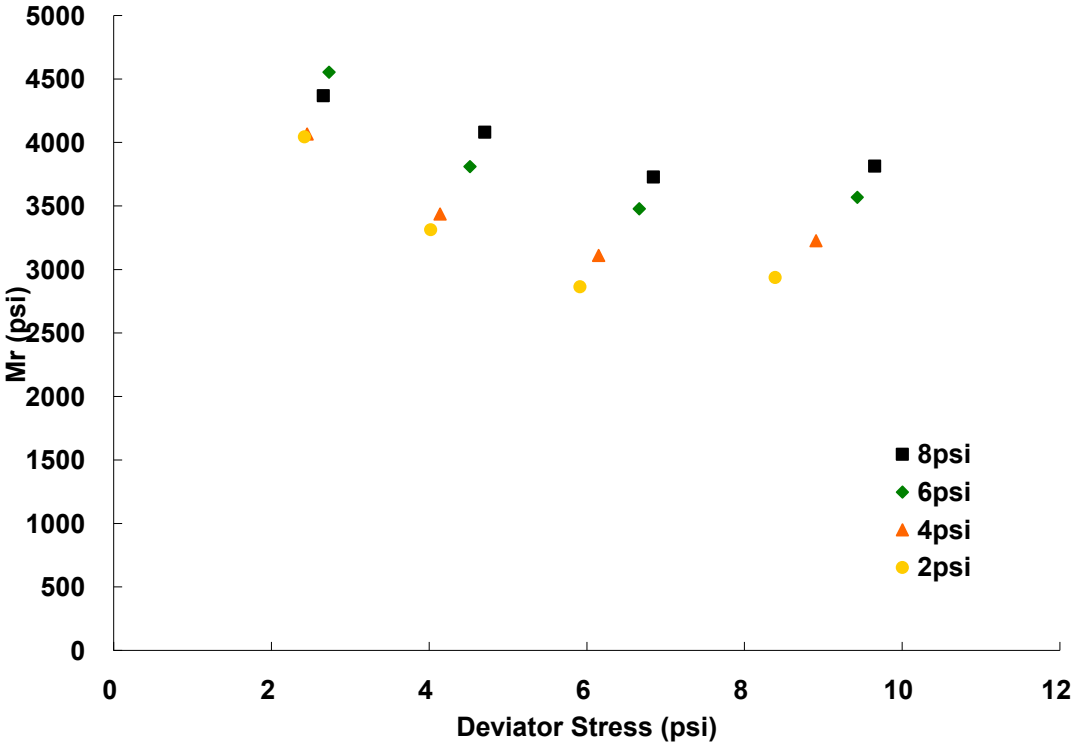

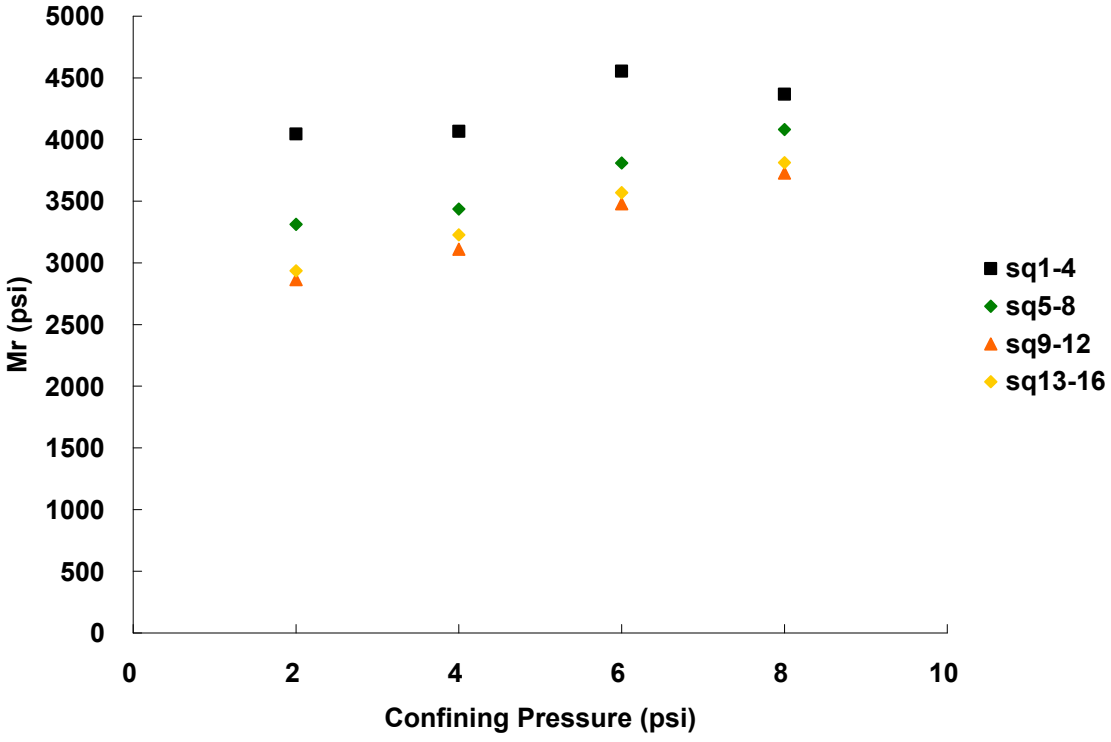

Owatonna 8.5-10.5 feet:

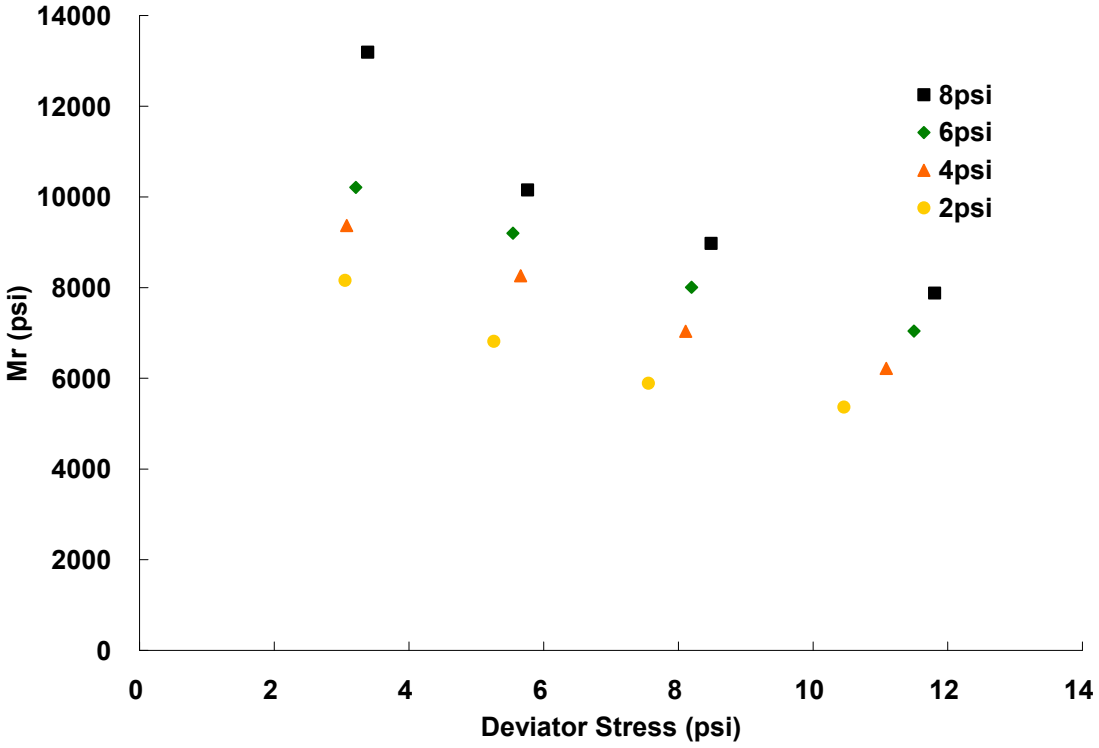

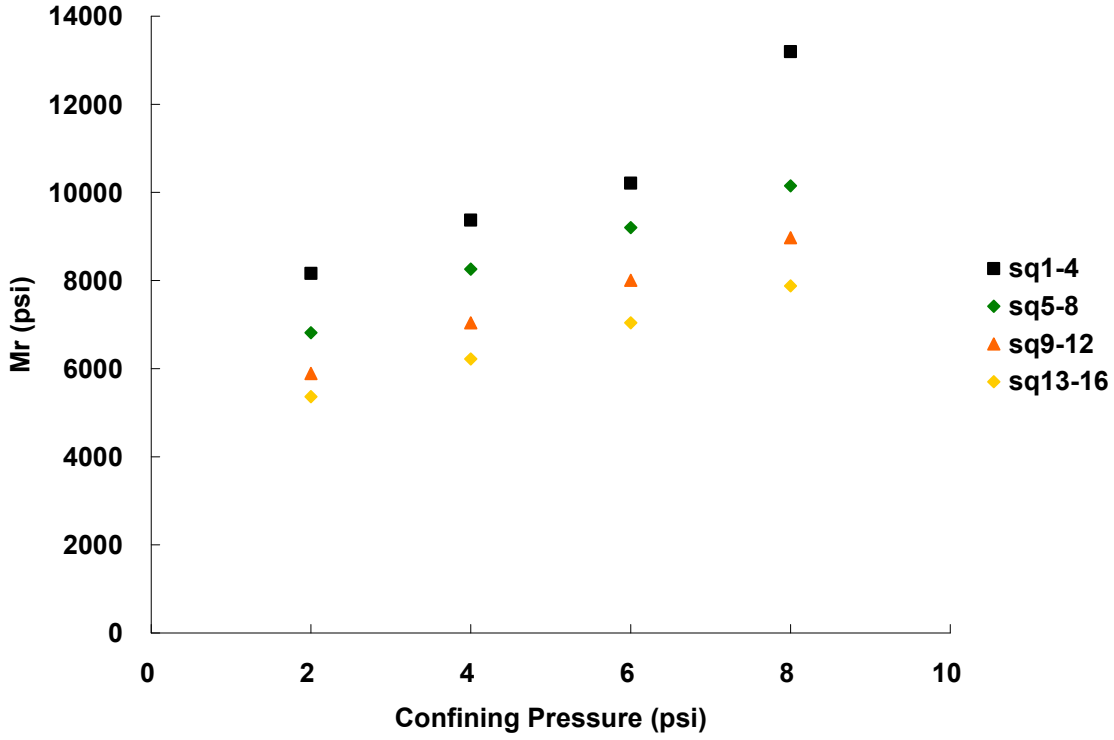

Owatonna 13.5-15.5 feet:

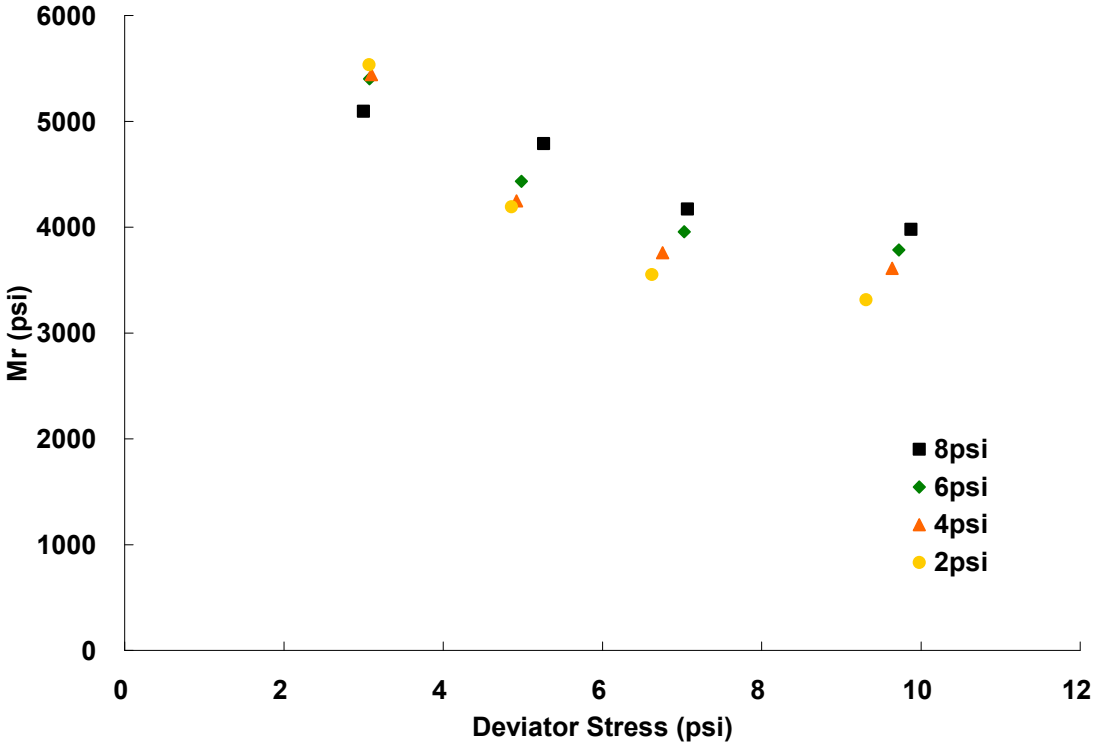

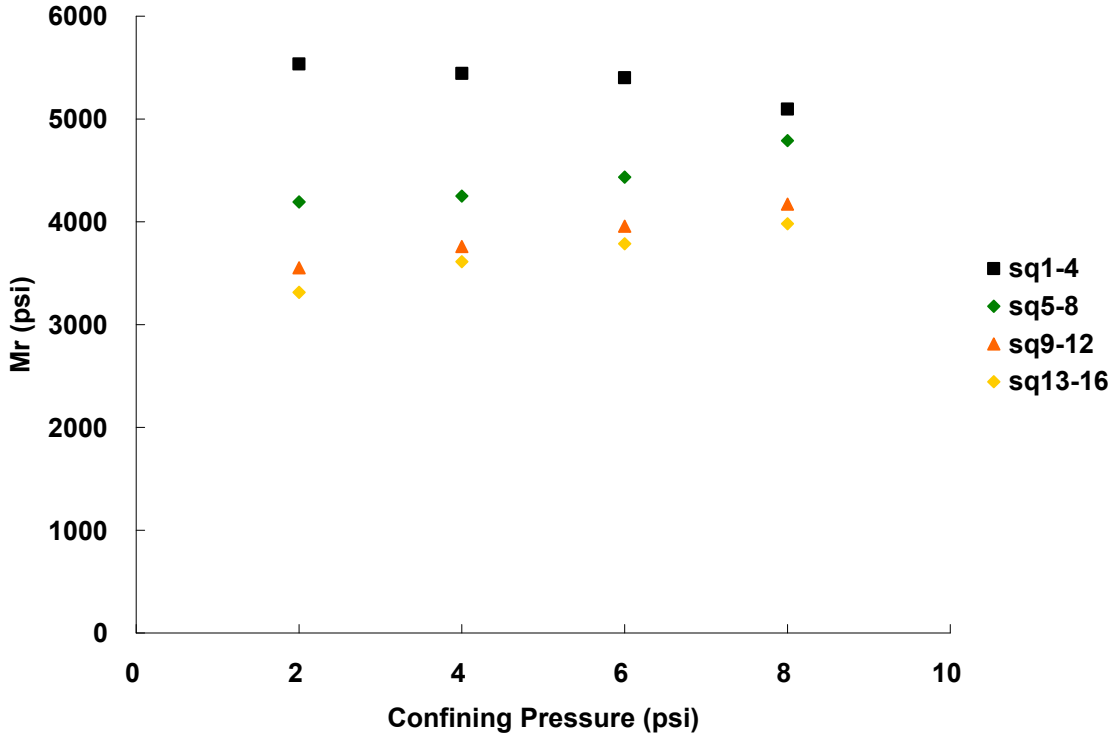

Forest Lake 13.5-15.5 feet:

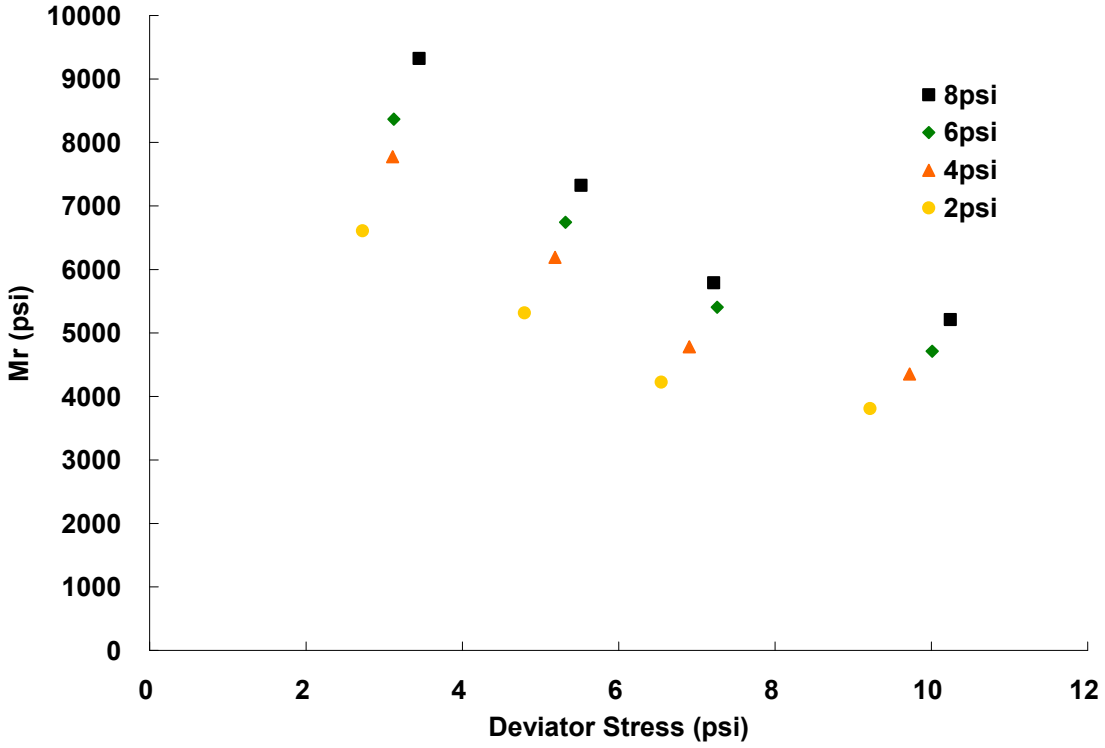

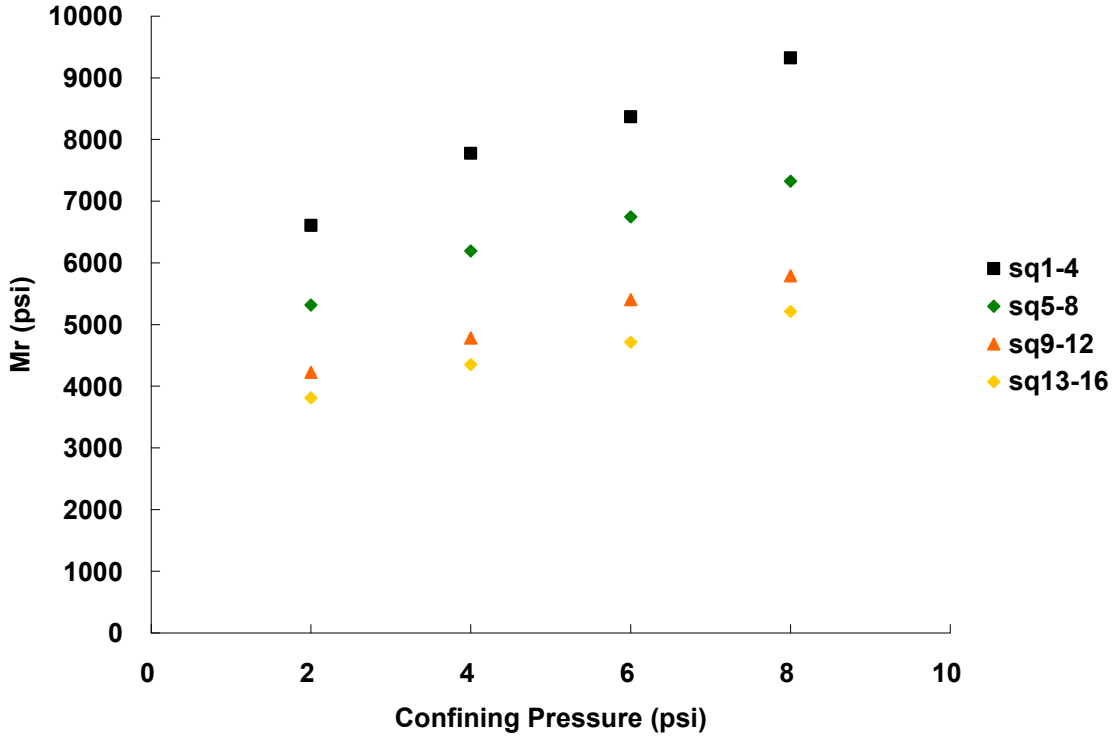

Forest Lake 18.5-20.5 feet:

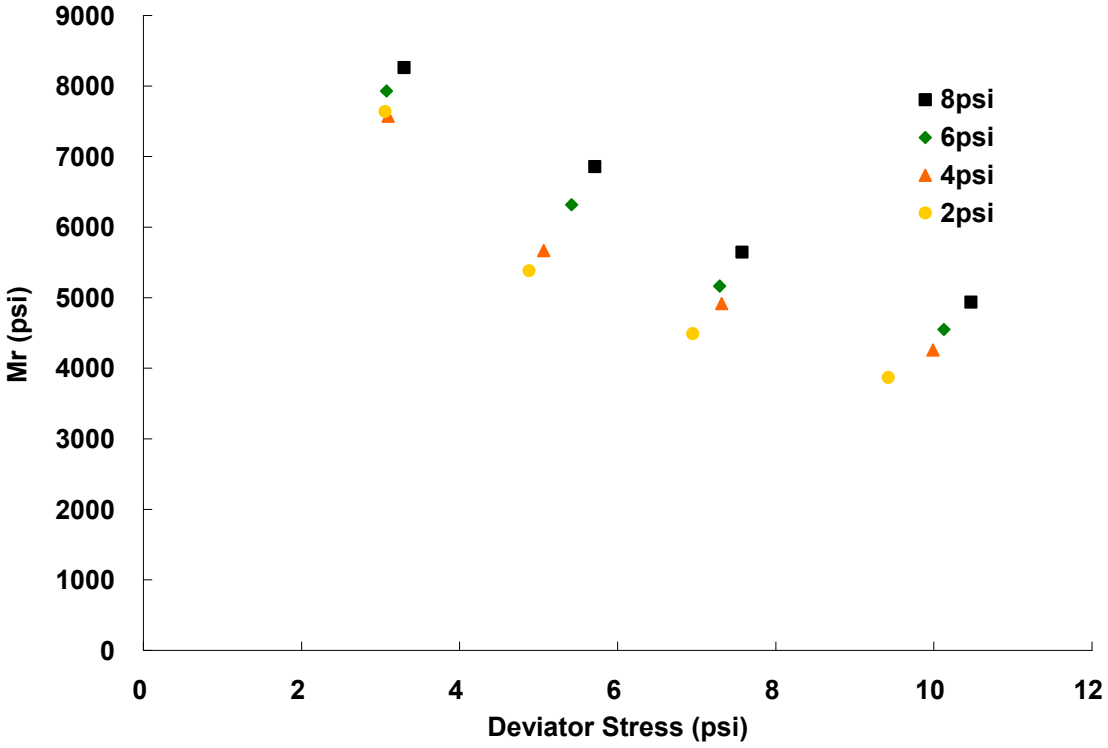

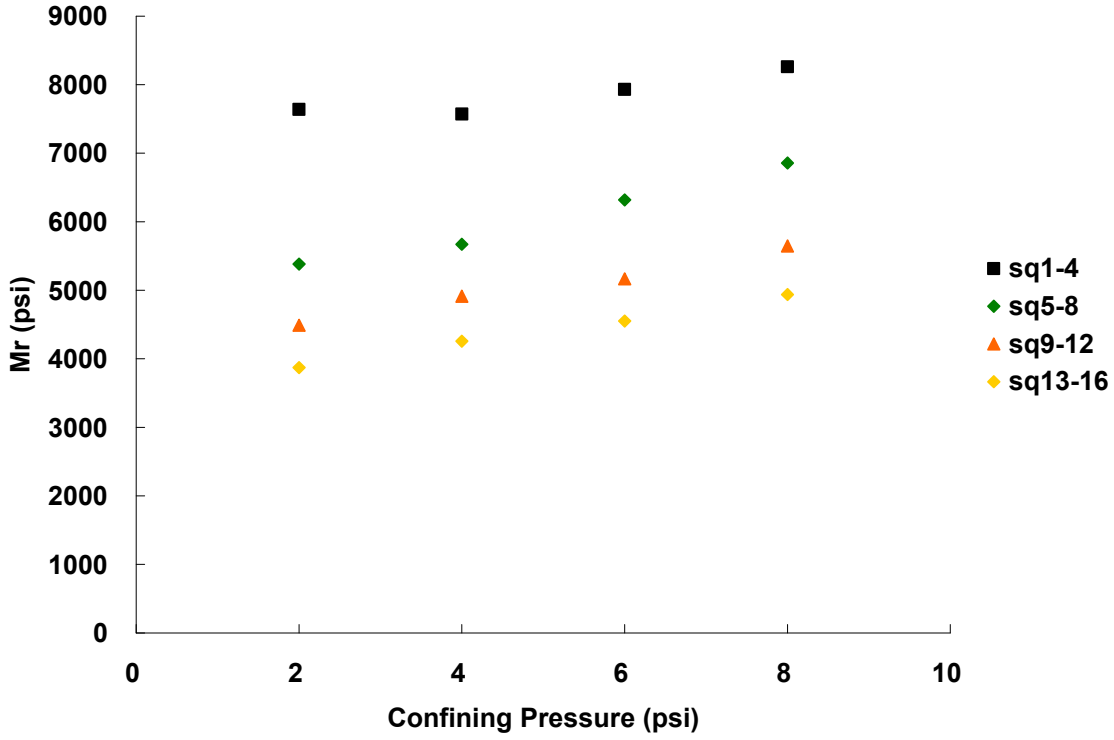

Appendix K

Resilient Modulus Testing Apparatus

The following description of the key pieces of the resilient modulus testing apparatus is based upon those by Davich et al. (2004) and Swenson et al. (2006) in which largely the same testing apparatus was used.

Load Frame:

MTS Systems, Inc. 858 servo-hydraulic load frame controlled by MTS Systems, Inc. TestWare hardware and TestStar software programmed to apply the specified haversine pulse axial load.

Triaxial Cell:

Research Engineering triaxial cell consisting of a plexiglass chamber friction fit to top and bottom platens fitted with air ports allowing for differential pressurization between sample interior and exterior as well as electrical ports to allow for internal placement of load cell and LVDTs for more accurate measurement and control of applied forces.

Pressure Regulation System:

Humboldt Flexpanel I pressure regulation system for monitoring and control of internal triaxial cell air pressure.

Load Cell:

22.2 kN (5,000 lb) load cell attached to the load frame allowing by a rod passing through the top platen of the triaxial cell allowing for internal measurement of the applied vertical force.

LVDTs:

Three spring-loaded LVDTs attached to a two piece aluminum harness spaced at 3 inches and held to the specimen via friction with the latex membrane. Readings were recorded via LabView software at a rate of approximately 400/sec.

Appendix L

CPT Seismic Traces

CPT seismic waterfall plots (provided by Mn/DOT):

Florence:

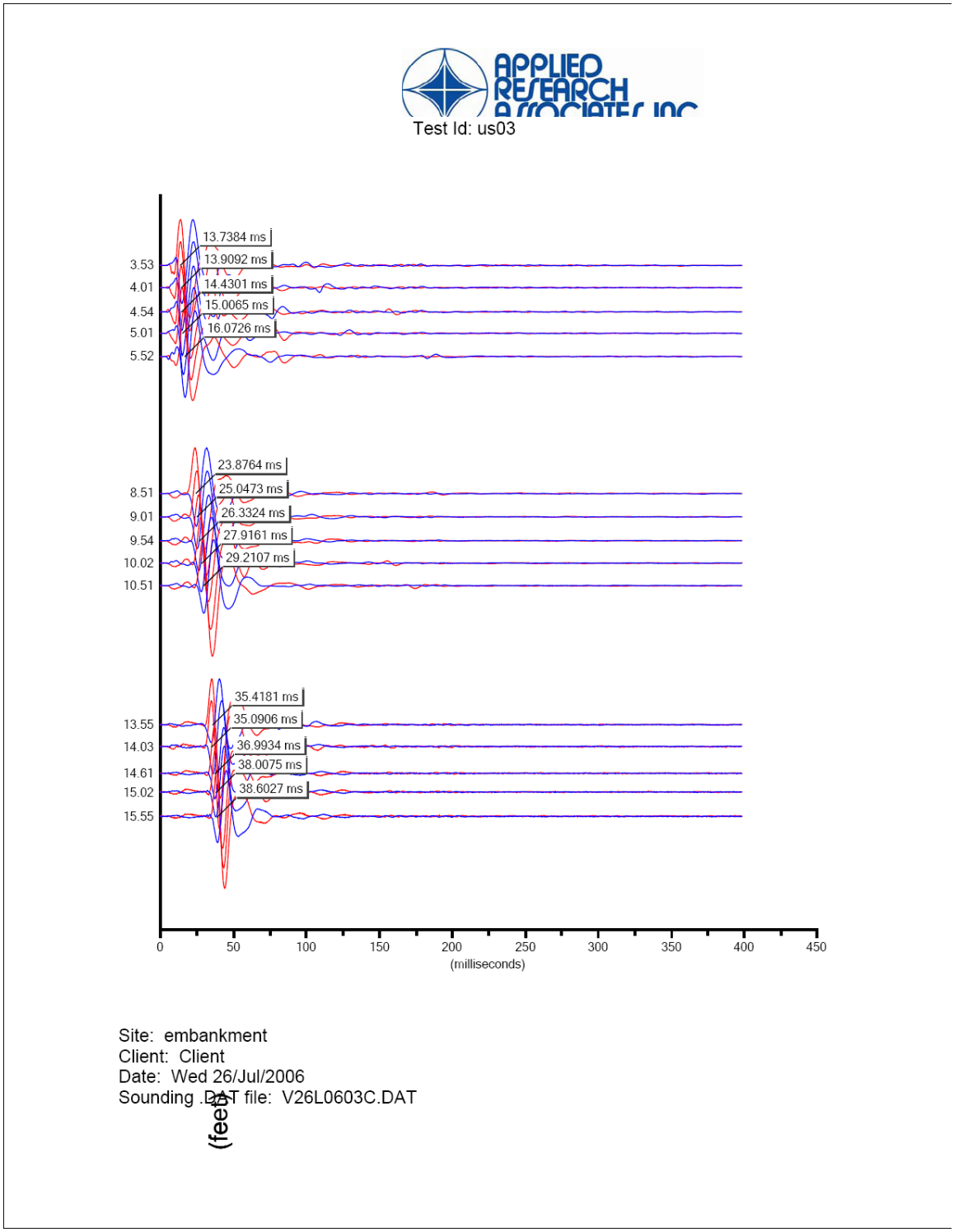

Owatonna:

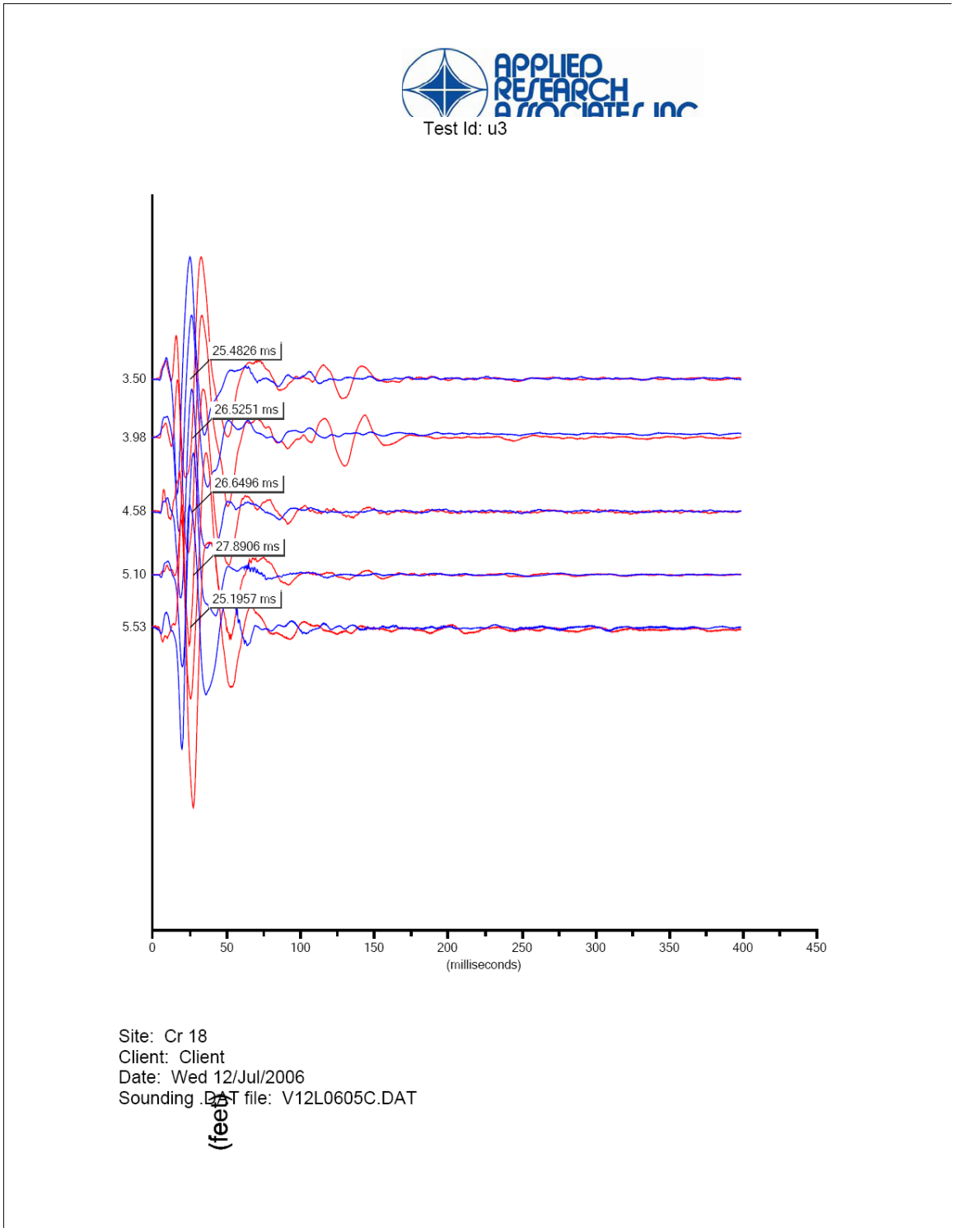
APPLIED RESEARCH ASSOCIATES, INC
Test Id: u3
25.4826 ms
26.5251 ms
26.6496 ms
27.8906 ms
25.1957 ms
3.50
3.98
4.58
5.10
5.53
0
50
100
150
200
250
300
350
400
450
(milliseconds)
Site: Cr 18
Client: Client
Date: Wed 12/Jul/2006
Sounding .DAT file: V12L0605C.DAT
(feet)

APPLIED RESEARCH ASSOCIATES, INC

Test Id: u3

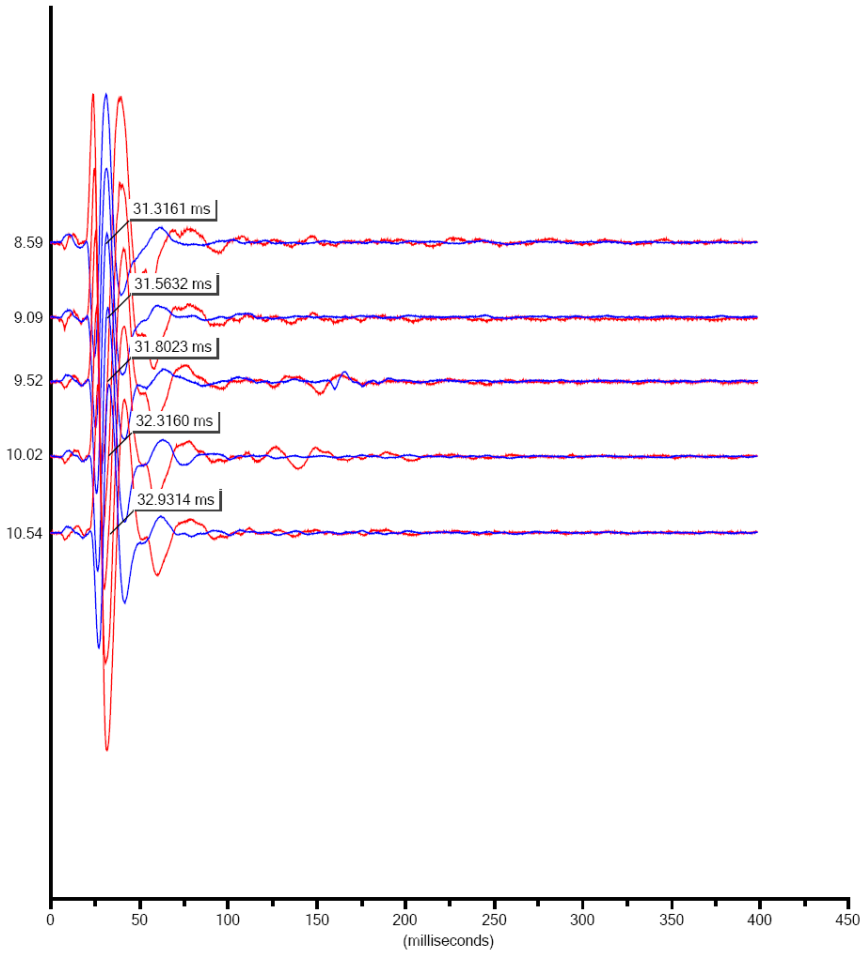

Site: Cr 18
Client: Client
Date: Wed 12/Jul/2006
Sounding .DAT file: V12L0605C.DAT

(feet)

Forest Lake:

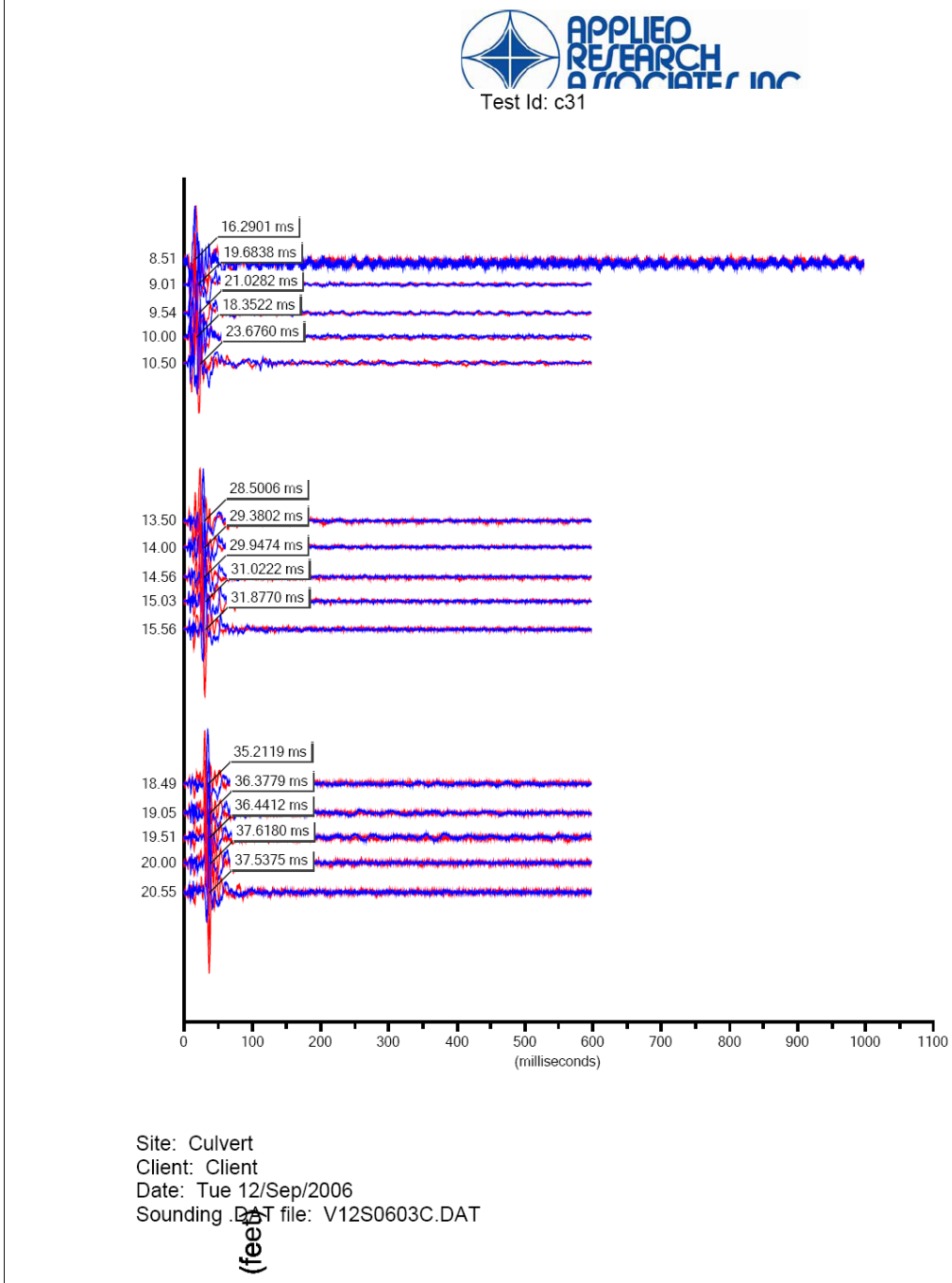
APPLIED RESEARCH ASSOCIATES, INC
Test Id: c31
16.2901 ms
19.6838 ms
21.0282 ms
18.3522 ms
23.6760 ms
8.51
9.01
9.54
10.00
10.50
28.5006 ms
29.3802 ms
29.9474 ms
31.0222 ms
31.8770 ms
13.50
14.00
14.56
15.03
15.56
35.2119 ms
36.3779 ms
36.4412 ms
37.6180 ms
37.5375 ms
18.49
19.05
19.51
20.00
20.55
0
100
200
300
400
500
600
700
800
900
1000
1100
(milliseconds)
Site: Culvert
Client: Client
Date: Tue 12/Sep/2006
Sounding .DAT file: V12S0603C.DAT
(feet)